보건학박사 학위논문

Characterization of aerosols and estimation of deposition in the respiratory tract from PHMG humidifier disinfectant

PHMG가 함유된 가습기 살균제의 공기 중 입자 특성과 인체 침착량 추정

2020년 **2**월

서울대학교 대학원

환경보건학과 환경보건학 전공

김 선 주

Characterization of aerosols and estimation of deposition in the respiratory tract from PHMG humidifier disinfectant

Advised by **Professor Chungsik Yoon**

A Dissertation Submitted in Partial Fulfillment of the
Requirements for the Degree of
Doctor of Philosophy in Public Health

To the Faculty of the Graduate School of Public Health at
Seoul National University
by
Sunju Kim

Data approved: December, 2019

Domyung Paek _____

Kyungho Choi _____

Seungmuk Yi _____

Donguk Park _____

Chungsik Yoon _____

PHMG가 함유된 가습기 살균제의 공기 중 입자 특성과 인체 침착량 추정

지도교수 윤 충 식

이 논문을 보건학 박사학위논문으로 제출함

2019년 10월

서울대학교 대학원

환경보건학과 환경보건학전공

김 선 주

김선주의 박사학위 논문을 인준함

2019년 12월

위 원 장 백 도 명 (인)

부 위 원 장 최 경 호 (인)

위 원 이 승 묵 (인)

위 원 박 동 욱 (인)

위 원 윤 충 식 (인)

ABSTRACT

Sunju Kim

Department of Environmental Health Sciences (Environmental Health Sciences)

Graduate School of Public Health

Seoul National University

Advised by Prof. Chungsik Yoon, Ph.D., CIH

Ultrasonic humidifiers are commonly used in Korea because of cold and dry weather during winter and early spring, but there can be problems due to microbial growth in the humidifier reservoir. Humidifier disinfectants were widely used from 1994 to 2011 in Korea to prevent microbial contamination in ultrasonic humidifiers, but sales were then prohibited by the government following an outbreak of severe lung injury among humidifier disinfectant users. The main raw materials used for humidifier disinfectants were polyhexamethyleneguanidine (PHMG), oligo(2-(2-ethoxy)ethoxyethyl guanidine chloride (PGH), and methylchloroisothiazolinone/methylisothiazolinone (CMIT/MIT). Of these, PHMG phosphate (CAS No. 89697-78-9) was the most widely sold product, accounting for the overwhelming majority of fatalities. Therefore, this study aimed to identify the characteristics of PHMG in aqueous solution and investigate the behavior of airborne particles generated by the use of PHMG as a humidifier disinfectant; determine the difference in oligomer types and content between PHMG products and aerosols and

estimate the airborne concentration of oligomers during humidifier use; and calculate the inhaled and deposited doses or fractions in the human lung using the ICRP and MPPD models for particles generated when a humidifier disinfectant containing PHMG was sprayed.

First, three types of PHMG were selected (manufactured in Korea, USA, and China), with dynamic light scattering (DLS) used to determine their behavioral characteristics in aqueous solution. To determine the airborne behavioral characteristics, PHMG was diluted to obtain high (62.5–65 ppm) and low (6.25–6.5 ppm) concentrations, and then real-time monitoring instruments were used to measure the effect of using a diffusion dryer and thermodenuder for controlling moisture in a cleanroom. A polycarbonate filter sample was analyzed by field emission-scanning electron microscope (FE-SEM)-energy dispersive spectrometry to determine the particle morphology. The DLS intensity results for the three products showed a slightly right-shifted (~100 nm) bimodal distribution relative to the airborne particle size distribution. The size of the airborne PHMG particles increased during the spraying due to aggregation, with the particle size of aggregated particles confirmed by FE-SEM to be approximately ≥20 nm. As the PHMG concentration increased by 10 times, the airborne concentrations measured using a real-time monitoring instrument increased by 2–3 times for nanoparticles and 45–85 times for 1–10-μm particles during humidifier operation; however, 99% of the particles generated could be classified as PM_1. Without ventilation, even after operating the humidifier, the PHMG particles could be airborne for approximately 2 h until the background

concentration was reached. Therefore, we found that airborne behavior was affected by the PHMG concentration, but this did not vary according to product manufacturer.

Second, LC-qToF was used to identify PHMG components in raw materials and airborne, and post-acquisition data processing was analyzed using UNIFI software. Samples in the air were diluted with the same conditions using three types of PHMGs to evaluate the behavioral characteristics (Chapter 2) at 8 h and had an impinger at 0.5 m and 1 m when the humidifier was sprayed. PHMG has been known to exist in the linear type (type A–C) and branched or cyclic type (type D–G). As a result of PHMG raw material analysis, various types existed, as shown in previous studies, among which the Oxy product was classified as type A–E, and BOC and Scunder products were classified as type A–E, except for type D. Additionally, the three products were composed of oligomers with 1–3 monomers, and compared to the linear type, dimer had the highest quantity in all products in type A and C. The linear structure in the Oxy product accounted for 90.6%, and Scunder and BOC products had linear structures of 78.6% and 75.8%, respectively. As the number of monomers increased (as the molecular weight increased), they were not detected at low concentrations. In a branched or cyclic structure, dimer of type E has the highest quantity in all products. In PHMG components of samples in the air, samples at 0.5 m showed a similar pattern with the component of raw materials, and dimers had the highest quantity in types A and C, and monomers in type B. However, high concentration samples collected at 1 m (65 ppm for Oxy product and 62.5 ppm and 125 ppm for Scunder and BOC products, respectively) were mainly detected for the low-molecular-

weight compounds, such as monomer or dimer. Additionally, the concentration of the oligomer in air was estimated to be 35.89 μg/m^3 at 6.5 ppm and 390.96 μg/m^3 at 65 ppm for the Oxy product.

Finally, based on data obtained in Chapter 2, inhaled and deposited doses were estimated using the ICRP and MPPD models. The ICRP model is widely used to evaluate the particle deposition in the respiratory tract for the general population and uses empirical equations based on experimental data, whereas the MPPD model is based on the ICRP model. Four types of scenarios were used in this study: adults and children and then daily and during sleep. Although the results of the two models varied due to differences in input parameters, the trend was similar. Infants and children tended to have similar or higher deposition doses and fractions than adults. Moreover, the areas of deposition were divided into the head airway, tracheobronchial, and alveolar regions. When the humidifier was sprayed, the highest number concentration was found at 15.4 nm, and the highest deposition fraction or dose by PM_1 was noted in the pulmonary and head airways.

Therefore, this study investigated the characteristics of raw materials of humidifier disinfectant containing PHMG sprayed in the air, and then estimated the inhaled and deposited dose in humans using the ICRP and MPPD models. Particles in raw materials of PHMG had a bimodal distribution in the region near 100 nm, and raw materials of PHMG consisted of oligomers in the linear type (type A–C). Characteristics of PHMG in the air were identified — most particles were PM_1 and existed as aggregated single particles of approximately 20 nm in size. Aerosol had a high proportion of monomers,

and the proportions of type C monomers were high at 1 m. Infants and young children showed high deposition doses or fractions in the ICRP and MPPD models.

Key words: humidifier disinfectant, PHMG, DLS, FE-SEM, SMPS, OPS, PAS, LC-qToF, ICRP model, MPPD mode, inhalation exposure, deposited dose, inhaled dose, exposure model

Student Number: 2015-30659

CONTENTS

LIST OF TABLES

LIST OF FIGURES

LIST OF APPENDICES

CHAPTER I.

Background

I-1.Humidifier disinfectant incident and the previous studies

Korea has four distinct seasons, and is cold and dry in winter and early spring. Ultrasonic humidifiers are commonly used during this time, but there can be problems due to microbial growth in the humidifier reservoir. Humidifier disinfectants were widely used to prevent microbial contamination in ultrasonic humidifiers from 1994 to 2011, but sales were then prohibited by the government following an outbreak of severe lung injury among humidifier disinfectant users (Park et al., 2018).

However, although similar symptoms were already reported as acute interstitial pneumonia observed in children from spring in 2006, the result in the previous study was estimated due to some viruses (Cheon et al., 2008). After that, the Korea Centers for Disease Con

trol and Prevention (KCDC) reported an odds ratio of lung injury of 47.3 (95% CI: 6.1–369.7) in a case-controlled epidemiologic study investigating lung injury associated with humidifier disinfectant in 2011 (KCDC, 2011). Prior to the ban, about 600,000 humidifier disinfectants were sold each year, with about 20 different types of product being available.

Humidifier disinfectant is diluted with water in a certain ratio prior to operation. The main raw materials used for humidifier disinfectants were polyhexamethyleneguanidine-phosphate (PHMG-P; CAS No. 89697-78-9), oligo(2-(2-ethoxy)ethoxyethyl guanidine chloride (PGH; CAS No. 374572-91-5), and a mixture of chloromethylisothiazolinone (CMIT; CAS No. 26172-55-4) and methylisothiazolinone (MIT; CAS No. 2682-20-4) (Paek et al., 2015). Among component of these humidifier disinfectants, product containing PHMG phosphate (PHMG) was the most widely sold product, accounting for the overwhelming majority of fatalities. The most representative product among them was 'Oxysaksak' manufactured in Oxy company.

As of May 2019, the number of deaths resulting from lung injuries associated with humidifier disinfectant was 1,403, and this number is expected to increase (ACCEH, accessed 13 May 2019). This was recognized incident by consumer product due to chemical abuse. It was assumed that there were many more victims than the known damage because it was documented by the first paper in 2006. Moreover, the outside of the oxy product was remarked as 'this component used in product is safe.' because this is focused on the toxicity of components, and the exposure route was not considered at all.

The properties of PHMG are basically known as follows. PHMG is a water-soluble chemical that is part of the guanidine group. The guanidine-based chemicals are widely used as a biocide, and PHMG has been used as a component in household chemical products, such as wet wipes and cleaning products, because it has a strong bacteriostatic action and relatively low toxicity (Aleshina et al., 2001; Mashat, 2016; Song et al.,

2014). The surface of bacterial cells with a negative charge is stabilized by Mg^{2+} and Ca^{2+}. The oligoguanidines used as disinfectant, displace the stabilizing status of Mg^{2+} and Ca^{2+} ions and induce the death of bacteria because phospholipids in membranes have cellular leakage and loss of essential cellular components (Buchberger et al.; Gilbert and Moore, 2005; Wei et al., 2009).

In addition, the incident caused by PHMG, a guanidine-based compound commonly used as a disinfectant, was not the first case in Korea. Deaths due to consumption of antiseptic liquid were reported in Russia from August 2006 to May 2007. During this period, 12,500 people were hospitalized citing health problems after drinking illegally manufactured vodka containing PHMG, which was intended for sterilization purposes in hospitals; 175 (9.4%) of the victims died. Accordingly, several studies of the oral toxicity of PHMG have been conducted in Russia (Ostapenko et al., 2011; Solodun et al., 2011). Ostapenko, Brusin et al. (2011) showed that 600 mg/kg was a lethal dose, and a 90-day chronic toxicity test identified signs of kidney and liver toxicity following a dose as low as 0.06 mg/kg.

Before the humidifier disinfectant fatalities in Korea, there was little information available regarding the inhalation toxicity of PHMG; however, a number of such studies were conducted in Korea thereafter. Some studies have reported that mice exposed to PHMG-P through intratracheal instillation showed severe pulmonary inflammation, fibrosis, and thymic atrophy (Song et al., 2014), and aerosol particles containing PHMG-P induced the generation of reactive oxygen species (ROS), and pulmonary inflammatory

and fibrotic changes (Kim et al., 2016). A number of studies on the toxicity of PHMG-P substances have been conducted in recent years

After incident, many epidemiologic studies were conducted, various studies have concluded that there is a clear relationship between lung injury and humidifier disinfectant. Among the epidemiological studies, the main conclusions were follow as. In particular, there were studies focused in children aged <6 years old and pregnant women because they were mainly the victims. Among the victims of lung injury, the majority of the victims were 125 (56.6%) for children aged < 6 years and under 35 (15.8%) for pregnant women, and they would be more vulnerable to humidifier disinfectant lung injury when exposed to chemicals within short period in early life (Park et al., 2016; Park et al., 2018). In addition, three categories, biological susceptibility, a temporal cycle of exposure and recovery, and spatial conditions and density of disinfectant, were investigated for assessing dose-response relationships in a nationwide study to classify all potential cases of humidifier disinfectant lung injury in Korea. analysis indicated associated strongly with recurrent, intense, acute exposure without sufficient recovery time between exposures, more so than long term cumulative exposure (Paek et al., 2015).

However, although the humidifier disinfectant incident was caused by a lack of understanding of the chemical exposure route, there have been few exposure assessment studies based on realistic environment until now. One study of harmful particle generation when sprayed PHMG conducted simulations in small and large rooms in an apartment during fall and winter. They did not conclude that PHMG caused lung disease

at the measured exposure levels (3.22 + 5.13 μg/m^3 in fall and 0.21 + 2.11 μg/m^3 in winter) and particle size distributions (PSDs) with maximum concentration (149–157 nm). However, until now, research on the PHMG aerosols has had limitations. airborne concentration could not be concluded that it was caused by PHMG particles was because there is no control over the moisture particles generated in the airborne. The studies on PHMG properties and concentration generated in the airborne were not considered by the PHMG properties as polymer. Most of the studies considering the properties of PHMG, which is a polymer, were mostly about the analysis method and the analysis of the composition of PHMG raw materials solution.

Therefore, humidifier disinfectant incident is one of the major incidents caused by consumer products, and it is important to make assessments based on the actual exposure environment and route.

I-2.Objectives and study design

Specific details on the purposes were (1) to identify the characteristics of PHMG in aqueous solution, and investigate the behavior of airborne particles generated by use of PHMG as a humidifier disinfectant (Chapter 2); (2) to identify the difference in oligomer types and content between PHMG products and aerosols and to estimate the airborne concentration of oligomers during humidifier use (Chapter 3); (3) to estimate inhaled and deposited doses in the human lung by using the ICRP and MPPD model for the particles generated when a humidifier disinfectant containing PHMG was sprayed (Chapter 4).

(1) Chapter 1. Humidifier disinfectant incident and the previous studies (Backgrounds)

(2) Chapter 2. Behavioral Characteristics of Polyhexamethyleneguanidine (PHMG) Particles in Aqueous Solution and Air when Sprayed into an Ultrasonic Humidifier

(3) Chapter 3. Characterization of Polyhexamethyleneguanidine (PHMG) oligomers in solutions and aerosols emitted during humidifier use

(4) Chapter 4. Estimates of an inhaled and deposited dose by inhalation exposure to humidifier disinfectant containing Polyhexamethyleneguanidine (PHMG)

(5) Chapter 5. Summary and conclusions

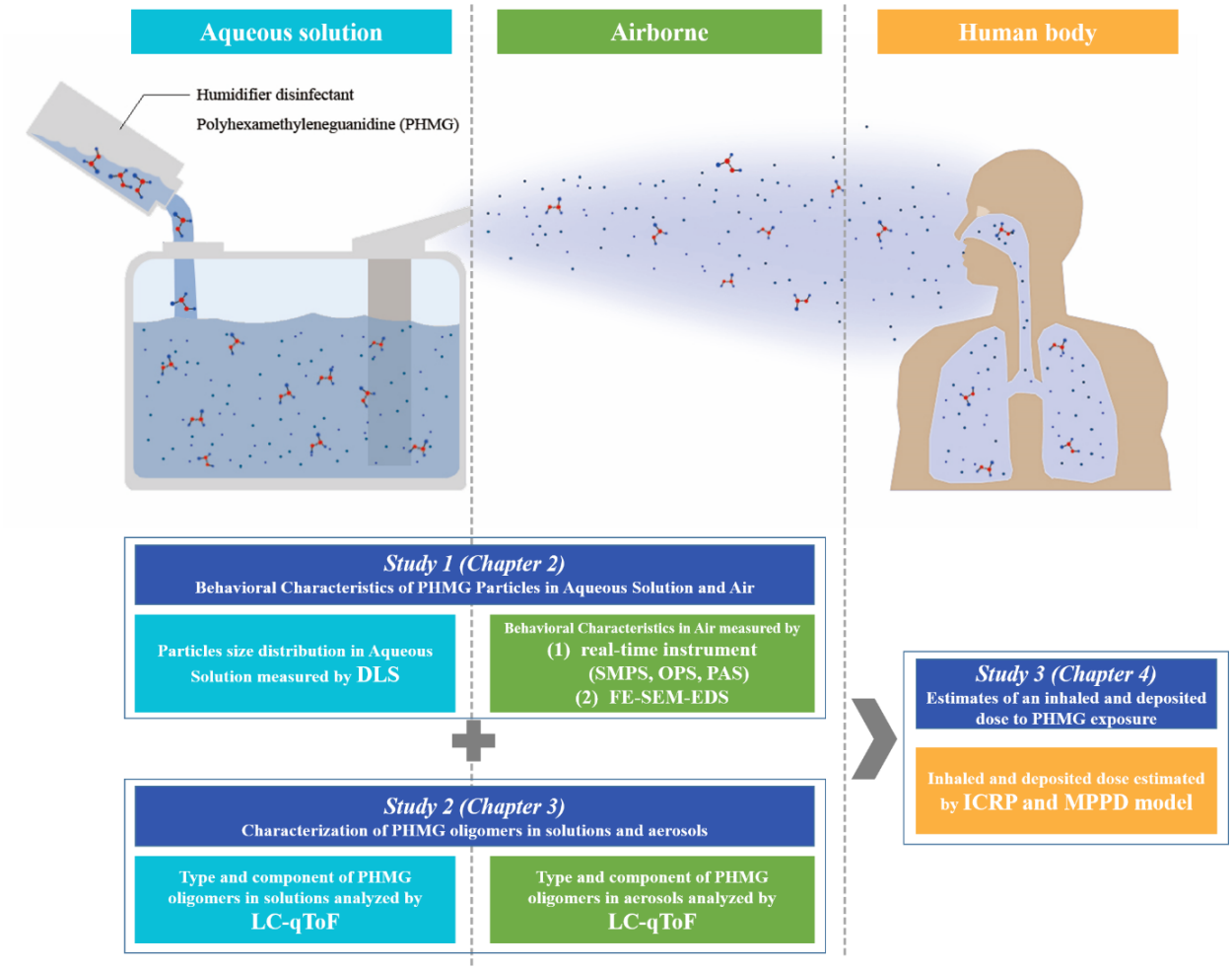

Figure I-1 . The framework of this study.

CHAPTER II.

Behavioral Characteristics of Polyhexamethyleneguanidine (PHMG) Particles in Aqueous Solution and Air when Sprayed into an Ultrasonic Humidifier

II-1. Introduction

Korea has four distinct seasons, and is cold and dry in winter and early spring. Ultrasonic humidifiers are commonly used during this time, but there can be problems due to microbial growth in the humidifier reservoir. Humidifier disinfectants were widely used to prevent microbial contamination in ultrasonic humidifiers from 1994 to 2011, but sales were then prohibited by the government following an outbreak of severe lung injury among humidifier disinfectant users (Park et al., 2018). The Korea Centers for Disease Control and Prevention (KCDC) reported an odds ratio of lung injury of 47.3 (95% CI: 6.1–369.7) in a case-controlled epidemiologic study investigating lung injury associated with humidifier disinfectant (KCDC, 2011). Prior to the ban, about 600,000 humidifier disinfectants were sold each year, with about 20 different types of product being available. As of May 2019, the number of deaths resulting from lung injuries associated with humidifier disinfectant was 1,403, and this number is expected to increase because there are patients who have used humidifier disinfectants in the past and have developed severe lung diseases (ACCEH, accessed 13 May 2019).

Humidifier disinfectant is diluted with water in a certain ratio prior to operation. The main raw materials used for humidifier disinfectants were polyhexamethyleneguanidine (PHMG), oligo(2-(2-ethoxy)ethoxyethyl guanidine chloride (PGH), and methylchloroisothiazolinone/methylisothiazolinone (CMIT/MIT) (Paek et al., 2015).

Among these disinfectants, PHMG phosphate (PHMG-P; CAS No. 89697-78-9) was the most widely sold product, accounting for the overwhelming majority of fatalities. Polyhexamethyleneguanidine is a water-soluble chemical that is part of the guanidine group. It is widely used as a biocide in household chemical products, such as wet wipes and cleaning products, because it has a strong bacteriostatic action and relatively low toxicity (Aleshina et al., 2001; Song et al., 2014).

Deaths due to consumption of antiseptic liquid were reported in Russia from August 2006 to May 2007. During this period, 12,500 people were hospitalized citing health problems after drinking illegally manufactured vodka containing PHMG, which was intended for sterilization purposes in hospitals; 175 (1.4%) of the victims died. Accordingly, several studies of the oral toxicity of PHMG have been conducted in Russia (Ostapenko et al., 2011; Solodun et al., 2011). Ostapenko, Brusin et al. (2011) showed that 600 mg/kg was a lethal dose, and a 90-day chronic toxicity test identified signs of kidney and liver toxicity following a dose as low as 0.06 mg/kg. Before the humidifier disinfectant fatalities in Korea, there was little information available regarding the inhalation toxicity of PHMG; however, a number of such studies were conducted in Korea thereafter. Some studies have reported that mice exposed to PHMG-P through intratracheal instillation showed severe pulmonary inflammation, fibrosis, and thymic atrophy (Song et al., 2014), and aerosol particles containing PHMG-P induced the generation of reactive oxygen species (ROS), and pulmonary inflammatory and fibrotic changes (Kim et al., 2016). A number of studies on the epidemiology and toxicity of

PHMG-P substances have been conducted in recent years; however, there have been few exposure assessment studies based on realistic particle concentrations.

There have only been a few studies of harmful particle generation when sprayed PHMG. The first such paper was published as part of a short epidemiological investigation by the KCDC. Lee and Yu (2017) conducted simulations in small and large rooms in an apartment during fall and winter. The airborne PHMG concentration in this study was 3.22 + 5.13 μg/m3 in fall and 0.21 + 2.11 μg/m3 in winter; the particle size distribution (PSD) maximum was at 149–157 nm. The second study reported aerosol generation results from a toxicity experiment with rats, but a nanoparticle generator was used rather than a humidifier for aerosol generation, and the experiment was conducted in a chamber in which only the nose of the rat was exposed (Kim et al., 2016).

There were several limitations to the above studies. The concentrations and PSDs of the disinfectant droplets could not be determined because the influence of moisture and the dilution solvent was not considered. The aim of this study was to identify the characteristics of PHMG in aqueous solution, and investigate the behavior of airborne particles generated by use of PHMG as a humidifier disinfectant.

II-2. Methods

II-2-1. Preparation of PHMG

Table Ⅱ-1 provides details of the PHMG materials used in our experiment. The experiment was conducted with two PHMG solutions and one product containing PHMG. One of the PHMG solutions contained approximately 20–25% PHMG (BOC, USA) and the other contained approximately 25% PHMG (Scunder, China). The other product used was oxysaksak, which contains approximately 0.1% PHMG (Oxy, Korea). It has a lavender aroma and is known to be responsible for most cases of lung injury. Because there was no legal requirement to produce a safety data sheet (SDS) for the Oxy product at the time of the sale, no specific safety information was available; however, data on the raw materials, including the amount of PHMG used in the product, were available.

Table II-1. Information on PHMG products used for this experiment

No.	Name	Ingredient by SDS	CAS No.	Content* (%)	Approximated concentration (%)	Dilution ratio	Nominal Diluted concentration (ppm)	Company (Manufactured country)
1	Oxy Product	Polyhexamethyleneguanidine Phosphate	89697-78-9	95	1300 ppm** (0.1%)	200:1***	6.50	Oxy (Korea)
		Hexamethylenediamine	124-09-4	1				
		Sodium Chloride	7647-14-5	4		20:1	65.00	
2	BOC product	Polyhexamethyleneguanidine Phosphate	89697-78-9	20-25	250,000 ppm (25%)	40,000:1	6.25	BOC (USA)
		Water	7732-18-5	75-80		4,000:1	62.50	
3	Scunder product	Polyhexamethyleneguanidine Phosphate	89697-78-9	25				Scunder (China)
		Water	7732-18-5	74.5		40,000:1	6.25	
		Ash content	-	0.5	250,000 ppm (25%)			
		Hexamethylenediamine	124-09-4	N.D.		4,000:1	62.50	
		Guanidine hydrochloride	50-01-1	N.D.				

* This content was indicated by SDS.

** Oxy product was only indicated for information on the ingredients for raw materials of PHMG used in product.

*** 200:1 was labelled on the product surface as recommended dilution ratio by Oxy manufactured company.

II-2-2. Characterization of PHMG in aqueous solution

Dynamic light scattering (DLS; Zetasizer Ultra; Malvern Instruments, UK) was used to confirm the particle distributions in solutions of the raw test materials. Each sample was measured three times. The BOC and Scunder products were analyzed under the same conditions as the Oxy product, but the analysis results were not stable. Therefore, all samples were analyzed without dilution because of the sensitivity of the DLS. Samples were placed in cuvettes (DTS0012; Malvern) and analyzed in a minimum volume of 1 ml. According to the PHMG SDS (Table Ⅱ-1), the dispersant used in the DLS was water, because water was used as the solvent during the production of the PHMG material. The refractive index and absorption values of the sample used to calculate the number size distribution were 1.520 and 0.001, respectively, and the temperature of the sample was 25℃. The DLS analysis could accommodate particles over the range of 0.1–10,000 nm. The software used for sample analysis was ZS XPLORER (ver. 1.00). All DLS size distribution results are presented as relative values.

II-2-3. Measurement and analysis of airborne PHMG particles

II-2-3-1. Cleanroom set up

All experiments were conducted in a 40.3 m^3 (7.0 m [L] × 2.4 m [W] × 2.4 m [H]) class 1,000 cleanroom fitted with a high-efficiency particulate air (HEPA) filter, enabling background particles smaller than 0.5 μm to be limited to less than 1,000 particles/ft^3. The purified air provided by the ventilation system flowed into the room via inlets on the ceiling, while the outlet air flowed out of the room through vents in the walls. The cleanroom was ventilated before measurements were conducted to ensure that the background concentration was kept below 100 particles/cm^3 (#/cm^3), with the concentration measured by a scanning mobility particle sizer (SMPS; Nanoscan; TSI, USA). Once measurements of the background concentration began, the ventilation system was turned off. All experiments were conducted using a temperature and humidity meter (TR-72U Thermo recorder; T&D Corporation, Japan). The temperature and humidity in the cleanroom before the humidifier began operating were maintained at about 20℃ and 50%, respectively.

The ultrasonic humidifier (H-U977, Ohsung, Korea) used for the experiment had a 6.5 L tank containing the spray liquid, and had a design used commonly in household humidifiers. The humidifier could be operated at a spray output rate of approximately 320 ml/h and the spray volume was set to the maximum in this study.

The Oxy product was recommended using about 10 ml product per water 2-3 L when humidifier water replace. Therefore, the recommended dilution for the Oxy product was 200:1, but previous studies had used dilution of up to 20:1 to simulate a “worst-case scenario”. The Oxy product concentrations investigated in previous studies were slightly different among the products investigated, but were about 1,300 ppm on average. As shown in Table Ⅱ-1, the exact PHMG concentration in each product was unknown and there was no standard PHMG solution on the market with a known concentration. We therefore took the approximate concentration suggested by the manufacturer as the nominal maximum concentration. The concentration of Oxy product was calculated to be about 6.5 ppm at 200:1 dilution, and about 65 ppm at 20:1 dilution. The dilution factors for the BOC and Scunder products were set to produce similar concentrations. The maximum concentrations of the two solutions (A and B) were about 25% (250,000 ppm); they were diluted to about 6.25 ppm (40,000:1) and 62.5 ppm (4,000:1), respectively. Distilled water was generated by a commercial purification system (Milli-Q; Merck Millipore, Germany) and then used to dilute PHMG in all experiments. The dilutions produced low concentrations of 6.5 ppm (Oxy product) and 6.25 ppm (BOC and Scunder products), and high concentrations of 65 ppm (Oxy product) and 62.5 ppm (BOC and Scunder products).

II-2-3-2. Instrumental measurement of airborne PHMG particles

The SMPS and an optical particle sizer (OPS; Model 3330; TSI) were used for real-time monitoring of the particle number concentration in the ranges of 10–420 nm and 0.3–10 μm, respectively. The particle cut points of the OPS were set to 0.3, 0.5, 1.0, 3.0, 5.0, and 10.0 μm, for a total of six channels. A portable aerosol spectrometer (PAS; Model 1.109; Grimm, Germany) was used to measure the mass concentration of the PM_1, $PM_{2.5}$, and PM_{10} fractions. All real-time instruments logged data at 1-min intervals.

The temperature was maintained at about 15℃ during operation, and increased to 20℃ thereafter. Humidity was maintained at 100% during operation, and decreased to about 60% thereafter.

A diffusion dryer and thermodenuder were used to minimize moisture because measurements were affected by the high humidity during the experiment. The diffusion dryer was filled with silica gel to evaporate the moisture particles. The thermodenuder, which had a heating zone set to 200℃ and an adsorption section filled with active charcoal, was used to remove volatile and semi-volatile compounds. The silica gel in the diffusion dryer was replaced periodically, i.e., when it turned pink. These instruments were connected to the inlets of all measuring equipment.

The diffusion dryer and thermodenuder were used to minimize the effect of moisture when operating the humidifier. In previous experimental studies using a thermodenuder,

decreases of about 94–98% in the number concentration of particles measured by SMPS have been reported depending, on the particle components and flow rates (An et al., 2007; Fierz et al., 2007). The same thermodenuder used in this study also reduced the number concentration of airborne particles by 81.5% in our previous humidifier study (Park et al., 2017). In that study, we investigated the most efficient combination of dryer and thermodenuder. Optimal efficiency was obtained when the diffusion dryer was connected ahead of the thermodenuder. When connecting in this order, the nanoparticle number concentration decreased by about 75% for a PHMG concentration of 65 ppm (Kim, 2018).

For integrated sampling, we used a 37-mm polycarbonate (PC) filter with a pore size of 0.4 μm (SKC, USA) equipped with a pump (GilAir; Sensidyne, USA) operated at 2 L/min for electron microscopy analysis.

The sampling zone was set to 0.5 m from the instrument for the SMPS, OPS, and PAS. The thermo recorder and PC filter of the real-time monitoring instruments were placed 0.5 m from the instrument, but for the SMPS they were also placed at 1 m because of instrumental constraints.

The real-time monitoring instruments sampled for a total 5 h 30 min. The background concentration was measured for 30 min before operating the humidifier. The humidifier was then operated for 4 h. After turning off the humidifier, the airborne concentration was measured for a further 1 h. The PC filter for integrated monitoring was operated during the 4 h period in which the humidifier was operated.

II-2-3-3. Analysis of airborne PHMG particles

The data measured by the real-time monitoring instrument were divided into before (n = 30), during (n = 240), and after (n = 60) humidifier operation. The data were subjected to a normality test and were shown to have a geometric distribution. The geometric mean (GM) and geometric standard deviation (GSD) were analyzed using Excel 2016 (Microsoft Office Professional Plus 2016; Microsoft Corp., USA), based on the data collected from the real-time monitoring instruments, i.e., SMPS, OPS, and PAS. The regression equation of the concentration reduction after operation of the humidifier was determined by plotting the data, and analysis of covariance (ANCOVA) was analyzed to identify the difference by concentration of product, and time was set covariance. Data analysis was performed using SPSS version 20.0 (IBM Inc., USA).

Field emission-scanning electron microscope-energy dispersive spectrometry (FE-SEM-EDS; Merlin Compact; Zeiss, Germany) was used for morphological analysis of the PHMG particles on the PC filter sampled during humidifier operation. The filter sample was pretreated with a chromium (Cr) coating (Model K-575X; Emitech, France) or platinum (Pt) coating (Model MSC-101; JEOL, Japan) for 120 s before the FE-SEM analysis. To identify the PHMG components of the particles, phosphorus (P) was a target in the EDS analysis. The Cr coating was applied without overlapping the P analysis peak. The Pt coating could overlap with the P peak due to the resolution of the microscope, but

it had a high conductivity and the analytical efficiency was good. The Pt coating was used in the Oxy product analysis because of the high analytical efficiency.

II-3. Results

II-3-1. Characteristics of PHMG in aqueous solution

Figure Ⅱ-1 shows the PSD, summarized in terms of the relative concentration of different particle sizes in solution according to the DLS measurement of the undiluted solution of each product. This was also converted to a PSD according to the number concentration (Appendices Figure 1).

The intensity graphs, i.e., the raw DLS data, indicated a bimodal distribution. The peaks within the range of 1–10 nm for all three products were similar to those shown in Appendices figure 1. The BOC and Scunder products had their highest peaks at 4 and 3 nm within the 1–10 nm range, respectively, while the highest peak for the Oxy product occurred at 2 nm. However, the intensity graphs were broadly similar for all three products. The second-highest peaks occurred at 126 nm for the Oxy product, and at 24 and 18 nm for the BOC and Scunder products, respectively.

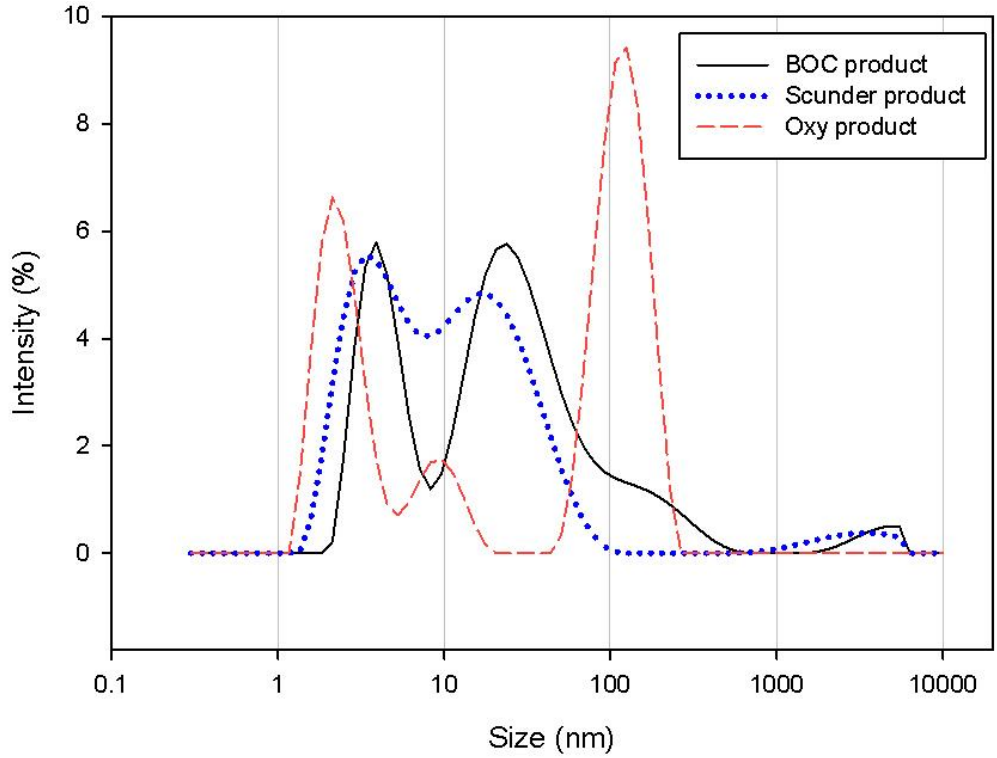

Figure II-1. The relative intensity distribution of PHMG products in aqueous solution analyzed by the dynamic light scattering (DLS).

II-3-2. Behavioral characteristics of airborne particles during and after humidifier operation

Figure Ⅱ-2 shows the GM and GSD, calculated by classifying the concentrations measured by the real-time instruments during and after humidifier operation. The detailed concentration was attached in appendices table 1. The humidifier was operated with only distilled water (i.e., 0 ppm PHMG) as a control, enabling the particle concentration attributable to distilled water in the diffusion dryer and thermodenuder to be measured as a background concentration. The total number concentration for airborne particles smaller than 420 nm, as measured by the SMPS, was about 4,000 #/cm^3, regardless of the sampling distance (i.e., 0.5 or 1 m), with more than 98% of them being nanoparticles smaller than 100 nm. In addition, the particle number concentration in the size range of 0.3–1.0 μm, as measured by the OPS, was 1 #/cm^3, and the mass concentration of the PM_1 size fraction, as measured by the PAS, was 0.19 μg/m^3. After operating the humidifier, the total particle concentration measured by the SMPS decreased to about 300 #/cm^3, with 93% of them being nanoparticles. The particle number concentration in the size range of 0.3–1.0 μm was 1 #/cm^3 and the mass concentration of PM_1 was 0.14 μg/m^3. The number concentration of particles smaller than 420 nm was decreased by an average of 93%, but there was little difference in the particle number and mass concentrations of particles larger than 0.3 μm during versus after humidifier operation.

In addition, ANCOVA analysis was performed with the covariance of the time to determine the difference in the airborne concentration by the spraying concentration in the same product, and airborne concentration was showed by spraying concentration in both during and after operation regardless of time.

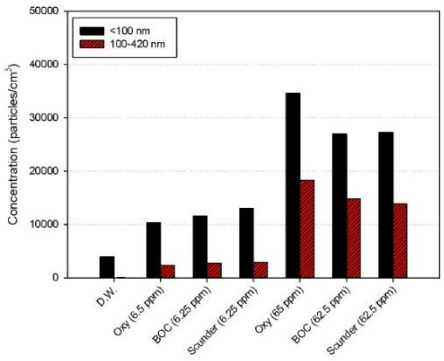

(a) During operation (SMPS 0.5 m)

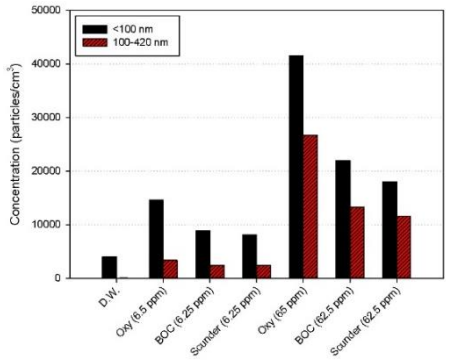

(b) During operation (SMPS 1.0 m)

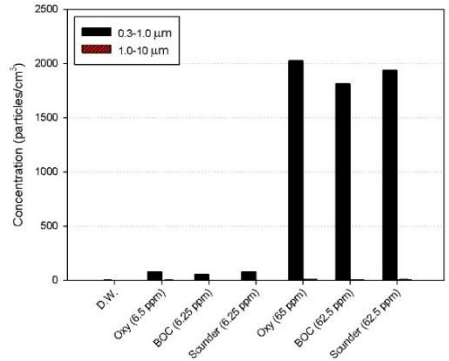

(c) During operation (OPS 0.5 m)

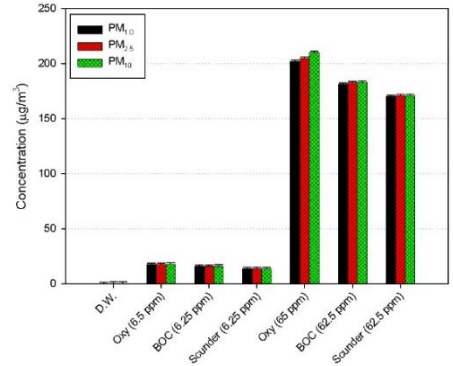

(d) During operation (PAS 0.5 m)

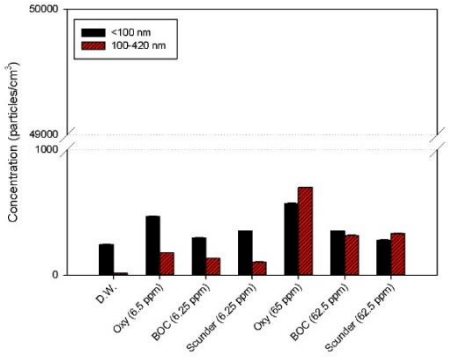

(e) After operation (SMPS 0.5 m)

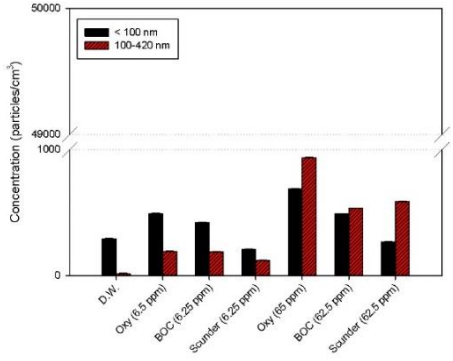

(f) After operation (SMPS 1.0 m)

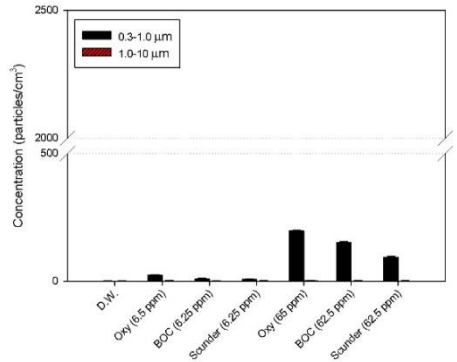

(g) After operation (OPS 0.5 m)

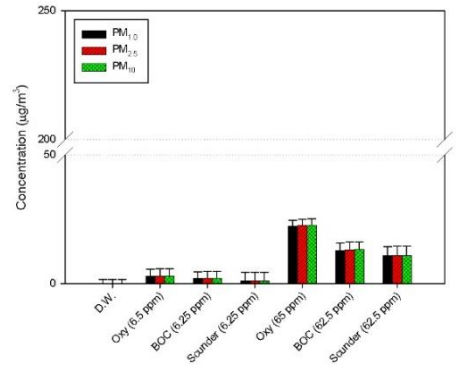

(h) After operation (PAS 0.5 m)

Figure II- 2 . Geometric mean (GM) and geometric standard deviation (GSD) of PHMG concentration measured by real-time monitoring instruments (The bonferroni correction of ANCOVA analysis was performed, and the p-value in all cases was <0.001).

To investigate the behavior of airborne PHMG particles, trends over time were assessed. Figure Ⅱ－3 is a graph showing temporal variation in the airborne concentration before, during, and after humidifier operation. Because all three PHMG products tended to display similar trends, the figures presented here show Oxy products as a representative material, while the results for BOC and Scunder products are given in Appendices figure 2. The airborne concentration increased sharply as soon as the humidifier was turned on after measuring the background concentration for 30 min. Over the 4 h period of humidifier operation, a similar concentration tended to be maintained. However, in the SMPS results, the number concentration tended to decrease slightly over the 4 h period. After the humidifier was turned off, the concentration decreased steeply, with the decrease eventually becoming more gradual.

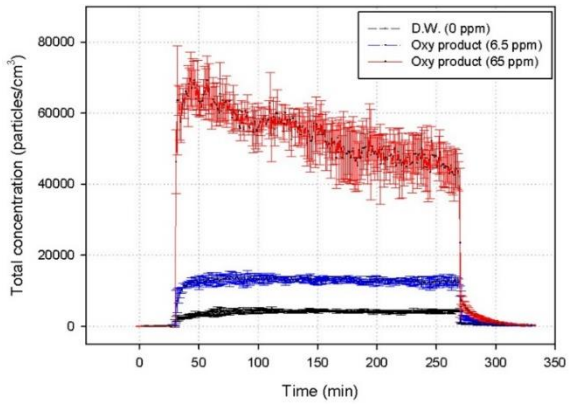

(a) The number concentration measured by SMPS (10-420 nm)

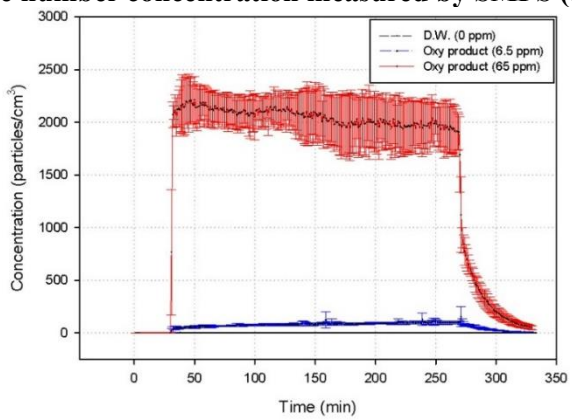

(b) The number concentration measured by OPS (0.3-1.0 μm)

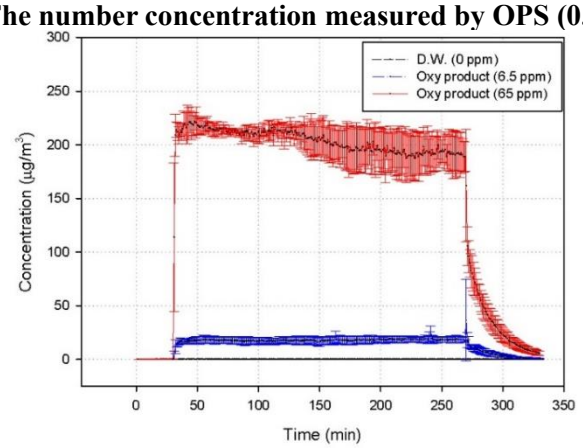

(c) The mass concentration measured by PAS (PM_1)

Figure II- 3 . Time-varying concentration in airborne at different PHMG concentration for Oxy product.

We confirmed the behavior of airborne PHMG particles during humidifier operation. As the concentration of the diluted PHMG increased 10 times from 6.5 to 65 ppm, the airborne concentrations measured by the real-time monitoring instruments were compared to determine how the airborne concentration changed.

Figure Ⅱ－2 gives the number concentrations during humidifier operation. The fraction of particles smaller than 100 nm, as measured by the SMPS, increased by about three times over the operating period for the Oxy product, and about twice for the BOC and Scunder products. The number concentration of particles in the 100–420 nm size range increased 7.9 times over the operating period for the Oxy product, 5.5 times for the BOC product, and 4.8 times for the Scunder product. The number concentration of particles in the 0.3–1.0 μm size range, as measured by the OPS, increased by about 26 times over the operating period for the Oxy product, 32 times for the BOC product, and 25 times for the Scunder product. The number concentration of particles in the 1–10 μm size range increased by about 45 times over the operating period for the Oxy product, 85 times for the BOC product, and 82 times for the Scunder product. When the PHMG was diluted 10 times, the particle number concentration increased as the particle size increased, and the mass concentration also displayed a similar increase when the PHMG was diluted.

The behavior of the PHMG particles was characterized in terms of the proportion of different size classes, and the size distribution of the particles generated during humidifier operation. Figure Ⅱ－2 shows that in terms of the particle number concentration measured by the OPS, 99% of all particles were in the size range of 0.3–1.0 μm during humidifier operation, regardless of the dilution concentration. The

proportion of particles in the PM_1 size fraction measured by the PAS was in the range of 96–99%. The number and mass concentrations of particles smaller than 10 μm were dominated by particles smaller than 1 μm.

There was little difference in the nanoparticle concentrations measured by the SMPS among the different dilution concentrations. Figure Ⅱ－4 shows: (a) the ratio of nanoparticles to total particles, and (b) the GM size of particles measured by the SMPS. The total number concentration in Figure Ⅱ－4 (a) is given for particles in the 10–420 nm size range, as measured by the SMPS. The ratio of nanoparticles to total particles was 81% at the high dilution concentration and 65% at the low dilution concentration. The higher the concentration, the more the ratio of nanoparticles to total particles decreased over the operating period. This was the opposite pattern to that observed in the particle size graph. Figure Ⅱ－4 (b) shows that the higher the dilution concentration, the larger the particle size. At the 6.5 ppm PHMG concentration, the average particle size was about 47 nm, while it was about 63 nm at the 65 ppm PHMG concentration.

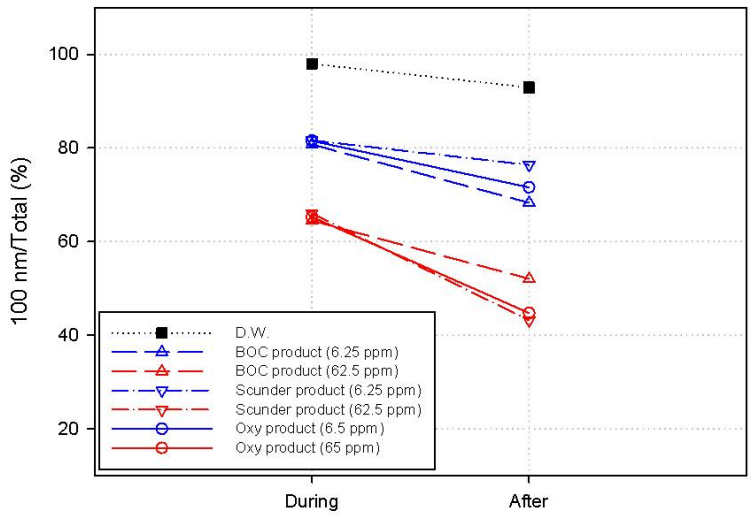

(a) The proportion of nanoparticle measured by SMPS(<100 nm / <420 nm)

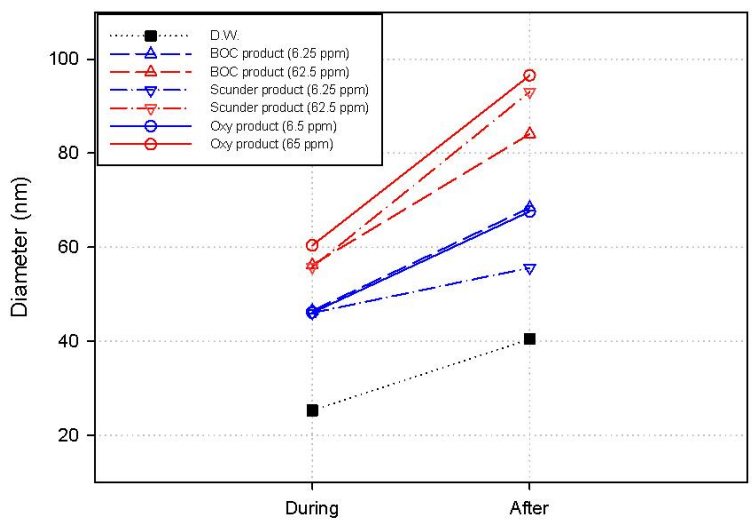

(b) The average particle diameter measured by SMPS

Figure II- 4 . Average of (a) the proportion of nanoparticle and (b) the particle diameter during and after operating humidifier.

Regarding the distribution and concentration by particle size, Figure Ⅱ－5 (a) and (b) show the PSD measured by the SMPS in the 0.5 and 1 m sampling zones during humidifier operation, respectively. As shown in Figure Ⅱ－5 (a), the highest peak in the PSD occurred at 86.6 nm for the low dilution concentration, and at 115.5 nm for the high dilution concentration. There was a second peak at 15.4 nm for both dilution concentrations. There was little difference in the PSD between the three products at the low dilution concentration, but the peak concentration for the Oxy product at a particle size of 115.5 nm was more than 2,000 #/cm^3 higher than the peak concentrations for the other products at the high dilution concentration.

At both dilution concentrations (Figure Ⅱ－5 (b)), the PSD in the 1 m sampling zone was similar to that at 0.5 m; however, the peak concentration at a particle size of 115.5 nm for the Oxy product was about twice that of the other products. Therefore, there was no significant difference in the PSD among the three products at the same dilution concentration, but there was a slight difference in the size distribution between the different dilution concentrations depending on the sampling distance. A bimodal distribution was observed regardless of the PHMG concentration and sampling distance, but this distribution was more clearly observed at the high dilution concentration.

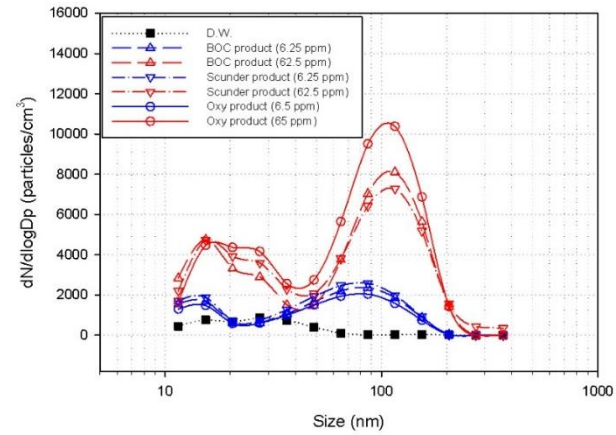

(a) During humidifier operation (0.5 m)

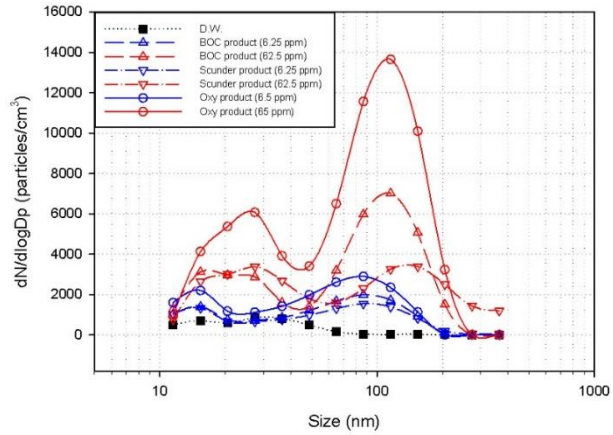

(b) During humidifier operation (1 m)

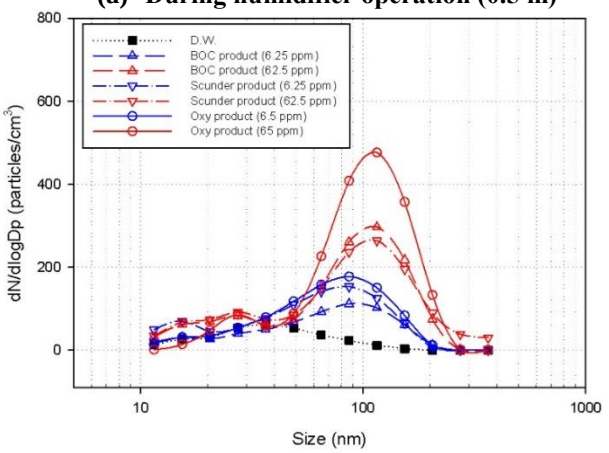

(c) After humidifier operation (0.5 m)

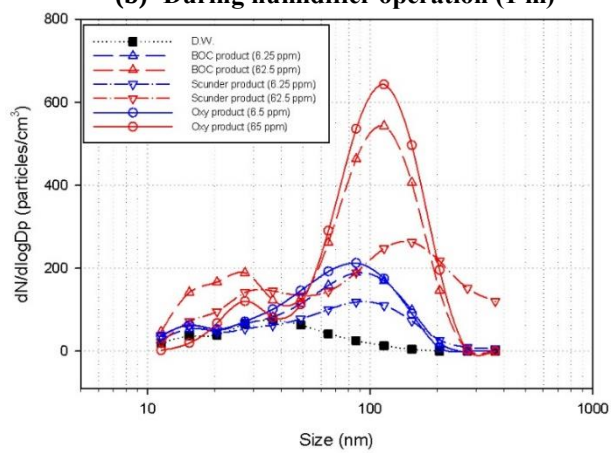

(d) After humidifier operation (1 m)

Figure II-5. Particle size distribution (PSD) at a different distance during and after humidifier operation measured by SMPS.

We examined the behavior of airborne particles after operating the humidifier. The average concentration measured at 1 h after operating the humidifier was different depending on the dilution concentration. Figure Ⅱ－2 shows that after operating the humidifier, as the dilution concentration was increased 10 times, the particle number concentration was increased 0.8–1.2 times for nanoparticles, 2.4–3.9 times for the 100–420 nm particle size range, 8.3–15.2 times for the 0.3–1.0 μm particle size range, and 44.7–114.0 times for the 1–10 μm particle size range. In terms of the mass concentration, the PM_1 fraction increased 6.2–10.5 times. However, the proportion of PM_1 among all particle sizes (> 97%), and the proportion of particles below 1 μm in the total number concentration (99%), was similar to that during humidifier operation.

Regarding the concentration of airborne residual PHMG particles after operating the humidifier, figure Ⅱ－6 shows the measurements made after 1 h of humidifier operation, including the exponential regression graph obtained via the nonlinear regression analysis. The figure only shows data for the Oxy products, with the data for BOC and Scunder products shown in Appendices figure 3.

The time required to reach the average background concentration before operating the humidifier was calculated using a regression equation. The average background concentration was measured during a 30 min period before operating the humidifier for all products, and the concentrations obtained were 58.55 #/cm^3 for nanoparticles measured by the SMPS, 0.34 #/cm^3 for particles smaller than 1 μm measured by the OPS, and 0.13 μg/m^3 for the PM_1 fraction measured by the PAS.

According to the SMPS measurements (Figure Ⅱ－6 (a)), the time to reach the background concentration for the Oxy product was about 93 min at 6.5 ppm and about 92 min at 65 ppm (BOC product: about 77 min at 6.25 ppm and about 76 min at 62.5 ppm, Scunder product: about 82 min at 6.25 ppm and about 73 min at 62.5 ppm). According to the OPS measurements (Figure Ⅱ－6 (b)), the time taken to decrease the concentration of particles below 1 μm to the background concentration for the Oxy product was 114 min at 6.5 ppm and 159 min at 65 ppm (BOC product: about 92 min at 6.25 ppm and about 140 min at 62.5 ppm, Scunder product: about 80 min at 6.25 ppm and about 109 min at 62.5 ppm). According to the PAS measurements (Figure Ⅱ－6 (c)), the time taken for the PM_1 fraction to reach the background concentration for the Oxy product was about 95 min at 6.5 ppm and 139 min at 65 ppm (BOC product: about 82 min at 6.25 ppm and about 106 min at 62.5 ppm, Scunder product: about 82 min at 6.25 ppm and about 99 min at 62.5 ppm).

Figure Ⅱ－5 (c) and (d) show the PSD in the 0.5 and 1 m sampling zones, respectively, as measured by the SMPS after operating the humidifier. The highest peak for all three products at 6.5 ppm occurred at 86.6 nm, while the highest peak at 65 ppm was at 115.5 nm. The PSD and concentration after operating the humidifier in the 1 m sampling zone (Figure Ⅱ－5 (d)) were similar to that at 0.5 m (Figure Ⅱ－5. (c)). The PSD after operating the humidifier did not have a prominent peak at 15.4 nm.

Figure Ⅱ－4 (a) also shows that compared to during humidifier operation, the proportion of nanoparticles after humidifier operation decreased from 81% to 72% at the

low dilution concentration, and from 65% to 47% at the high dilution concentration. The average particle size after humidifier operation increased from 46 to 64 nm at the low dilution concentration, and from 58 to 91 nm at the high dilution concentration (Figure Ⅱ－4 (b)).

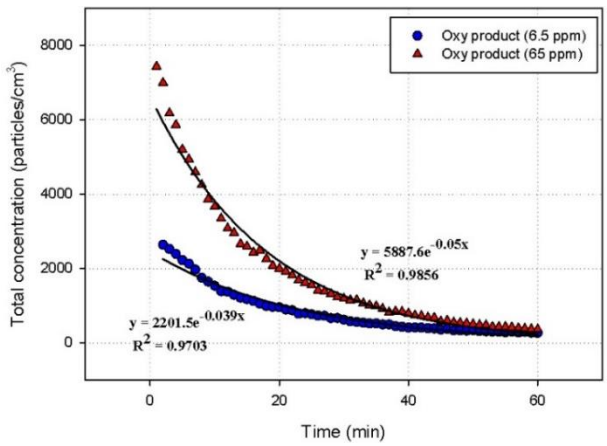

(a) The number concentration measured by SMPS (10-420 nm)

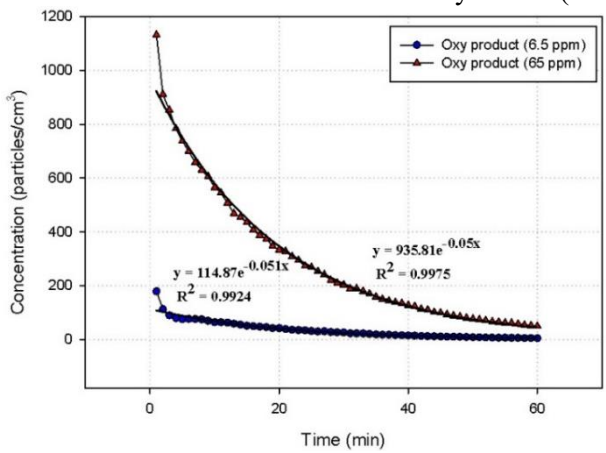

(b) The number concentration measured by OPS (0.3-1.0 μm)

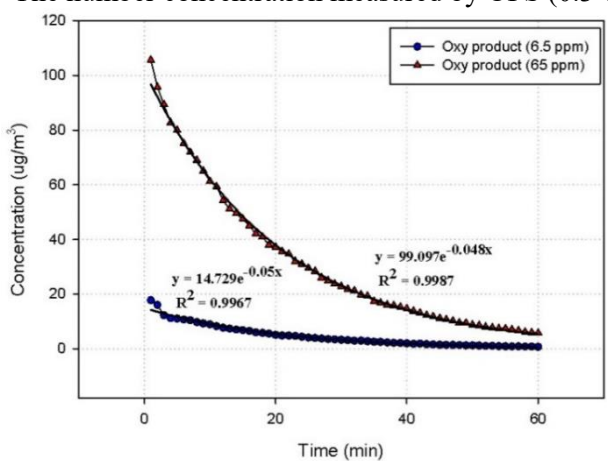

(c) The mass concentration measured by PAS (PM1.0)

Figure II-6. Time-varying concentration including exponential regression curve after humidifier operation for Oxy product.

II-3-3. Field emission-scanning electron microscope-energy dispersive spectrometry analysis

Figure Ⅱ-7 shows FE-SEM images of samples classified by PHMG material and dilution concentration. In the case of the Oxy product, more aggregated particles were found at the higher dilution concentration than at the low dilution concentration, while the particle sizes of the BOC and Scunder products showed no significant differences between the two dilution concentrations. Some particles were also collected from the inside of the pores of the filter. Most particles were not present as single particles, with small particles being present in an aggregated form. These particles were also analyzed by EDS and were considered to contain PHMG, because phosphate was detected at levels between 0.1% and 0.42% (Appendices figure 5). The average single particle size was about 20 nm or more for all three samples, while the agglomerated particle size was 150–400 nm for the BOC and Scunder products, and 200-600 nm for the Oxy product.

For the Oxy product sample collected in the 1 m sampling zone (Appendices figure 4), the maximum size of the agglomerated particles was 860–1,200 nm for the high dilution concentration sample.

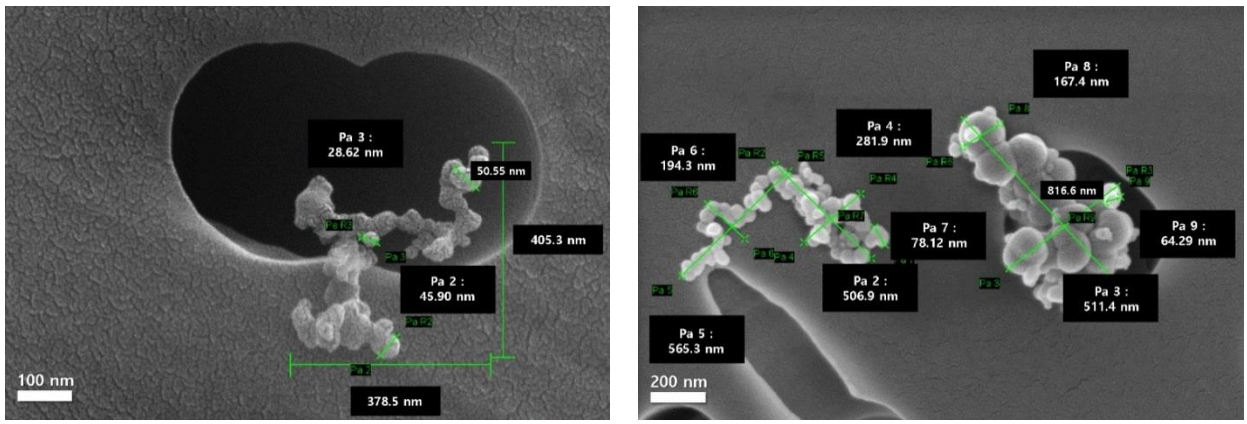

(a) Oxy product (left : 6.5 ppm, right : 65 ppm)

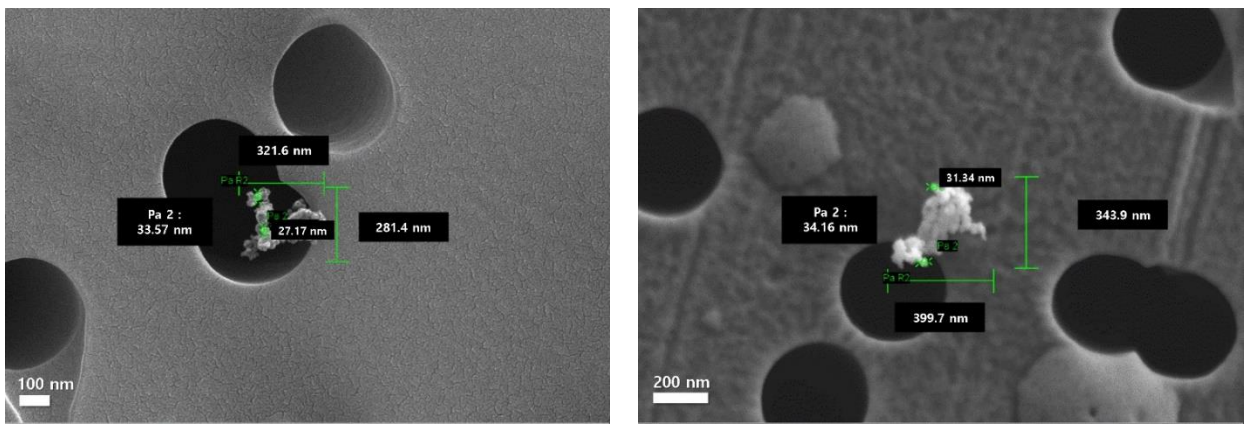

(b) BOC product (left : 6.25 ppm, right : 62.5 ppm)

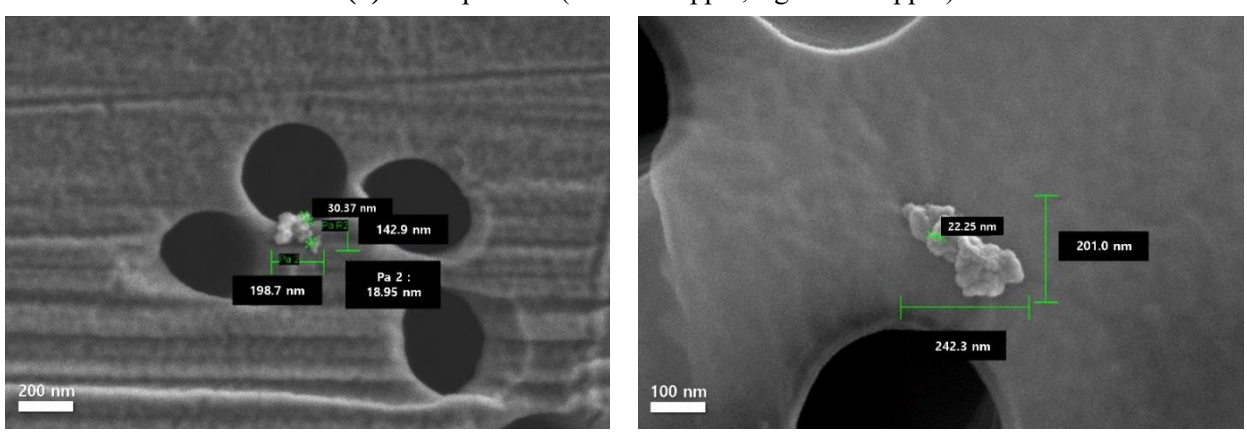

(c) Scunder product (left : 6.25 ppm, right : 62.5 ppm)

Figure II- 7 . FE-SEM image of samples during humidifier operation at 0.5 m.

II-4. Discussion

In this study, the characteristics of PHMG in aqueous solution were identified, and the behavior of airborne PHMG particles was confirmed. The study compared three different products containing PHMG, which was the main causative agent in the extremely high incidence of humidifier lung disease in Korea (Hong et al., 2014; Kim et al., 2014). The Oxy product was the main causative agent, but some other products containing PHMG were also used as a humidifier disinfectant. However, PHMG solution, including humidifier disinfectant products containing PHMG, was difficult to sell and purchase legally in Korea after the incident. We therefore conducted experiments to investigate the behavior of particles generated from PHMG products using PHMG raw material solutions currently on sale in other countries.

The distribution of PHMG in aqueous solution was measured by DLS. The raw DLS data, expressed as an intensity distribution, were similar between the BOC and Scunder products, whereas there was a difference in the distribution for the Oxy product, for which a multimodal distribution was observed. However, the particle number size distribution was monomodal in all three PHMG products. The intensity determined using the Rayleigh approximation was proportional to the sixth power of the particle diameter. This was because scattered light intensity is dependent on particle size, and the intensity could then be converted to a number size distribution. According to previous studies, DLS tends to be inherently sensitive to large particles (Anderson et al., 2013; Elizalde et

al., 2000; Mahl et al., 2011; Souza et al., 2016). The particles constituting the solution had a multimodal distribution (within a range of approximately 100 nm) in terms of the intensity distribution, but it was estimated that most particles were in the 1–10 nm size range.

The three solutions could not be diluted and analyzed because of the measurement limitations of DLS (Xu, 2015), i.e., it was presumed that there was a difference in the multimodal distribution of intensity due to the differences in PHMG concentration. In the BOC and Scunder products, except for the 25% PHMG content and the residue (ash, hexamethylenediamine, and guanidine hydrochloride were present in the Scunder product at about 0.5%), the remainder of the product was mostly water. However, for the Oxy product, the components present in the actual product were not known (only information about the PHMG content was available). Most of the product, except for the 0.1% PHMG content and some lavender flavoring, was inferred to be water.

The PHMG PSD measured by DLS in aqueous solution (Figure Ⅱ－1) and the airborne PSD measured by SMPS (Figure Ⅱ－5) were compared. However, it was difficult to directly compare the two size distributions due to the differences in measuring principle among instruments, but it was possible to determine the size distributions based on the measurements.

Although there was no peak in the PSD at about 100 nm in aqueous solution, there was a peak at 115.5 nm in the airborne particles. The bimodal PSD of all three products in aqueous solution was slightly shifted to the right, similar to the airborne distribution. For

the Oxy product, it was considered that the concentration of 115.5 nm particles compared to the other products was higher because this product had a peak at 126 nm in the size distribution in aqueous solution. The FE-SEM analysis results also confirmed that more aggregated particles were produced using the Oxy product compared to the other products.

It was inferred that the particle size increased as the particles in aqueous solution became airborne, because the nanoparticles had a tendency to agglomerate (Buseck and Adachi, 2008; Ham et al., 2015). In addition, the size distribution graph after operating the humidifier (Figs. 5 (c) and (d)) indicated that the peak at 15.4 nm almost disappeared and the bimodal distribution weakened. As a result, it was assumed that the size of PHMG particles generated when the humidifier was operated was about 100 nm, but most of the particles remaining after humidifier operation were agglomerated and then settled under gravity, with only a few nanoparticles remaining airborne.

Distilled water was used to dilute the PHMG. In the control group, only distilled water was sprayed. In this study, when the humidifier was operated with only distilled water (i.e., no PHMG) the nanoparticle number concentration was about 4,000 #/cm^3, the number concentration of particles in the 0.3–1 μm size range was 1 #/cm^3, and the PM_1 concentration was 0.19 μg/m^3.

The concentration of distilled water droplets measured after combining the diffusion dryer and the thermodenuder was close to zero in the case of OPS and PAS; however, the concentration measured by the SMPS was about 4,000 #/cm^3. In our previous study, the dehumidifier efficiency of the diffusion dryer and the thermodenuder was about 76% for

nanoparticles, 86% for the 0.3–1 μm size range, and 98% for the 1.0–10 μm size range. In other studies, the number concentration of airborne distilled water droplets in the range of 10 nm to 10 μm was measured using ultrasonic atomization without a diffusion dryer or thermodenuder. A bimodal distribution was observed, including a peak at 1.0–10.0 μm (Kudo et al., 2017). The 100 nm to 230 μm PSD measured by a Spraytec was also reported to have a bimodal distribution (Wang et al., 2008). In this study, about 24% of the nanoparticles were distilled water droplets that were not removed by the dehumidifier, and almost all of the relatively large (≥ 300 nm) particles were eliminated by the combination of a diffusion dryer and thermodenuder.

However, the concentration of Oxy product particles measured by the SMPS was three times higher at 6.5 ppm, and 13 times higher at 65 ppm, then the concentration of distilled water droplets. Therefore, the concentration of distilled water droplets would not have a significant effect on the concentration of diluted PHMG particles. It was considered that the distilled water used in the experiment could contain various nano-sized residues from the original tap water, because the pore size of the HEPA filter used in the distilled water instrument was 0.3 μm. Most particles larger than 0.3 μm were removed by filtration, but some nanoparticles may have remained in the distilled water.

As shown in figure Ⅱ－3, during humidifier operation, the concentration measured by the SMPS gradually decreased at the high dilution concentration, with all three products displaying the same trend (appendices figure 2), whereas for the concentrations measured by the OPS in the 0.3–10.0 μm range there was no fluctuation. In addition, we found no fluctuation in the mass concentration of small particles (figure Ⅱ－3 (c)).

As shown in figure Ⅱ－4 (a), the proportion of nanoparticles measured by the SMPS in this study was 81% at the low dilution concentration and 65% at the high dilution concentration. When the concentration was high, the probability of aggregation between airborne particles increased, as did the particle size (Hung et al., 2010). In addition, the FE-SEM results (figure Ⅱ－7 and Appendices figure 4) showed that more agglomerated particles were produced at the higher dilution concentration. As shown in the OPS measurement data in figure Ⅱ－3, particle sizes were mostly below 1.0 μm.

This experiment was conducted without ventilation or an external air inflow from before until after operating the humidifier, with the only exception being when the researcher entered the cleanroom to turn the humidifier on and off (about 30 s). In the humidifier disinfectant lung disease incident, victims rarely ventilated their rooms due to the cold and dry winter weather (Lee et al., 2012; Park et al., 2015). Therefore, these experimental conditions were similar to the environment referenced by other reports of this incident.

As shown in figure Ⅱ－6, the particle concentration 1 h after humidifier operation was higher than the background concentration before operating the humidifier. The time taken for the concentration to decrease to the average background level at the high and low dilution concentrations, as measured by the SMPS, OPS, and PAS, was at least 2 h and 40 min. The time taken for the particle concentration to decrease to background levels was longer for the Oxy product than for the BOC and Scunder products, and was faster for all three products at the high dilution concentration than at the low dilution concentration, as shown by the SMPS measurements. Due to their ability to aggregate, nanoparticle concentrations decreased at a similar rate at both dilution concentrations

(Hotze et al., 2010). It was found that particles containing PHMG may remain airborne for at least 2 h and 40 min after operating the humidifier under conditions of no ventilation. If the room was ventilated, the concentration of PHMG could decrease at a faster rate. The FE-SEM analysis indicated that particles were present at a single size of 20 nm or more, but most were aggregated, resulting in nano- to micro-sized particles. The concentration of microsized particles increased over time due to the agglomeration of PHMG particles.

Prior to the lung injury incident caused by the humidifier disinfectant, there had been some studies on the airborne particle concentration generated through the use of various humidifier solvents, and their associated health effects. For example, there have been studies on the airborne particle concentration due to minerals in tap water (Highsmith et al., 1988; Sain et al., 2018). In a previous study of PHMG, SMPS measurements of particle concentration and the size distributions of distilled water droplets, tap water droplets, and tap water with PHMG revealed that the total concentration (GM of particle size) was 5,860 #/cm^3 (86 nm), 30,400 #/cm^3 (143 nm), and 24,200 #/ cm^3 (149 nm), respectively, when the humidifier was operated at its highest level (20) (Lee and Yu, 2017). Umezawa et al. (2013) found a large difference in airborne particle concentration between tap water and distilled water. The number concentrations of distilled and tap water droplets were about 700 #/cm^3 and 50,000 #/cm^3, while their mass concentrations were < 0.01 mg/m^3 and about 0.46 mg/m^3, respectively. It was therefore difficult to isolate the characteristics of PHMG, because the effect of other particles in the tap water was not considered. As seen in the above studies, there was no significant difference in

particle concentration between tap water alone and tap water with PHMG, because the PHMG particles were dominated by the minerals and other particles in tap water.

This study had some advantages over previous studies. First, it considered the effect of moisture concentration on the airborne particle concentration when the humidifier was operated, by incorporating a diffusion dryer and thermodenuder. Thus, the experimental environment represented the optimal conditions under which to determine the behavior of PHMG particles.

Second, this experiment was conducted in a cleanroom to minimize the effect of other particles when operating the humidifier. Accordingly, the background particle concentration could be reduced to a minimum before operating the humidifier. The outside air passed through a HEPA filter into the clean room, minimizing the concentration of externally generated particles in the room. When obtaining real-time instruments, the standard background concentration in all experiments was set to 100 #/cm^3 for the SMPS, regardless of sampling distance, and the total particle concentration in the 0.3–10 μm size range measured by OPS was less than 1 #/cm^3. The PM_1, $PM_{2.5}$, and PM_{10} mass concentration were 0.3 μg/m^3 or less.

Finally, PHMG products manufactured in different countries were used in this experiment. Previous studies have typically used one product, or only PHMG manufactured in Korea. Because we used PHMG products manufactured in different countries in this study, the behavior of various humidifier disinfectant products containing PHMG could be inferred. The different PHMG products produced a similar airborne PSD and concentration even though the manufacturers differed.

However, this study also had some limitations. The first concerned the limit of detection of the measurement instruments. The SMPS, OPS, and PAS are commercially available real-time instruments that can measure particle sizes above 10 nm, while a DLS can detect particles in the range of 0.1–10,000 nm. Although particle sizes below 10 nm in aqueous solution and airborne particle samples could therefore not be assessed (Fissan et al., 2014), the intensity in aqueous solution was mostly around 100 nm. As the particles in aqueous solution were released to the atmosphere, the FE-SEM analysis of airborne particles confirmed that the aggregated particle size was larger than 20 nm. Therefore, because the particles in aqueous solution agglomerated once they were airborne, this limitation of particle size measurement would likely have little effect on the results.

A second limitation was the pore size of the PC filter used in the FE-SEM analysis. It may have been possible for smaller particles to pass through the filter pores during sampling because, in some samples, small particles were deposited on the walls of the pores, as shown in Fig 7 (c). We used FE-SEM to measure particle size and detect P as a target element, rather than quantify the concentration of PHMG aerosol. We found that in addition to agglomerated particles, single particles were also present in airborne samples, as shown in appendices figure Ⅱ－2 (a).

II-5. Conclusions

The PSD in the aqueous solution (DLS intensity) and airborne samples had a bimodal distribution, which was slightly right-shifted in the region near 100 nm. The particles analyzed by FE-SEM were mostly aggregated, and the single particle size was also about 20 nm.

When the PHMG input concentration increased, the airborne particle concentration generated during humidifier operation increased as the particle size increased. However, most of the particles contributing to the mass concentration of PHMG were smaller than 1 μm, and the PM_1 concentration was almost 99% of the PM_{10} concentration regardless of the initial PHMG concentration. In addition, without ventilation, the PHMG particles could remain airborne even after operating the humidifier at the concentration recommended by the manufacturer, with a period of about 2 h required to reach the background concentration.

Although the three PHMG products were manufactured in different countries, we found that the behavior of airborne particles was mostly affected by the input concentration of PHMG rather than differences due to the manufacturer of the product. The results of our study are likely to be representative of the concentrations and behavioral characteristics of particles produced through the use of various PHMG products.

Therefore, inhalation exposure to substances for which the toxicological information is unknown, such as humidifier disinfectants, may continue in our daily lives. Although it is

important to know the toxicity of a substance, it is also important to know airborne behavior including the size, shape, residual time, moving distance of its components to prevent adverse health effects in terms of the precautionary principle.

There were many policy changes in Korea after the incident. The toxicity assessment policy for consumer products has been strengthened and a new law on biocidal products was enacted, the ‘Safety Control Act of Household Chemical Products and Biocidal Products (K-BPR)’. In this context, this study provides basic data for assessing consumer products while considering exposure route because of the increasing interest in exposure to consumer products in Korea.

This paper was published in Environmental research.

CHAPTER III.

Characterization of Polyhexamethyleneguanidine (PHMG) oligomers in solutions and aerosols emitted during humidifier use

III-1. Introduction

The negatively charged surface of bacterial cells is stabilized by the cations Mg^{2+} and Ca^{2+}. Oligoguanidines, used as disinfectants, displace Mg^{2+} and Ca^{2+} and result in bacterial death, caused by cellular leakage and loss of essential cellular components (Buchberger et al.; Gilbert and Moore, 2005; Wei et al., 2009). Therefore, guanidine-based chemicals are widely used as biocides; polyhexamethylene guanidine phosphate (PHMG-P; CAS No. 89697-78-9) has been used in household products, such as wet wipes and cleaning supplies, due to its strong bacteriostatic action and relatively low toxicity (Aleshina et al., 2001; Mashat, 2016; Song et al., 2014).

Humidifier disinfectant products containing PHMG were widely used to prevent microbial contamination due to microbial growth in the ultrasonic humidifier reservoir (Alvarez-Fernández et al., 1998; Shiue et al., 1990) from 1994 to 2011 in Korea (Park et al., 2018). However, the inhalation of aerosols containing humidifier disinfectants has resulted in an outbreak of severe lung injury. Consumer products containing the disinfectant PHMG were sold the most, accounting for the overwhelming majority of the fatalities, and the sale of PHMG was prohibited by the Korean government.

Several studies on the epidemiology, toxicology, and analysis of the guanidine-based chemicals have been conducted. However, only a few studies have analyzed airborne PHMG; most have analyzed PHMG raw materials. PHMG is a polymer containing various

oligomers, and thorough chemical characterization remains challenging due to the presence of complex PHMG oligomer mixtures with different structures (Buchberger et al.).

PHMG polymers are mainly analyzed by matrix-assisted laser desorption/ionization-time of flight-mass spectrometry (MALDI-TOF-MS), high performance liquid chromatography (HPLC), and liquid chromatography-mass spectrometry (LC-MS) (Bae et al., 2019; Choi et al., 2016; Yang et al., 2013). However, since there is no oligomer standard solution for each subtype, previous studies have focused on identifying various oligomers in the stock solution of PHMG. Despite the epidemiological investigation of the health effects of PHMG-containing humidifier disinfectants and the analysis of PHMG concentration in products and aerosols, different subtypes of PHMG in solution and aerosols have not been identified.

In this study, liquid chromatography-time of flight-mass spectrometry (LC-qToF-MS) was used for more accurate measurements of the mass value of the parent molecular ions, which is typically analyzed by LC/MS, and determine the exact mass value of the fragment ions. In addition, the development of software programs has made it possible to accurately identify targeted materials, and the analysis data were processed to improve the accuracy of PHMG oligomer classification. The aim of this study was to identify the different PHMG oligomer types and content in products and aerosols and estimate the airborne concentration of oligomers during humidifier use.

III-2. Materials and Methods

III-2-1.Materials

Table Ⅲ-1 provides details of the PHMG materials used in this experiment. The experiment was conducted with two PHMG solutions and one product containing PHMG. The product was Oxy product which contains approximately 0.1% PHMG and a lavender aroma (brand name oxysaksak, Oxy, Korea). One of the PHMG solutions contained approximately 20–25% PHMG (BOC, USA) and the other contained approximately 25% PHMG (Scunder, China). Among the products containing PHMG, oxy products were selected because many patients with lung injury occurred among users who used oxy products.

Because there was no legal requirement to produce a safety data sheet (SDS) for the Oxy product at the time of the sale, no specific safety information was available. However, the ingredient listed in Table Ⅲ－1 is the information of PHMG raw materials contained in the product because data on the raw materials were provided by a report submitted to the government for product approval.

The oligomer peaks were identified using an internal standard (FC-8302, FUTURECHEM, Korea). The guanidine carbon in the internal standard was replaced by the carbon isotope of mass 13. A 10-ppm internal standard solution was added to all

oligomer standards, and each oligomer solution had a retention time within about 0.5 min of the time at which the internal standard was detected.

Table III-1. Information on PHMG products used for this experiment

No.	Name	Ingredient by SDS	CAS No.	Content* (%)	Approximated concentration (%)	Dilution ratio	Nominal Diluted concentration (ppm)	Company (Manufactured country)
1	Oxy Product	Polyhexamethyleneguanidine Phosphate	89697-78-9	95	1300 ppm** (0.1%)	200:1***	6.50	Oxy (Korea)
		Hexamethylenediamine	124-09-4	1				
		Sodium Chloride	7647-14-5	4		20:1	65.00	
2	BOC product	Polyhexamethyleneguanidine Phosphate	89697-78-9	20-25	250,000 ppm (25%)	40,000:1	6.25	BOC (USA)
						4,000:1	62.50	
		Water	7732-18-5	75-80		2,000:1	125	
3	Scunder product	Polyhexamethyleneguanidine Phosphate	89697-78-9	25		40,000:1	6.25	Scunder (China)
		Water	7732-18-5	74.5				
		Ash content	-	0.5	250,000 ppm (25%)	4,000:1	62.50	
		Hexamethylenediamine	124-09-4	N.D.				
		Guanidine hydrochloride	50-01-1	N.D.		2,000:1	125	

* This content was indicated by SDS.

** Oxy product was only indicated for information on the ingredients for raw materials of PHMG used in product.

*** 200:1 was labelled on the product surface as recommended dilution ratio by Oxy manufactured company.

III-2-2.Sampling of airborne PHMG

III-2-2-1. Cleanroom set up

All experiments were conducted in a 40.3 m^3 (7.0 m [L] × 2.4 m [W] × 2.4 m [H]) class 1,000 cleanroom fitted with a high-efficiency particulate air (HEPA) filter, enabling background particles smaller than 0.5 μm to be limited to less than 1,000 particles/ft^3. The purified air provided by the ventilation system flowed into the room via inlets on the ceiling, while the outlet air flowed out of the room through vents in the walls. The cleanroom was ventilated before turning on the humidifier, the ventilation system was turned off once starting sampling. The temperature and humidity in the cleanroom before the humidifier began operating were maintained at about 20℃ and 50%, respectively. During operation, the temperature was maintained at about 15℃, and increased to 20℃ thereafter, and humidity was maintained at 100%, and decreased to about 60% thereafter.

The ultrasonic humidifier (H-U977, Ohsung, Korea) used for the experiment had a 6.5 L tank containing the spray liquid, and had a design used commonly in household humidifiers. The humidifier could be operated at a spray output rate of approximately 320 ml/h and the spray volume was set to the maximum in this study.

III-2-2-2. Sampling

The recommended dilution for the Oxy product was 200:1, but previous studies had used dilution of up to 20:1 to simulate a “worst-case scenario”. The Oxy product concentrations investigated in previous studies were slightly different among the products investigated, but were about 1,300 ppm on average. As shown in Table Ⅲ－1, the exact PHMG concentration in each product was unknown and there was no standard PHMG solution on the market with a known concentration. We therefore took the approximate concentration suggested by the manufacturer as the nominal maximum concentration. The concentration of Oxy product was calculated to be about 6.5 ppm at 200:1 dilution, and about 65 ppm at 20:1 dilution. The dilution factors for the BOC and Scunder products were set to produce similar concentrations. The maximum concentrations of the two solutions (A and B) were about 25% (250,000 ppm); they were diluted to about 6.25 ppm (40,000:1) and 62.5 ppm (4,000:1), respectively. In addition, it is difficult to get Oxy sample as Oxy products are no longer available for sale. Therefore, an additional experiment on 125 ppm concentration (2000:1) was conducted for BOC and Scunder products except for the Oxy product (130 ppm (10:1) based on Oxy product). Distilled water was generated by a commercial purification system (Milli-Q; Merck Millipore, Germany) and then used to dilute PHMG in all experiments.

The previous study was conducted at a flow rate of 1 L/min based on NIOSH 5521 (Lee and Yu, 2017). However, due to the low concentration of airborne PHMG, in this study,

we used a 30 mL impinger equipped with a pump (GilAir; Sensidyne, USA) and operated at 2 L/min. Ten milliliters of distilled water (Milli-Q; Merck Millipore, Germany) was used in the impinger as an adsorbing liquid. The sampling zone was set to 0.5 m and 1 m, and samples were collected three times while the humidifier was running over the course of 8 h.

To determine the loss of the impinger, the humidifier was operated at 125 ppm, the highest Scunder and BOC concentration, and the same impinger was analyzed in series at 0.5 m. A total of six samples were analyzed and the measurements were repeated three times for each product; not all samples were detected in the third impinger. Therefore, the recovery was determined using the intensity detected in the first impinger compared to the sum of the intensities detected in the first and second impingers. Based on the average of the ratios of all the oligomers, 84% were used to estimate the concentration in air. The LOD of each oligomer was measured seven times at the concentration of about 10 ppm and calculated as three times the standard deviation.

III-2-3.Analysis of PHMG

III-2-3-1. Conditions of LC-qToF

The conditions for LC/MS analysis are shown in Table Ⅲ－2. The Waters ACQUITY UPLC I-Class TUV system and Masslynx ver. 4.1 software were used. Chromatographic separation was performed on an ACQUITY UPLC BEH C18 2.1 × 100 mm (1.7 μm) column (Waters, USA), and the column temperature was set at 40℃. The total run time was 15 min, and the sample injection volume was 10 μL. All chemicals were of HPLC grade and ≥ 99.9% pure. A binary mobile phase system composed of 0.1% trifluoroacetic acid (Lot No. STBF4960V, Sigma-Aldrich, USA) in distilled water (A) and 100% acetonitrile (Lot No. SHBH4463V, Sigma-Aldrich, USA) (B) at a flow rate of 0.4 mL/min was used. The gradient elution program was the following: 0–1 min, 95% (A); 1–10 min, 95–80% (A); 10–13 min, 80% (A); 13–13.5 min, 80–95% (A); 13.5–15 min, 95% (A). The temperature of all samples was maintained at 10℃.

A SYNAPT G2-Si HDMS mass spectrometry system was used in electrospray ionization (ESI) and positive ion modes (+H). The ESI parameters were set as follows: capillary voltage, 3 kV; cone voltage, 30 V; source temperature, 120℃; desolvation temperature, 300℃; desolvation gas flow rate, 800 L/h. The mass analyzer scanned over a mass range of 100–1500 Da in a full scan. Data were acquired in continuum mode. Dual-dynamic collision energy was 25–45 V.

Five standard (STD) solutions of PHMG in three products (Oxy, Scunder, and BOC) were prepared at the concentration of 1, 5, 10, 50, and 100 ppm separately.

Table III- 2 . LC-qToF analysis conditions (mass and UPLC conditions)

UPLC Conditions			
LC System	Waters ACQUITY UPLC I-Class & TUV		
Processing Software	Masslynx		
Column	ACQUITY UPLC BEH C18 1.7um, 2.1 X 100 mm		
Column Temp	35℃		
Sample Temp	10℃		
Flow Rate	0.4 mL/min		
Mobile Phase A	0.1% Trifluoroacetic acid (TFA) in distilled water		
Mobile Phase B	100% Acetonitrile (ACN)		
Total Run Time	15 min		
Injection Volume	10 $\mu\ell$		
Gradient	Time (min)	A (%)	B (%)
	0	95	5
	1	95	5
	10	80	20
	13	80	20
	13.5	95	5
	15	95	5

Mass conditions	
MS system	SYNAPT G2-Si HDMS
Source	ESI POSITIVE
Capillary voltage(kV) :	3
Cone voltage(V)	30
Source Temp. (℃)	120
Desolvation Temperaterue (℃):	300
Desolvation gas rate(L/Hr):	800
Acquisition mode	MSe
Mass Range (Da)	100~1,500

III-2-3-2. Data processing using Unifi

Post-acquisition data processing was performed using Unifi software (v.1.8.2, Waters, USA). This program takes into consideration the estimated peak intensity, molecular weight, and molecular structure of the sample and presents the information in the form of a Molfile.

Previous studies have shown that there are a total of seven types of PHMG oligomers: linear structures (types A–C) and cyclic and branched structures (type D–G) (figure Ⅲ－1). Therefore, polymers with various molecular structures and mass are present in the same PHMG sample. Table Ⅲ－3 shows the mass for each polymer type and the monomer when the ion mode is positive (+ H). In this study, each oligomer is represented by a combination of the type and number of the monomer. For example, the dimer of type A is referred to as A2. Therefore, the intensity of all oligomer types was compared to the Molfile containing molecular structure (figure Ⅲ－1) and mass (table Ⅲ－3) information. Each Molfile PHMG oligomer was created using Chem3D program (PerkinElmer, USA). Target match tolerance was set to 10 ppm.

For the UNIFI program analysis, we have set some criteria for locating the corresponding oligomers. Firstly, we have identified the oligomer peaks using the Masslynx program. Secondly, the oligomer peaks were detected above the background concentration. Finally,

all standards were confirmed to have similar high and low fragments, and the oligomer peaks and their intensity were identified based on standards.

Table III- 3 . Mass by oligomer type of PHMG in positive mode(+H)

The linear structures										
Type A			Type B			Type C				
A1	$C_7H_{18}N_4$	159.1610	B1	$C_{13}H_{31}N_5$	258.2658	C1	$C_8H_{20}N_6$	201.1828		
A2	$C_{14}H_{33}N_7$	300.2876	B2	$C_{20}H_{46}N_8$	399.3924	C2	$C_{15}H_{35}N_9$	342.3094		
A3	$C_{21}H_{48}N_{10}$	441.4142	B3	$C_{27}H_{61}N_{11}$	540.5190	C3	$C_{22}H_{50}N_{12}$	483.4360		
A4	$C_{28}H_{63}N_{13}$	582.5408	B4	$C_{34}H_{76}N_{14}$	681.6456	C4	$C_{29}H_{65}N_{15}$	624.5626		
A5	$C_{35}H_{78}N_{16}$	723.6674	B5	$C_{41}H_{91}N_{17}$	822.7722	C5	$C_{36}H_{80}N_{18}$	765.6892		
A6	$C_{42}H_{93}N_{19}$	864.7940	B6	$C_{48}H_{106}N_{20}$	963.8988	C6	$C_{43}H_{95}N_{21}$	906.8158		
A7	$C_{49}H_{108}N_{22}$	1005.9206	B7	$C_{55}H_{121}N_{23}$	1105.0254	C7	$C_{50}H_{110}N_{24}$	1047.9420		
The branched or cyclic structures										
Type D			Type E			Type F			Type G	
D1	$C_{26}H_{61}N_9$	498.4971	E1	$C_7H_{16}N_3$	142.1344	F1	$C_8H_{18}N_5$	184.1744	G1	$C_{20}H_{44}N_7$	382.3658
D2	$C_{33}H_{76}N_{12}$	639.6237	E2	$C_{14}H_{31}N_6$	283.2610	F2	$C_{15}H_{33}N_8$	325.3010	G2	$C_{27}H_{59}N_{10}$	523.4924
D3	$C_{40}H_{91}N_{15}$	780.7503	E3	$C_{21}H_{46}N_9$	424.3876	F3	$C_{22}H_{48}N_{11}$	466.4276	G3	$C_{34}H_{74}N_{13}$	664.6190
D4	$C_{47}H_{106}N_{18}$	921.8769	E4	$C_{28}H_{61}N_{12}$	565.5142	F4	$C_{29}H_{63}N_{14}$	607.5542	G4	$C_{41}H_{89}N_{16}$	805.7456
D5	$C_{54}H_{121}N_{21}$	1063.0035	E5	$C_{35}H_{76}N_{15}$	706.6408	F5	$C_{36}H_{78}N_{17}$	748.6808	G5	$C_{48}H_{104}N_{19}$	946.8722
D6	$C_{61}H_{136}N_{24}$	1204.1301	E6	$C_{42}H_{91}N_{18}$	847.7674	F6	$C_{43}H_{93}N_{20}$	889.8074	G6	$C_{55}H_{119}N_{21}$	1087.9988
D7	$C_{68}H_{151}N_{27}$	1345.2567	E7	$C_{49}H_{106}N_{21}$	988.8940	F7	$C_{50}H_{108}N_{23}$	1030.9340	G7	$C_{62}H_{134}N_{24}$	1229.1254

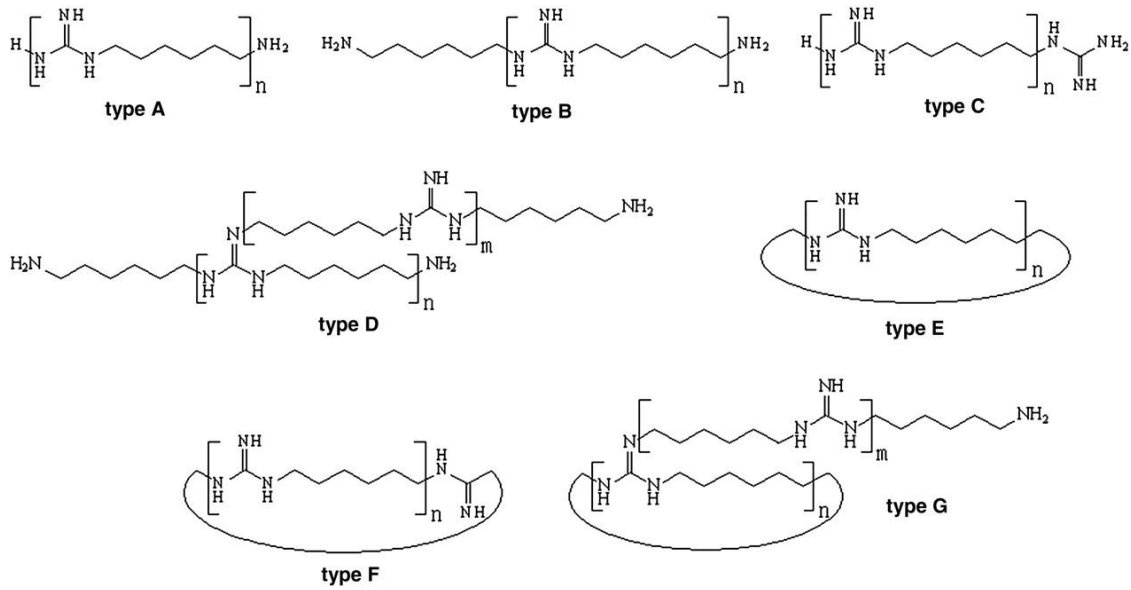

Figure III- 1 . Structures of a several of type of PHMG (referenced by study of Wei et al).

III-3. Results

III-3-1.Characteristics of raw materials in PHMG products

Figure Ⅲ－2 shows the chromatogram of the standard solution with the highest concentration (100 ppm) for each product. At the same concentration of PHMG, there was a difference in the relative intensity of the product peaks in the chromatogram: the peak height for B1 and C1 was similar for the Oxy product, but the B1 peak was barely visible for Scunder and BOC products.

The data for each product oligomer type based on the results of UNIFI analysis are shown in figure Ⅲ－3. The histogram of each oligomer depicts the peak intensity of all standard solutions. Firstly, the dimer peak of all type A and C linear products has the highest intensity. All the type B products have monomers and dimers of low molecular weights. B7 and C7 were not detected for any product concentration. For BOC products, only B1 and B2 were detected above STD 4 (50 ppm). Secondly, for the branched and cyclic structures, type D was only detected for the Oxy product as D1 (monomer) and D2 (dimer); E2 and E3 were detected as well.

For linear concentration standards, as the number of monomers increased (as the molecular weight increased), detection at low concentrations decreased. In addition, dimers had the

highest intensity except for those in B type. For the branched and cyclic structures, E2 had the highest intensity for all products. Based on the measurements for STD 5 (100 ppm), the sum of the intensities of all detected oligomers was 1,429,171 for Oxy, 992,976 for Scunder, and 768,955 for BOC.

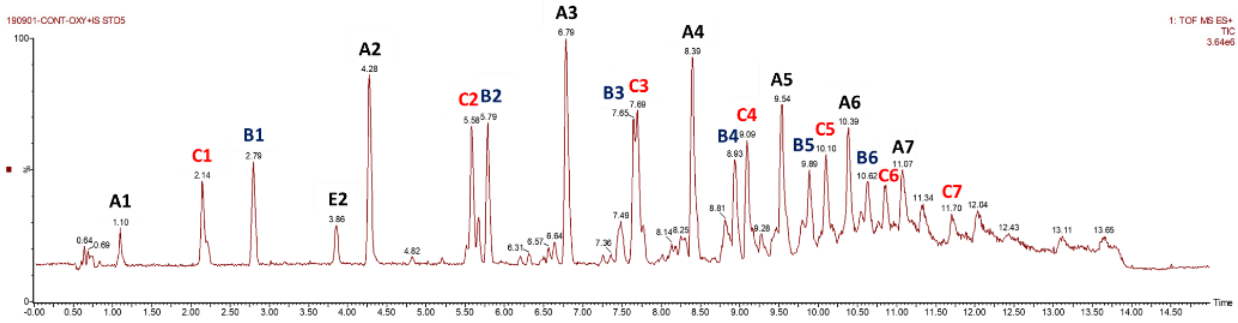

(a) Oxy product

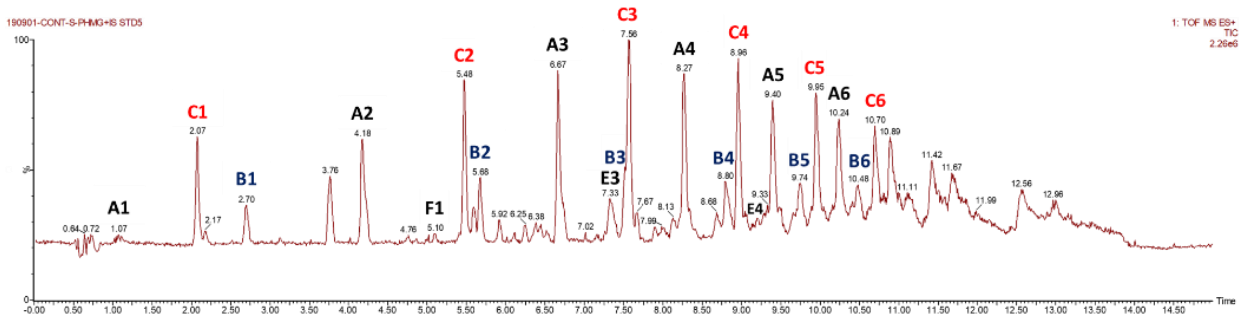

(b) Scunder product

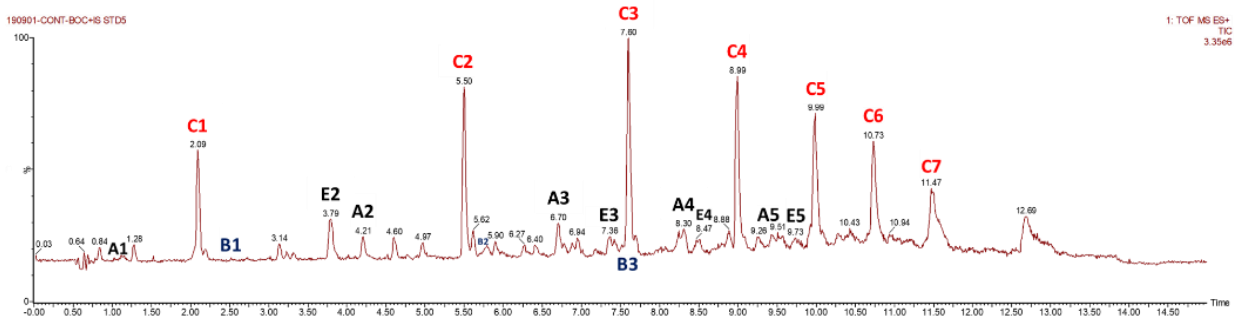

(c) BOC product

Figure III- 2 . Chromatogram of three PHMG products based on STD 5 (100 ppm).

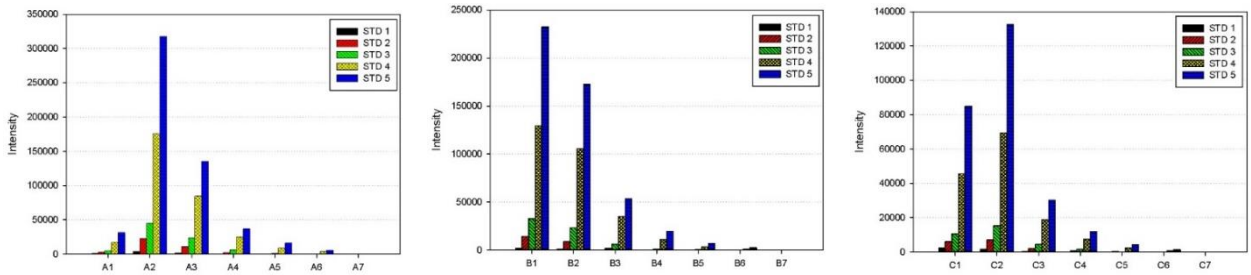

(a) Oxy product-Type A (b) Oxy product-Type B (c) Oxy product-Type C

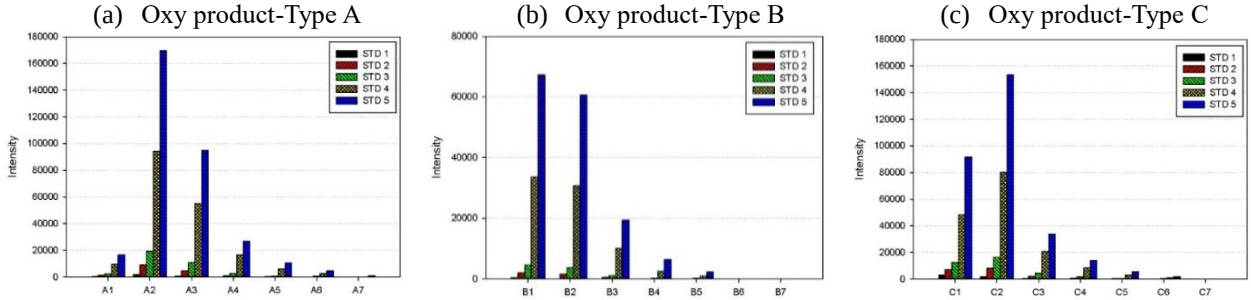

(f) Scunder product-Type A (g) Scunder product-Type B (h) Scunder product-Type C

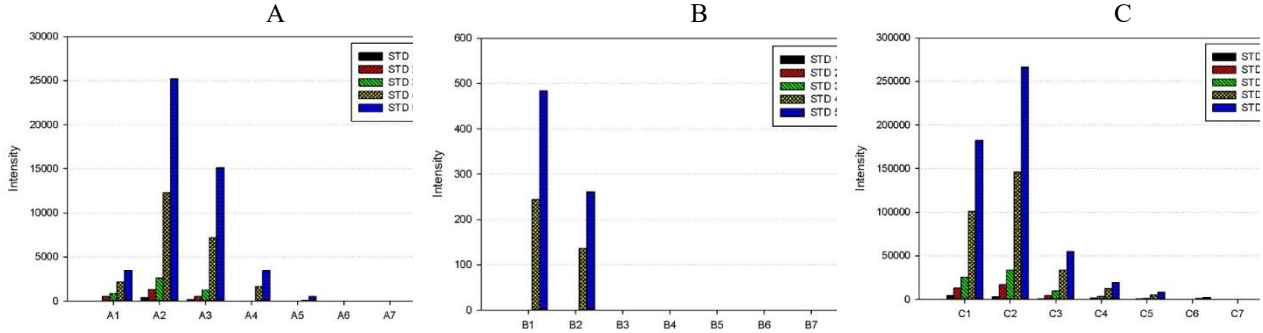

(k) BOC product-Type A (l) BOC product-Type B (m) BOC product-Type C

Figure III- 3 . Comparison on intensities of all PHMG STD.

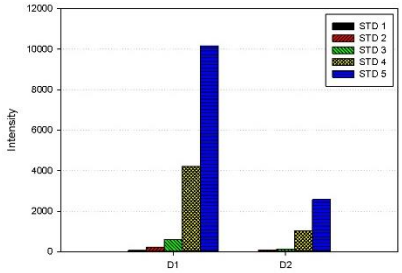

(d) Oxy product-Type D

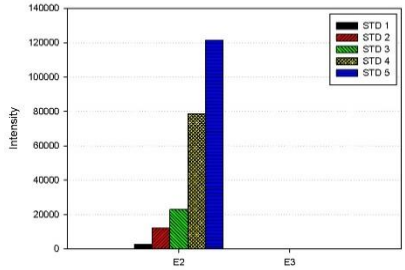

(e) Oxy product-Type E

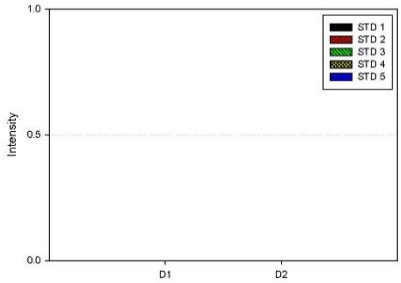

(i) Scunder product-Type D

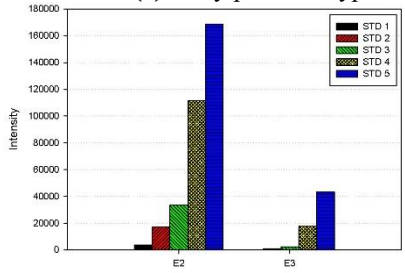

(j) Scunder product-Type E

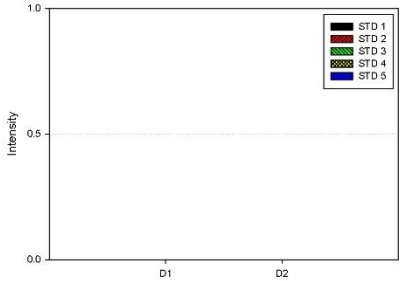

(n) BOC product-Type D

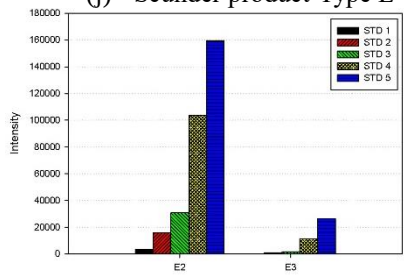

(o) BOC product-Type E

Figure III-4. Comparison on intensities of all PHMG STD (continued).

The proportion of oligomers in each type was similar in all products (figure Ⅲ－3); however, the intensity was different. The proportion of each oligomer is shown in figure Ⅲ－4 based on STD 5 (100 ppm) measurements (the sum of the intensities of all oligomers is 100%).

The comparison of the structure type proportion revealed that the linear structure of the Oxy product accounted for 90.6%, and most of the components had linear structure. On the contrary, Scunder and BOC samples contained 78.6% and 75.8% of the linear structures, respectively, and about 25% of the branched or cyclic structures.

In the Oxy product, type A (38%) was the most abundant followed by type B (34%), and the combination of types A and B accounted for 72% of the total. The Scunder product comprised 33% of type A, 30% of type C, and the combination of types A and C was about 63%. However, the most abundant components of the BOC product were type C (69%) and type E (24%), accounting for about 93% of the total.

The proportion of each oligomer was the following: A2 (22.2%), B1 (16.2%), and B2 (12.2%) for Oxy, and A2 (17.7%), E2 (17.0%), and C2 (15.4%) for Scunder. BOC contained C2 (34.6%), C1 (23.7%), and E2 (20.8%). Therefore, even the same PHMG products can have different oligomer components.

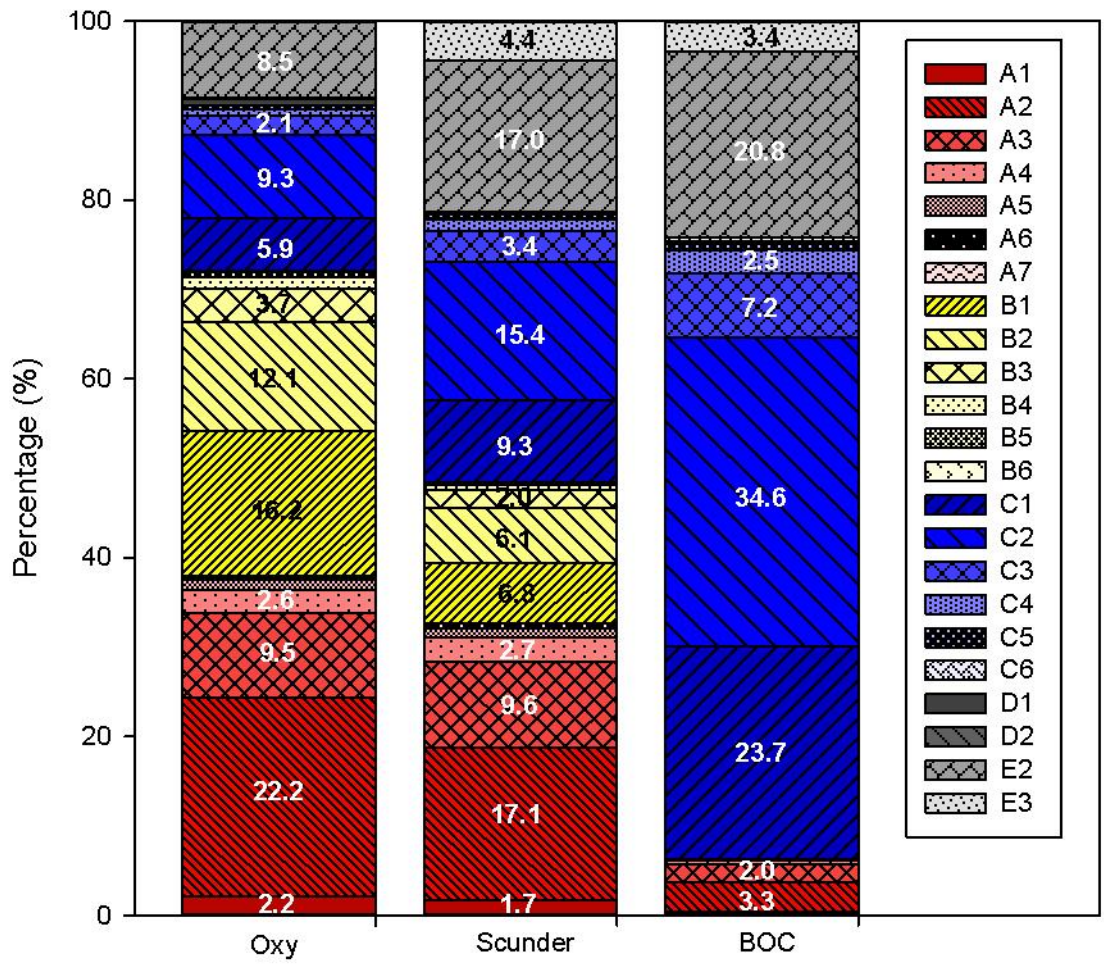

Figure III- 5 . The proportion of oligomer component in PHMG STD 5.

III-3-2.Intensity and estimated concentration of sample collected in the airborne

III-3-2-1. Intensity

Figure Ⅲ－5 shows the mean and SD of the intensity of three Oxy samples collected in the span of 8 hours. The black bar marks the 6.5 ppm PHMG concentration (200 dilutions; recommended dilution concentration), and the red bar marks 65 ppm PHMG. An additional experiment was conducted at 125 ppm of Scunder (figure Ⅲ－6) and BOC (figure Ⅲ－7), and the result of the experiment is marked by the green bar. In addition, the line graph in figure Ⅲ－5 marks to the intensity of STD 5.

In linear structures of all products, dimer was the most abundant structure in the types A and C, and monomer in the type B. However, type B was almost undetectable in the sample regardless of the distance in BOC products. The lowest concentrations (6.5 ppm and 6.25 ppm) were not detected for any oligomer types or products at 1 m. In addition, at high concentrations (65 ppm, 62.5 ppm, and 125 ppm), the low molecular weight monomers were detected the most regardless of the oligomer content in raw materials. C1 was the most pronounced.

The results of sampling at 0.5 m and 1 m are shown in Figure Ⅲ－5(g) and (f), and the

structures are branched or cyclic, type D (D1 and D2) and type E (E2 and E3) in all products. Type D was not detected in all concentrations of oxy at 1 m; however, D1 was detected in 6.5 ppm, and D1 and D2 were detected at 65 ppm. E2 had the most intensity out of all branched and cyclic structures. E2 was detected regardless of the distance at all concentrations except for the lowest concentration (6.25 ppm or 6.5 ppm) sampled at 1 m in all products.

At the lowest sample concentrations (6.5 ppm and 6.25 ppm) of the three products, C1 had the highest intensity at 0.5 m, and C1 proportion was 21.5%, 36.2%, and 54.4% for Oxy, Scunder, and BOC, respectively. For the Oxy product at 65 ppm and 0.5 m, A2 had the highest intensity (19.6%). For Scunder at 62.5 ppm and 125 ppm, E2 represented the highest proportion of the product, 21.3% and 18.3%, respectively. At 62.5 ppm and 125 ppm of BOC, C2 was detected the most (30.3% and 33.4%, respectively). Samples collected at 1 m contained the highest proportion of C1 except for Scunder at 125 ppm, which contained 43.3% of E2.

In all the three products, the overall oligomer composition was similar to that of each raw material solution at 0.5 m; however, the lowest concentration (6.5 ppm for Oxy, 6.25 ppm for Scunder and BOC) of each product was not detected for all oligomer types of at 1 m.

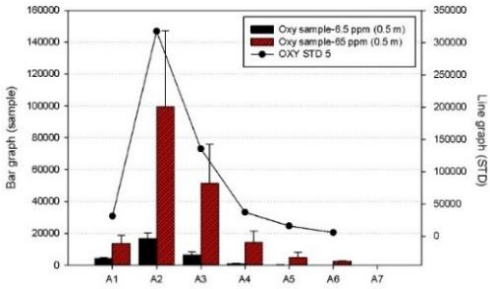

(a) Oxy product-type A (0.5 m)

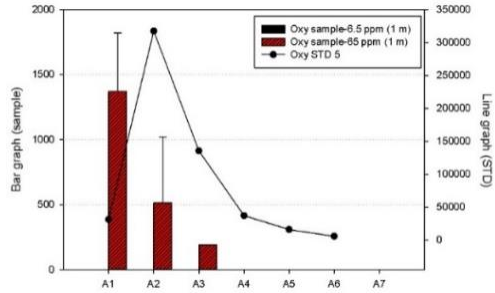

(b) Oxy product-type A (1 m)

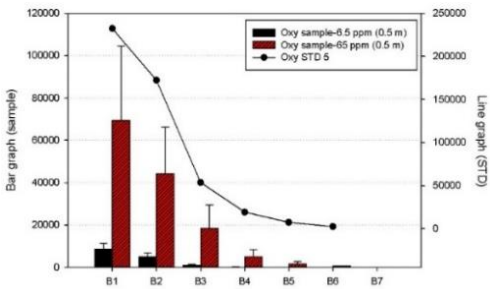

(c) Oxy product-type B (0.5 m)

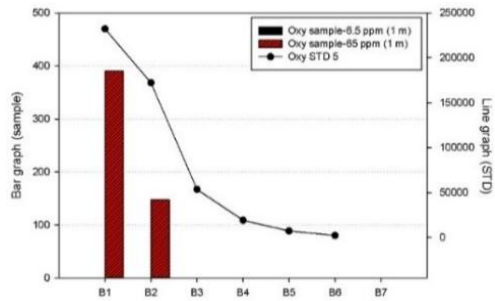

(d) Oxy product-type B (1 m)

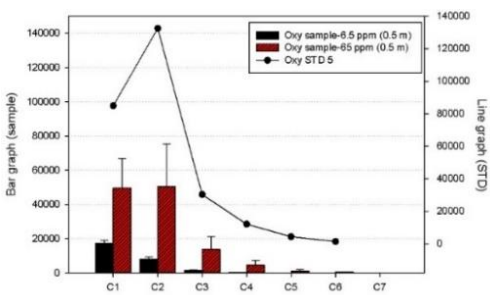

(e) Oxy product-type C (0.5 m)

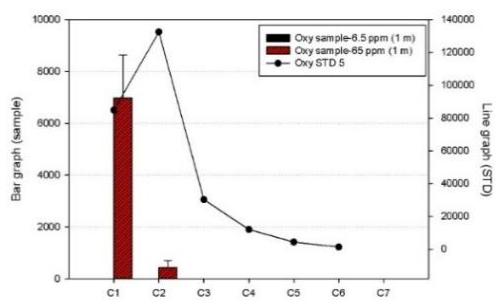

(f) Oxy product-type C (1 m)

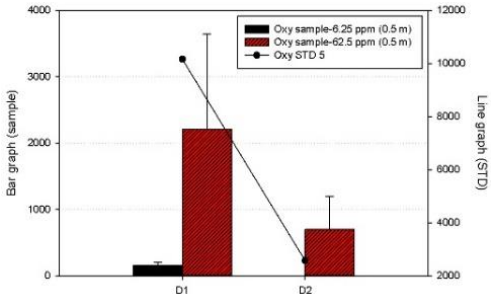

(g) Oxy product-type D (0.5 m)

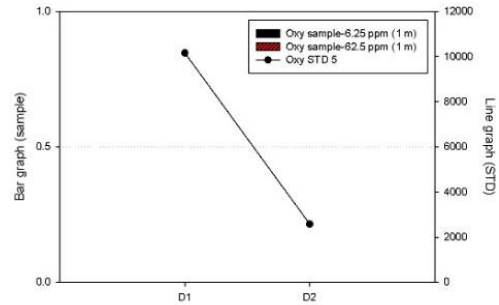

(h) Oxy product-type D (1 m)

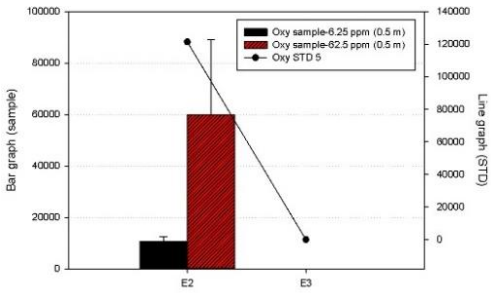

(i) Oxy product-type E (0.5 m)

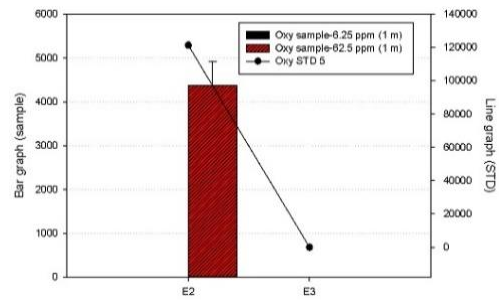

(j) Oxy product-type E (1 m)

Figure III- 6 . Comparison on intensity of oxy samples.

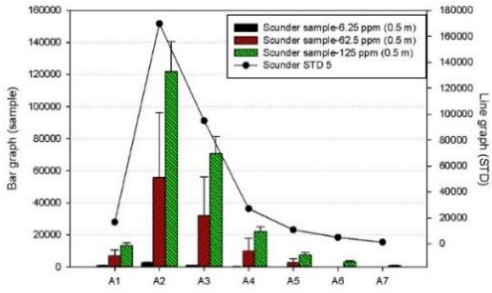

(a) Scunder product-Type A (0.5 m)

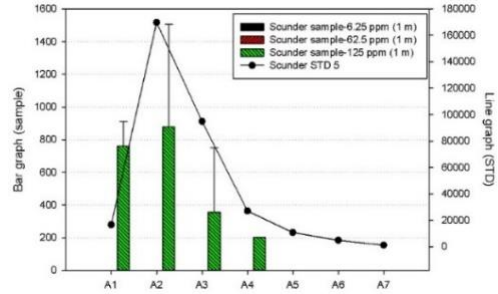

(b) Scunder product-Type A (1 m)

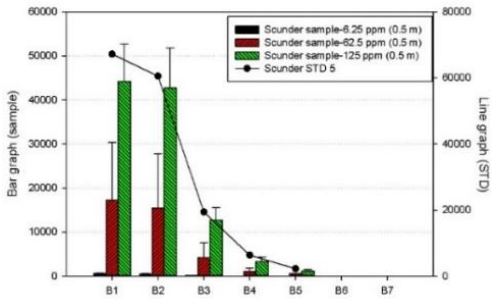

(c) Scunder product-Type B (0.5 m)

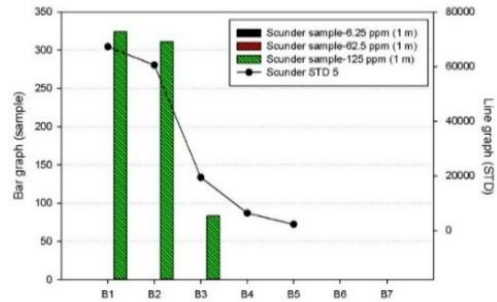

(d) Scunder product-Type B (1 m)

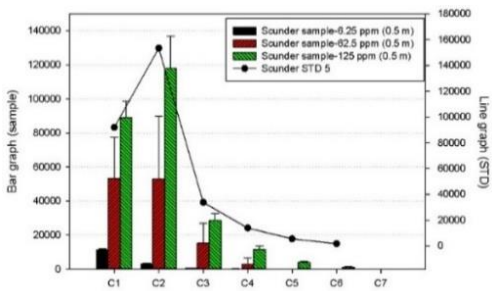

(e) Scunder product-Type C (0.5 m)

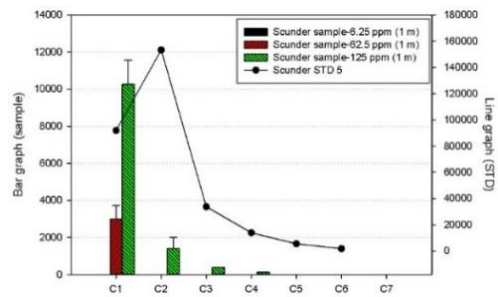

(f) Scunder product-Type C (1 m)

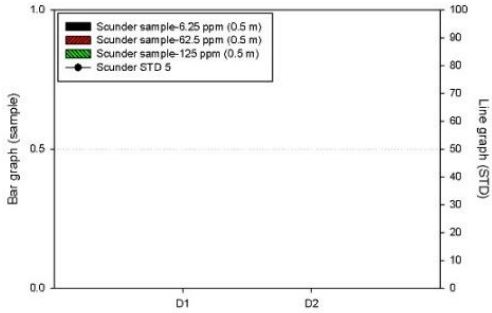

(g) Scunder product-type D (0.5 m)

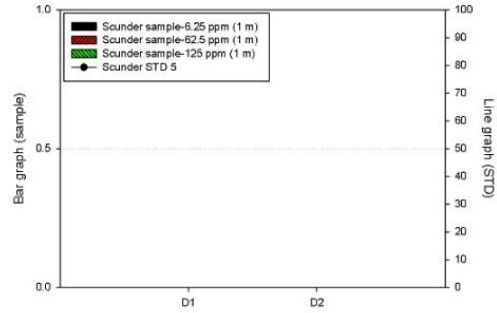

(h) Scunder product-type D (1 m)

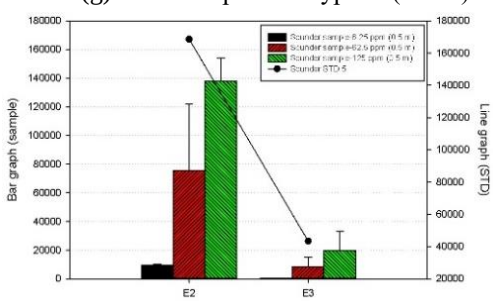

(i) Scunder product-type E (0.5 m)

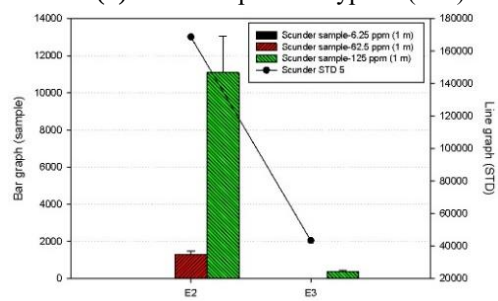

(j) Scunder product-type E (1 m)

Figure III- 7 . Comparison on intensity of Scunder samples.

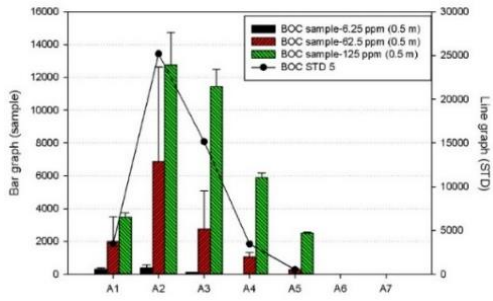

(a) BOC product-type A (0.5 m)

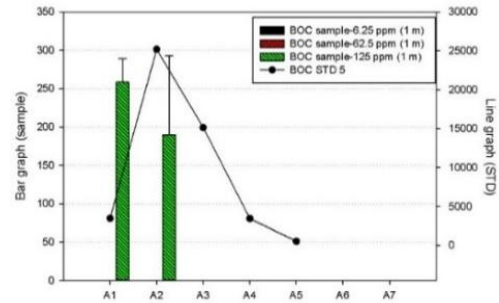

(b) BOC product-type A (1 m)

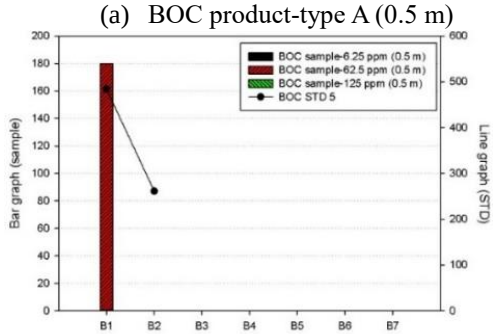

(c) BOC product-type B (0.5 m)

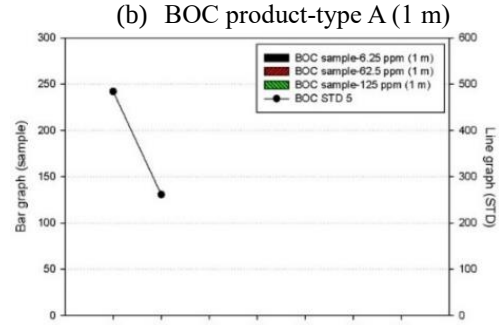

(d) BOC product-type B (1 m)

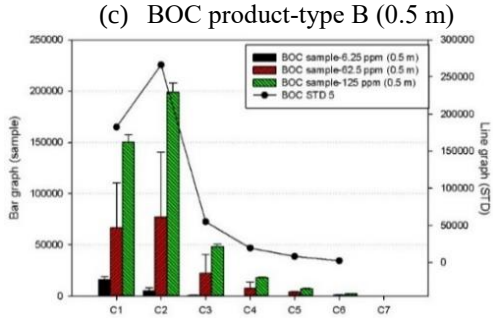

(e) BOC product-type C (0.5 m)

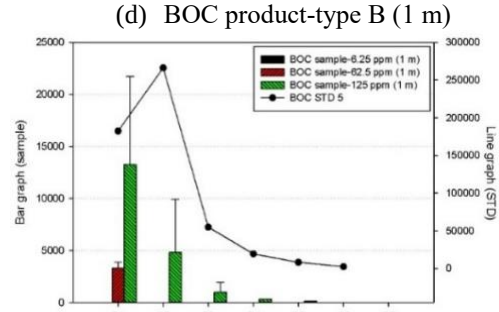

(f) BOC product-type C (1 m)

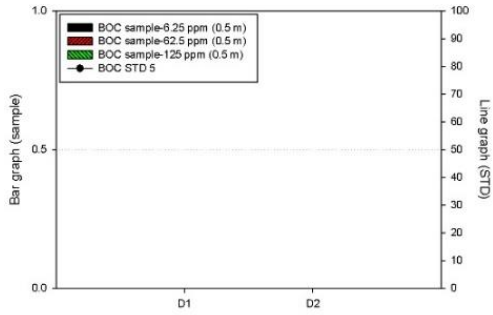

(g) BOC product-type D (0.5 m)

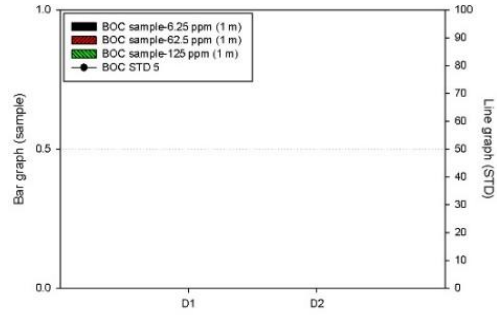

(h) BOC product-type D (1 m)

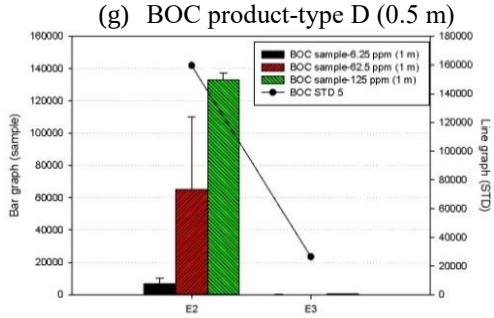

(i) BOC product-type E (0.5 m)

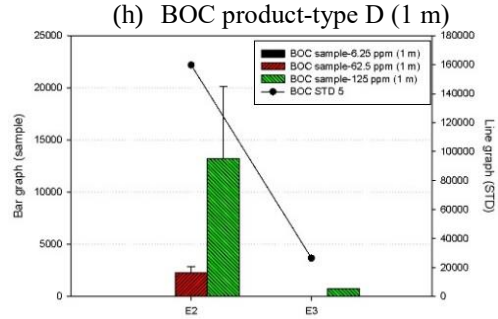

(j) BOC product-type E (1 m)

Figure III-８. Comparison on intensity of BOC samples.

III-3-2-2. Concentration estimation

Since there is no standard method to determine the concentration of each PHMG oligomer, we made the following assumption: the intensity is the same as the concentration regardless of the oligomer type. Therefore, after assuming that the total concentration of PHMG is the sum of all oligomer intensities in the standard detected for each product, the concentration corresponding to the X-axis for each oligomer was set according to the detected ratio. For example, when the concentration of 100 ppm equals the intensity of 100 (the sum of all oligomer intensities), if the intensity of A1 is 10, the concentration of A1 in PHMG is 10 ppm.

The linear equation for the standard curve was calculated for each product and oligomer, and the concentration of each sample was estimated (appendices figure 2(a)–(c)). The negative values for all samples were excluded. The mean concentration and SD for all the three products are shown in Table Ⅲ－4.

The change in the experimental humidifier spraying concentration was proportional to the change in the total airborne concentration of PHMG at 0.5 m. For instance, when the PHMG spraying concentration for Oxy was increased about 10 times from 6.5 ppm to 65 ppm, the total collected airborne concentration increased about 11 times from 35.89 $\mu g/m^3$ to 390.96 $\mu g/m^3$. As the spraying concentration increased from 62.5 ppm to 125 ppm for

Scunder and BOC, the airborne concentration increased 2.2 and 2.4 times, respectively.

At the lower spraying concentration, the higher mass PHMG oligomers were not detected.

At 1 m, all product samples were detected at concentrations above 6.25 ppm or 65 ppm, and the samples contained mainly linear monomers. C1 was the main component at all concentrations except for 125 ppm at 1 m. The proportion of C1 was 89% for the 65 ppm sample of Oxy and 100% for the 62.5 ppm Scunder product. In branched or cyclic structures, E2 was the most abundant, and C1 and E2 accounted for about half the structures in the 125 ppm samples of BOC and Scunder products.

Table III-4. Summary of geometric mean (GM) and geometric standard deviation (GSD) of PHMG concentration (unit : μg/m^3)

product	Conc	distance	The linear structure													The branched and cyclic structure				Total
			Type A					Type B				Type C				Type D		Type E		
			A1	A2	A3	A4	A5	B1	B2	B3	B4	C1	C2	C3	C4	D1	D2	E2	E3	
Oxy	6.5 ppm	0.5 m	2.67 (0.51)	6.18 (3.30)	1.72 (1.54)	0.04 (0.07)	-	2.09 (1.89)	0.79 (0.80)	-	-	12.64 (1.58)	3.83 (1.34)	0.44 (0.35)	0.003 (0.003)	0.01 (0.01)	-	5.47 (1.50)	-	35.89 (12.83)
		1 m	-	-	-	-	-	-	-	-	-	-	-	-	-	-	-	-	-	-
	65 ppm	0.5 m	10.69 (4.41)	76.73 (40.44)	39.90 (20.66)	10.91 (6.25)	3.78 (2.76)	53.35 (29.75)	33.38 (18.46)	14.36 (9.31)	3.78 (2.96)	40.14 (14.73)	39.99 (21.16)	10.90 (6.19)	3.50 (2.45)	1.73 (1.22)	0.55 (0.44)	47.28 (24.42)	-	390.96 (205.50)
		1 m	0.31 (0.39)	-	-	-	-	-	-	-	-	3.98 (1.46)	-	-	-	-	-	0.19 (0.33)	-	4.48 (2.18)
Scunder	6.25 ppm	0.5 m	0.89 (0.10)	0.13 (0.22)	-	-	-	-	-	-	-	11.66 (0.92)	0.83 (0.36)	0.05 (0.05)	-	-	-	6.76 (1.14)	-	20.33 (1.87)
		1 m	-	-	-	-	-	-	-	-	-	-	-	-	-	-	-	-	-	-
	62.5 ppm	0.5 m	8.05 (4.59)	65.78 (49.67)	37.55 (29.82)	11.79 (9.84)		20.23 (16.29)	18.22 (15.11)	4.92 (4.17)		64.07 (29.89)	62.60 (45.70)	18.29 (14.13)	3.06 (4.67)	-	-	88.62 (57.07)	9.93 (8.02)	413.12 (286.11)
		1 m	-	-	-	-	-	-	-	-		1.34 (0.87)	-	-	-	-	-	-	-	1.34 (0.87)

	125 ppm	0.5 m	16.10	148.08	85.68	26.82		53.90	52.05	15.47		109.11	143.81	34.60	14.21	-	-	166.56	24.09	890.50
			(2.09)	(21.85)	(12.38)	(3.57)		(9.97)	(10.88)	(3.39)		(11.25)	(22.12)	(4.71)	(2.17)			(18.46)	(16.48)	(138.86)
		1 m	0.51	-	-	-	-	-	-	-	-	10.41	-	-	-	-	-	8.94	-	19.86
			(0.18)									(1.39)						(2.29)		(3.62)
BOC	6.25 ppm	0.5 m	0.09	-	-	-	-	-	-	-	-	16.05	0.45	-	-	-	-	3.86	-	17.31
			(0.14)									(5.03)	(0.79)					(4.20)		(9.92)
		1 m	-	-	-	-	-	-	-	-	-	-	-	-	-	-	-	-	-	-
	62.5 ppm	0.5 m	2.99	10.34	4.06				-	-	-	99.54	115.06	33.74	11.47	-	-	76.60	-	353.81
			(2.59)	(9.12)	(3.63)							(71.60)	(100.70)	(29.40)	(9.97)			(56.40)		(283.30)
		1 m	-	-	-	-	-	-	-	-	-	-	-	-	-	-	-	-	-	-
	125 ppm	0.5 m	5.52	19.80	18.00			-	-	-	-	235.89	310.68	75.54	27.74	-	-	160.78	0.01	853.97
			(0.59)	(4.24)	(2.25)							(23.46)	(30.33)	(7.75)	(2.03)			(13.14)	(0.01)	(83.04)
		1 m	0.01	-	-	-	-	-	-	-	-	11.99	0.71	-	-	-	-	11.70	0.31	24.27
			(0.01)									(13.89)	(1.00)					(8.61)	-	(19.59)

III-4. Discussion

In this study, the oligomers in raw materials of PHMG products were characterized. In addition, the characterization and quantification of the airborne oligomer components were performed. This study compared three different products containing PHMG, which was the main causative agent for the extremely high incidence of the humidifier-related lung disease in Korea (Kim et al., 2014). The Oxy product was the main causative agent, but other products containing PHMG were also used as humidifier disinfectants. However, PHMG solution, including humidifier disinfectant products containing PHMG, was difficult to sell and purchase legally in Korea after the incident. Therefore, we qualitatively analyzed the purchased PHMG raw material solutions currently on sale in other countries.

PHMG is an extremely soluble guanidine-based polymer. It is synthesized from hexamethylene and guanidine salt. The structure of PHMG can be linear, branched, or cyclic. There are 7 types of PHMG structures: 3 linear (type A–C) and 4 branched or cyclic (type D–G) (Albert et al., 2003; Qian et al., 2008). In this study, it was confirmed that identical PHMG products can have different oligomer components. The linear A–C types were detected the most in all products. The content of type A–C oligomers was about 91% in the Oxy, 79% in Scunder, and 76% in BOC products. Type B was almost undetectable in BOC, and type C was 69% of the total. In addition, type D, branched or cyclic structure,

was only detected in Oxy products. E2 of type E was detected the most, amounting to about 20.8% in BOC and 8.5% in Oxy (figure Ⅲ－4). The branched and cyclic structures are type D–G, but only types D and E were detected in this study.

The results of the previous study analyzing the PHMG oligomer content in humidifier disinfectant products manufactured in Korea were similar. Type C oligomers were more abundant than type B oligomers and showed monotonically decreasing oligomer distributions. Linear types A–C were identified in the previous study, and types A–E in this study (Hwang et al., 2013).

In addition, as PHMG hydrochloride was synthesized in the previous study, the components of PHMG hydrochloride were analyzed under the conditions of increased time and temperature of the polycondensation reaction. As a result, the average molecular weight increased with the increasing reaction time and temperature above 170℃. In linear structures, the proportion of types A and C increased, and the proportion of type B decreased. In circular structures, the fraction of type D decreased and type E increased. As in the present study, the proportion of E2 increased when the reaction time increased in previous study (Wei et al., 2009).

Our results regarding the components of PHMG are consistent with those of the the previous studies. The longest reaction time and the highest average molecular weight among the three products were assigned to BOC products, and the shortest reaction time and low average molecular weight were assigned to the Oxy product.

Studies on the antimicrobial activity of PHMG suggest that the molecular weight should be at least 800–1300 Da (Albert et al., 2003; Chen et al., 2017). Therefore, the average molecular weight of the PHMG product was assumed to be that of the low mass oligomer (about 800 Da), not the high mass polymer. Not only PHMG is occupied to oligomer, but PHMB, which is known as guanidine-based biocide, has detected less than 6 oligomers (O'Malley et al., 2006). Therefore, it can be inferred that most of the guanidine-based chemicals exist mainly as oligomers.

In addition, when the humidifier was working, mainly C1 was detected at the dilution of 200:1 (6.5 ppm), which was the recommended Oxy dilution (figure Ⅲ－5). Similar results were obtained for other products. However, C1 was not the most abundant raw material component in all three products. The most detected monomer was C1 in Scunder and BOC products but B1 in Oxy. C1 weighs less than B1; however, there was about a 6-fold difference in the airborne concentration (Table Ⅲ－4). For the samples analyzed at 1 m, most monomers were detected at a high proportion, and C1 was detected at the highest proportion regardless of the concentration. We found that it was important to know the composition of raw materials in this experiment; however, the airborne PHMG oligomer composition was different from that of raw materials.

There are few studies on the detection of airborne polymers and oligomers, but there have been studies of volatilization as a function of molecular weight upon exposure to polymers composed of isocyanates. The study conducted by the National Institute of Occupational Safety and Health (NIOSH) in the US revealed that the lower molecular weight isocyanates

are a vapor inhalation hazard; conversely, the higher molecular weight isocyanates do not readily volatilize but are still an inhalation hazard if aerosolized (Streicher et al., 1998). Although PHMG is not volatile, it could be inferred that if the proportion of the low molecular weight molecules in raw materials is large, it may still spread once aerosolized by a humidifier.

Although it has been about 10 years since the humidifier disinfectant incident occurred, there have been few studies to characterize the components of airborne PHMG. Several studies have concentrated on the PHMG oligomer analysis, and one study analyzed the concentration of airborne PHMG. However, the exact structure of PHMG oligomers could not be identified (Lee and Yu, 2017). The results for the dilution of 200:1 in Lee and Yu's study were similar to the estimated concentration in this study. The total concentration of the Oxy product was 35.89 $\mu g/m^3$ (Table Ⅲ−4) and 30.5 $\mu g/m^3$ based on Lee and Yu's analysis. Thus, the estimated concentration is very similar to the actual total concentration. In addition, the airborne concentration increased linearly with the dilution ratio and we observed a similar trend.

An earlier study has estimated the concentration of airborne PHMG ($\mu g/m^3$) based on the concentration of PHMG in the humidifier disinfectant product ($\mu g/ml$), the daily usage of disinfectant (ml), the average daily use of the humidifier (hr), the room volume (m^3), and air change per hour (ACH=1). The concentration of airborne PHMG was estimated to be 68.3 $\mu g/m^3$ which is about 1.9 times higher than our result.

In the previous studies, MALDI-ToF, which has been used mainly for polymer analysis, was used to analyze PHMG. However, if the homogeneity of the sample matrix was not maintained, the analysis results were affected. Therefore, LC-qToF-MS was used in this study. The UNIFI program can more accurately process the data because the intensity is determined based on the mass and structure of target materials.

However, this study has some limitations. First is the sampling method of PHMG. In this study, samples were collected using an impinger. Since there is no proven method for sampling airborne PHMG, the isocyanate detection method NIOSH 5521 was used. The NIOSH method sampling flow rate was 1 L/min, but the flow rate of 2 L/min was used in this study for more efficient intensity measurement. Our method is estimated to be the most effective sampling method to identify oligomers. However, if a proven method of measuring PHMG in the airborne is found in the future, more accurate measurements will be possible.

The second limitation involved the estimation of the oligomer concentration. Since the intensity of each oligomer concentration is not known, it was assumed that all concentrations regardless of the oligomer type had the same intensity. Since there is no current methodology for quantifying individual oligomers due to technology limitations, the estimation used in this study is the most appropriate method.

III-5. Conclusions

In this study, we analyzed PHMG products manufactured in different countries and characterized the individual oligomers. In addition, we analyzed the airborne PHMG oligomers using a humidifier under the conditions of the actual humidifier disinfectant incident.

PHMG samples from different manufacturers contained different raw material components. Most PHMG samples contained type A–C linear structures and dimers and E2 branched or cyclic structures. The lower the PHMG concentration, the higher the content of the oligomers with a small number of monomers. The composition of the airborne PHMG was similar to that of raw materials in the samples collected at 0.5 m, and the proportion of monomers was high at 1 m. However, because there is no E1 in the branched and cyclic structures, mostly E2 was detected at 1 m.

The Oxy product that caused the most damage in the humidifier disinfectant incident mainly contained C1 monomers when the humidifier sprayed the manufacturer recommended concentration (6.5 ppm; 200:1 dilution); in addition, the airborne concentration was 35.89 $\mu g/m^3$.

CHAPTER IV.

Estimates of an inhaled and deposited dose by inhalation exposure to humidifier disinfectant containing Polyhexamethyleneguanidine (PHMG)

IV-1. Introduction

Humidifier disinfectants were first developed in 1994 as part of a consumer product to prevent the growth of microbes in an ultrasonic humidifier but were withdrawn from the Korean market in 2011 as they caused lung disease (Park et al., 2018). This incident, which was recorded as one of worst accidents caused by inhalation exposure to consumer products, has been the focus of epidemiological studies, clinical reports, and toxicological studies. Although it has been about a decade since the incident, only a few studies have assessed actual exposure concentrations and inhaled and deposited doses in a similar environment. In addition, it is important to consider the characteristics of each population in exposure assessments because the affected individuals are mainly children and pregnant women.

In the field of exposure science, various exposure assessment models have been developed to complement experimental measurements (Park et al., 2018b). There are some advantages of modeling particle deposition in the human respiratory tract. Health risk assessments and aerosol therapies for inhaled particles require information on local deposition patterns within the lungs, and where experimental studies are either forbidden owing to ethical considerations or are not feasible for health reasons, information on particle deposition is needed for all members of the population, from children to elderly

individuals, and for all particle sizes and breathing conditions (Hofmann, 2011).

In particular, the International Commission on Radiological Protection (ICRP) model is widely used to evaluate particle deposition in the respiratory tract among the general populations, and the model uses empirical equations based on experimental data and theory to characterize deposition via settling, inertia, and diffusion in the respiratory tract (Hinds, 1999). Additionally, the multiple-path particle dosimetry (MPPD) model uses the multiple-path method to calculate particle deposition in all airways of the lung and provides lobar- and airway-specific information. In each airway, deposition is calculated using theoretically derived efficiencies based on diffusion, sedimentation, impaction, and interception within the airway or airway bifurcation (ARA, 2016).

The humidifier disinfectant incident was a large accident that led to the development of lung diseases in a large number of patients following inhalation exposure to consumer products. It is important to determine estimated inhaled and deposited doses of humidifier disinfectants because until now, inhalation exposure has not been assessed using actual data. Therefore, this study aimed to estimate inhaled and deposited doses in the human lung using the ICRP and MPPD models for particles generated when a humidifier disinfectant containing polyhexamethyleneguanidine (PHMG) was sprayed.

IV-2. Methods

IV-2-1. Preparation of PHMG

The experiment was conducted with one product containing PHMG. The product used was oxysaksak, which contains approximately 0.1% PHMG (Oxy, Korea). It has a lavender aroma and is known to be responsible for most cases of lung injury. Because there was no legal requirement to produce a safety data sheet (SDS) for the Oxy product at the time of the sale, no specific safety information was available; however, data on the raw materials, including the amount of PHMG used in the product, were available.

IV-2-2. Measurement of airborne PHMG particles

IV-2-2-1. Cleanroom set up

All experiments were conducted in a 40.3 m^3 (7.0 m [L] × 2.4 m [W] × 2.4 m [H]) class 1,000 cleanroom fitted with a high-efficiency particulate air (HEPA) filter, enabling background particles smaller than 0.5 μm to be limited to less than 1,000 particles/ft^3. The purified air provided by the ventilation system flowed into the room via inlets on the ceiling, while the outlet air flowed out of the room through vents in the walls. The cleanroom was ventilated before measurements were conducted to ensure that the background concentration was kept below 100 particles/cm^3 (#/cm^3), with the concentration measured by a scanning mobility particle sizer (SMPS; Nanoscan; TSI, USA). Once measurements of the background concentration began, the ventilation system was turned off. All experiments were conducted using a temperature and humidity meter (TR-72U Thermo recorder; T&D Corporation, Japan). The temperature and humidity in the cleanroom before the humidifier began operating were maintained at about 20℃ and 50%, respectively.

The ultrasonic humidifier (H-U977, Ohsung, Korea) used for the experiment had a 6.5 L tank containing the spray liquid, and had a design used commonly in household humidifiers. The humidifier could be operated at a spray output rate of approximately 320 ml/h and the spray volume was set to the maximum in this study.

The recommended dilution for the Oxy product was 200:1, but previous studies had used dilution of up to 20:1 to simulate a “worst-case scenario”. The Oxy product concentrations investigated in previous studies were slightly different among the products investigated, but were about 1,300 ppm on average. As shown in Table Ⅱ－1, the exact PHMG concentration in each product was unknown and there was no standard PHMG solution on the market with a known concentration. We therefore took the approximate concentration suggested by the manufacturer as the nominal maximum concentration. The concentration of Oxy product was calculated to be about 6.5 ppm at 200:1 dilution, and about 65 ppm at 20:1 dilution.

Distilled water was generated by a commercial purification system (Milli-Q; Merck Millipore, Germany) and then used to dilute PHMG in all experiments. The dilutions produced low concentrations of 6.5 ppm and high concentrations of 65 ppm.

IV-2-2-2. Instrumental measurement of airborne PHMG particles

The SMPS and an optical particle sizer (OPS; Model 3330; TSI) were used for real-time monitoring of the particle number concentration in the ranges of 10–420 nm and 0.3–10 μm, respectively. The particle cut points of the OPS were set to 0.3, 0.5, 1.0, 3.0, 5.0, and 10.0 μm, for a total of six channels. A portable aerosol spectrometer (PAS; Model 1.109; Grimm, Germany) was used to measure the mass concentration of the PM1, PM2.5, and PM10 fractions. All real-time instruments logged data at 1-min intervals.

The temperature was maintained at about 15℃ during operation, and increased to 20℃ thereafter. Humidity was maintained at 100% during operation, and decreased to about 60% thereafter.

A diffusion dryer and thermodenuder were used to minimize moisture because measurements were affected by the high humidity during the experiment. The diffusion dryer was filled with silica gel to evaporate the moisture particles. The thermodenuder, which had a heating zone set to 200℃ and an adsorption section filled with active charcoal, was used to remove volatile and semi-volatile compounds. The silica gel in the diffusion dryer was replaced periodically, i.e., when it turned pink. These instruments were connected to the inlets of all measuring equipment.

The diffusion dryer and thermodenuder were used to minimize the effect of moisture when operating the humidifier. In previous experimental studies using a thermodenuder, decreases of about 94–98% in the number concentration of particles measured by SMPS have been reported depending, on the particle components and flow rates (An et al., 2007; Fierz et al., 2007). The same thermodenuder used in this study also reduced the number concentration of airborne particles by 81.5% in our previous humidifier study (Park et al., 2017). In that study, we investigated the most efficient combination of dryer and thermodenuder. Optimal efficiency was obtained when the diffusion dryer was connected ahead of the thermodenuder. When connecting in this order, the nanoparticle number concentration decreased by about 75% for a PHMG concentration of 65 ppm (Kim, 2018).

The sampling zone was set to 0.5 m from the instrument for the SMPS, OPS, and PAS. The real-time monitoring instruments sampled for a total 5 h 30 min. The background concentration was measured for 30 min before operating the humidifier. The humidifier was then operated for 4 h. After turning off the humidifier, the airborne concentration was measured for a further 1 h. The data used in this study was measured by 4h during the humidifier is operating and 1h after the humidifier is turning off.

IV-2-3. Respiratory deposition models

IV-2-3-1. International commission on radiological protection (ICRP) model

The ICRP model was primarily developed to estimate the dose to the organs and tissues, which resulted from the inhalation of radioactive particles by humans. This model uses empirical equations based on experimental data and theory to characterize regional and total deposition through settling, inertia, and diffusion in the regions of the respiratory system: (1) head airway, including the nose, mouth, throat, and upper airways; (2) tracheobronchial region; and (3) alveola (Hinds, 1999; ICRP, 1994). It can also estimate a wide range of particle sizes, essentially all aerosol particle sizes, under a complete range of breathing conditions. The equation has two parts: one for (a) inhaled and one for (b) deposited dose (Hinds, 1999; ICRP, 1994; Nazarenko et al., 2012).

(a)**Inhalaled dose (ID)** $= f_{nano} \cdot C_{inh} \cdot Q_{inh} \cdot T_{exposure} / Bw$

- ID = Inhaled aerosol dose per exposure event (Number: particles/kg/day, mass: ng/kg/day)
- f_{nano} = Fraction of ENMs in the inhaled aerosol
- C_{inh} = Aerosol concentration in inhaled air (Number: particles/L, mass: ng/L)
- Q_{inh} = Inhalation flow rate (L/min)
- $T_{exposure}$ = Duration of exposure (min)
- Bw= Body weight (kg)

$$\textbf{(b)Deposited dose (DD)} = \sum_{dp} \boldsymbol{DF_i\ (dp) \cdot\ ID\ (dp)}$$

$$\boldsymbol{DF_{NR}(dp)} = \frac{\mathbf{1}}{\mathbf{1} + \boldsymbol{exp}(\mathbf{6.84} + \mathbf{1.183\ \ln\ dp}} + \frac{\mathbf{1}}{\mathbf{1} + \boldsymbol{exp}\ (\mathbf{0.924} - \mathbf{1.885\ \ln\ dp})}$$

$$\boldsymbol{DF_{TR}(dp)}$$

$$= \frac{\left(\frac{\mathbf{0.00352}}{\boldsymbol{dp}}\right) \cdot [\boldsymbol{exp}(-\mathbf{0.234}\ (\boldsymbol{\ln\ dp} + \mathbf{3.40})^2) + \mathbf{63.9}\ \boldsymbol{exp}(-\mathbf{0.819}\ (\boldsymbol{\ln\ dp} - \mathbf{1.61})^2)]}{\mathbf{1} - \mathbf{0.5}(\mathbf{1} - \frac{\mathbf{1}}{\mathbf{1} + \mathbf{0.00076}\ \boldsymbol{dp}^{\mathbf{2.8}}})}$$

$$\boldsymbol{DF_{AR}(dp)} = \frac{\left(\frac{\mathbf{0.0155}}{\boldsymbol{dp}}\right) \cdot [\boldsymbol{exp}(-\mathbf{0.416}(\boldsymbol{\ln\ dp} + \mathbf{2.84})^2) + \mathbf{19.11}\boldsymbol{exp}(-\mathbf{0.482}(\boldsymbol{\ln\ dp} - \mathbf{1.362})^2)]}{\mathbf{1} - \mathbf{0.5}(\mathbf{1} - \frac{\mathbf{1}}{\mathbf{1} + \mathbf{0.00076}\ \boldsymbol{dp}^{\mathbf{2.8}}})}$$

$$\boldsymbol{DF_{TOTAL}(dp)} = \mathbf{0.0587} + \frac{\mathbf{0.911}}{\mathbf{1} + \boldsymbol{exp}(\mathbf{4.77} + \mathbf{1.485\ \ln\ dp})} + \frac{\mathbf{0.943}}{\mathbf{1} + \boldsymbol{exp}(\mathbf{0.508} - \mathbf{2.58\ \ln\ dp})}$$

- Dp = Midpoint aerosol particle size of instrumental measurement size channel in SMPS and OPS
- DFHA (dp) = Deposited fraction of inhaled aerosol in the head airway (HA)
- DFTR (dp) = Deposited fraction of inhaled aerosol in the tracheobronchial region (TR)
- DFAR (dp) = Deposited fraction of inhaled aerosol in the alveolar region (AR)
- DFTOTAL (dp) = Total deposited fraction of inhaled aerosol (sum of DFHA, DFTR and DFAR)

IV-2-3-2. Multiple-path particle dosimetry (MPPD) model

The MPPD model calculates the deposition and clearance of mono- and polydispersed aerosols in the human respiratory tract (ARA, 2016). For idealizing the human lung, eight options are available in the model; these include the Yeh-Schum, stochastic, age-specific, Weibel, and Pacific Northwest National Laboratories models. All these models fall under two categories: single- and multiple-path methods. Moreover, age-specific human lung geometries representing 10 distinct ages from 3 months to 21 years are provided. Furthermore, this model considers particle characteristics and various breathing patterns. The current version 3.04 is freely available at www.ARA.com and was used for modeling in this study.

IV-2-3-3. Input parameters for ICRP modeling

Table Ⅳ-1 shows the factors of the inhaled dose applied to the ICRP model. The inhalation rate was divided into the following categories: adult and children and then average and during sleep. The factors in adults were based on the Korean Exposure Factors Handbook published by the Korea Ministry of Environment. The average inhalation rate in men and women was 9.9 L/min, and the sleeping inhalation rate in men and women was 7.5 L/min.

The age of children selected in this study was <6 years because a previous study showed a significant increase in lung disease in these children (Park et al., 2018a). Infants aged <1 year were excluded from this study due to various factors. The daily average inhalation rate of 7.0 L/min in male and female children was based on the Korean Exposure Factors Handbook for Children published by the National Institute of Environmental Research (NIER). However, there were no data on the sleeping inhalation rate; thus, 4.3 L/min was used by referring to the EPA data.

The contact time was used based on that used in a previous study: 660 min (11 h) for average time (Paek et al., 2015; Park et al., 2015) and 480 min (8 h) for sleeping time (Park et al., 2016). The body weight (BW) used as a reference was 65.4 kg for adults, obtained from the health screening statistics published by the National Health Insurance Service, and 15.4 kg for children aged <6 years, obtained from the Korean Exposure Factors Handbook for Children published by the NIER. The spraying amount was obtained by

calculating the PHMG concentration in the product, and the daily amount was used as the amount of exposure when the disinfectant was sprayed during the contact time.

Table IV-1. Factors used for calculation of inhalation exposure for Oxy product in ICRP model

Factor			Oxy
Q_{inh}(Inhalation rate, L/min)	Adult	Average	9.9
		Sleeping	7.5
	Children (Age 1-5)	Average	7.0
		Sleeping	4.3
$T_{contact}$(min)	Average		660
	Sleeping		480
BW(kg)	Adult		65.43
	Children (Age 1-5)		15.44
Spraying amount (ml)	6.5 ppm or 6.25 ppm		0.00832
	65 ppm or 6.25 ppm		0.0832
Use amount (ml/day)	6.5 ppm or 6.25 ppm	8 hr	0.01664
		11 hr	0.02288
	65 ppm or 6.25 ppm	8 hr	0.1664
		11 hr	0.2288

IV-2-3-4. Input parameters for MPPD modeling

Table Ⅳ－2 shows the input parameters of the MPPD model. There are eight detailed models in the human MPPD model, with symmetric and asymmetric five-lobe versions considering the lung structure. Of these, two models were used in this study, and all of them used symmetric models considering the actual lung shape. These were the Yeh-Schum and age-specific five-lobe models, which are the most commonly used MPPD models.

Particularly, in the age-specific five-lobe model, some variables (FRC, URT volume, breathing frequency, and tidal volume) vary depending on age, and the variables applied in the MPPD model are shown in Table Ⅳ－1. However, variables for inhalant properties and some exposure scenario used experimental values. The particle property option used the multimodal mode, and data on mass concentrations were used. These values were converted to the number concentrations, as measured using SMPS and OPS. Each mode used the trimodal mode in 6.5 ppm and bimodal mode in 65 ppm, and the multimodal distribution used the particle size of each peak as the diameter. The inhalability of the particle was considered in the calculation. Body orientation was used to determine the deposition direction in the lung, and each variable was selected as “upright” for daily and “on back” for sleeping.

Table IV-2. Input parameters for MPPD model

Model	Month or year	1. Airway Morphometry		2. Inhalant Properties - Aerosol (single)			3. Exposure Scenario (Constant Exposure)				
		FRC (ml)*	URT volume (ml)**	Particle density	Aspect ratio	Particle properties	Acceleration of Gravity	Body Orientation	Aerosol concentration	Breathing frequency	Tidal volume
Yeh-Schum 5-lobe		3300	50							12	625
Age-specific 5-lobe	3 months	17.97	2.45							39	30.44
	21 months	38.41	6.52							28	81.22
	23 months	29.36	6.94						0.017 mg/m^3 (6.5 ppm) and 0.202 mg/m^3 (65 ppm)	27	86.79
	28 months	30.81	7.92	0.74 g/cm^3	1	Multimodal	981 cm/S2	"Upright" and "On back"		26	100.1
	3 yrs	48.2	9.47							24	121.3
	8+ yrs	501.32	21.03							17	278.2
	9+ yrs	683.03	22.44							17	295.8
	14 yrs	987.56	30.63							16	388.1
	18 yrs	1159.38	37.38							15	446.7
	21 yrs	2123.75	42.27							14	477.2

*FRC (ml) : functional residual capacity, **URT volume (ml) : upper respiratory tract

IV-3. Results

IV-3-1. ICRP model

Table Ⅳ-3 shows the inhaled dose concentration of the Oxy product. When the humidifier was sprayed, nanoparticles (<100 nm) accounted for the largest proportion of the size range and also accounted for 81% at 6.5 ppm and 62.9% at 65 ppm. In all scenarios, as sprayed concentrations increased from 6.5 ppm to 65 ppm, increasing all size ranges, the concentration of nanoparticles increased by approximately 3.4 times. Particularly, the inhaled dose at the 1–2.5-μm size increased by 27.2 times. In all scenarios, the daily inhaled dose at all concentrations was the highest in children aged <6 years: 8.5×10^9 at 6.5 ppm and 2.7×10^{10} at 65 ppm. In both concentrations, it is estimated that the inhaled dose of children aged <6 years is approximately three times higher than that of adults.

Table Ⅳ－4 shows the inhaled dose based on the mass concentration. The PM_1-to-PM_{10} ratio was 96.4% when the humidifier was sprayed at all concentrations and in all scenarios, with most of the particles having a size below 1 μm. As for the inhaled dose based on the number concentration, children aged <6 years had the highest daily inhaled dose based on the mass concentration, i.e., 1.5×10^7 at 6.5 ppm and 1.7×10^8 at 65 ppm. As the spraying concentration was increased by 10 times, the inhaled dose based on the mass concentration

increased 11.4 times.

Table IV- 3 . Inhaled dose of number concentration for Oxy product (unit: particles/bwkg/day)

Scenario			6.5 ppm (Average (SD))				65 ppm (Average (SD))			
			PM 0.011-0.1	PM 0.1-1.0	PM 1.0-2.5	PM 2.5-10	PM 0.011-0.1	PM 0.1-1.0	PM 1.0-2.5	PM 2.5-10
Humidifier on	Adult	Average	2.9E+09 (1.2E+08)	6.7E+08 (2.8E+07)	1.0E+05 (2.4E+04)	2.5E+04 (1.3E+04)	9.6E+09 (7.1E+08)	5.7E+09 (2.2E+08)	2.8E+06 (3.1E+05)	3.0E+04 (5.3E+03)
		Sleeping	1.1E+09 (4.9E+07)	2.7E+08 (1.1E+07)	4.1E+04 (9.5E+03)	9.9E+03 (5.2E+03)	3.9E+09 (2.8E+08)	2.3E+09 (9.0E+07)	1.1E+06 (1.2E+05)	1.2E+04 (2.1E+03)
	Child	Average	8.5E+09 (3.6E+08)	2.0E+09 (8.5E+07)	3.0E+05 (7.1E+04)	7.4E+04 (3.9E+04)	2.9E+10 (2.1E+09)	1.7E+10 (6.7E+08)	8.3E+06 (9.3E+05)	9.0E+04 (1.6E+04)
		Sleeping	2.8E+09 (1.2E+08)	6.5E+08 (2.8E+07)	9.9E+04 (2.3E+04)	2.4E+04 (1.3E+04)	9.4E+09 (6.9E+08)	5.5E+09 (2.2E+08)	2.7E+06 (3.0E+05)	2.9E+04 (5.2E+03)
Humidifier off	Adult	Average	1.8E+08 (6.3E+07)	7.7E+07 (2.8E+07)	1.4E+05 (1.8E+05)	2.7E+04 (2.2E+04)	2.6E+08 (3.7E+07)	3.5E+08 (5.1E+07)	7.6E+05 (1.7E+05)	9.9E+03 (1.2E+03)
		Sleeping	7.4E+07 (2.5E+07)	3.1E+07 (1.1E+07)	5.5E+04 (7.3E+04)	1.1E+04 (9.0E+03)	1.0E+08 (1.5E+07)	1.4E+08 (2.0E+07)	3.0E+05 (7.0E+04)	3.9E+03 (4.6E+02)
	Child	Average	5.5E+08 (1.9E+08)	2.3E+08 (8.5E+07)	4.1E+05 (5.4E+05)	8.0E+04 (6.7E+04)	7.6E+08 (1.1E+08)	1.0E+09 (1.5E+08)	2.3E+06 (5.2E+05)	2.9E+04 (3.4E+03)
		Sleeping	1.8E+08 (6.2E+07)	7.5E+07 (2.8E+07)	1.3E+05 (1.8E+05)	2.6E+04 (2.2E+04)	2.5E+08 (3.6E+07)	3.4E+08 (4.9E+07)	7.4E+05 (1.7E+05)	9.6E+03 (1.1E+03)

Table IV-４. Inhaled dose of mass concentration for Oxy product (unit: ng/bwkg/day)

Scenario			6.5 ppm (Average (SD))			65 ppm (Average (SD))		
			PM 1	PM 2.5	PM 10	PM 1	PM 2.5	PM 10
Humidifier on	Adult	Average	4.9E+06	5.0E+06	5.1E+06	5.6E+07	5.7E+07	5.8E+07
			(7.6E+05)	(7.1E+05)	(6.9E+05)	(3.3E+06)	(3.1E+06)	(2.7E+06)
		Sleeping	2.0E+06	2.0E+06	2.0E+06	2.2E+07	2.3E+07	2.3E+07
			(3.0E+05)	(2.8E+05)	(2.8E+05)	(1.3E+06)	(1.2E+06)	(1.1E+06)
	Child	Average	1.5E+07	1.5E+07	1.5E+07	1.7E+08	1.7E+08	1.7E+08
			(2.3E+06)	(2.1E+06)	(2.1E+06)	(9.8E+06)	(9.3E+06)	(8.1E+06)
		Sleeping	4.8E+06	4.9E+06	5.0E+06	5.4E+07	5.5E+07	5.6E+07
			(7.4E+05)	(6.9E+05)	(6.8E+05)	(3.2E+06)	(3.0E+06)	(2.6E+06)
Humidifier off	Adult	Average	1.3E+06	1.3E+06	1.3E+06	8.7E+06	8.9E+06	9.0E+06
			(5.0E+05)	(5.5E+05)	(5.9E+05)	(1.8E+06)	(1.9E+06)	(1.9E+06)
		Sleeping	5.0E+05	5.2E+05	5.3E+05	3.5E+06	3.6E+06	3.6E+06
			(2.0E+05)	(2.2E+05)	(2.4E+05)	(7.2E+05)	(7.5E+05)	(7.8E+05)
	Child	Average	3.7E+06	3.9E+06	4.0E+06	2.6E+07	2.7E+07	2.7E+07
			(1.5E+06)	(1.6E+06)	(1.8E+06)	(5.4E+06)	(5.6E+06)	(5.8E+06)
		Sleeping	1.2E+06	1.3E+06	1.3E+06	8.5E+06	8.7E+06	8.8E+06
			(4.9E+05)	(5.3E+05)	(5.7E+05)	(1.8E+06)	(1.8E+06)	(1.9E+06)

The deposited dose was divided into the head airway, tracheobronchial, and alveolar regions (figure Ⅳ－1~4). The deposited dose based on the number concentration measured using SMPS and OPS is shown in figure Ⅳ－1 and 3. figure Ⅳ－1 presents the deposited dose based on the number concentration classified by scenario and spraying concentration, and figure Ⅳ－3 presents the deposited dose by particle size distribution (PSD) of the number concentration by scenario and spraying concentration. Most of them showed a bimodal distribution of nanoparticles, and the alveolar region had the highest deposited dose in all concentrations and scenarios. As for the inhaled doses at all concentrations and scenarios, children aged <6 years had the highest daily deposited dose.

The alveolar region had the highest deposited dose, followed by the tracheobronchial and head airway regions. When the humidifier was sprayed, the highest deposited dose was 15.4 nm, noted in the alveolar region, followed by the tracheobronchial and head airway regions. The deposited dose in the alveolar region was 65.8% of the total deposited dose at 6.5 ppm and 67.2% of the total deposited dose at 65 ppm.

After the humidifier was sprayed, at 6.5 ppm, the alveolar region had the highest deposited dose, followed by the tracheobronchial and head airway regions. However, at 65 ppm, the alveolar region still had the highest deposited dose, followed by the head airway region and then the tracheobronchial region (figure Ⅳ－1). Moreover, we found that the highest deposited dose was between 48.7 and 64.9 nm at 65 ppm in the PSD (figure Ⅳ－3).

Figure Ⅳ-2 shows the PM_1 in the alveolar, tracheobronchial, and head airway regions. Unlike the number concentration, all scenarios showed a higher deposited dose in the order of the head airway, alveolar, and tracheobronchial regions. Furthermore, Scunder and BOC products showed similar patterns as Oxy products.

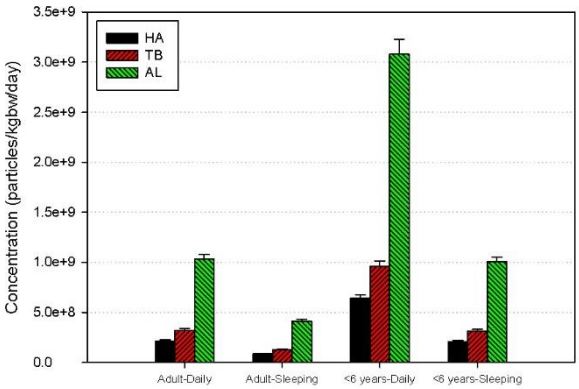

(a) Oxy product-6.5ppm (on)

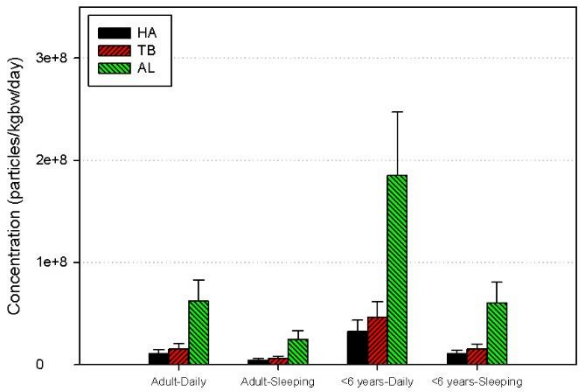

(b) Oxy product-6.5ppm (off)

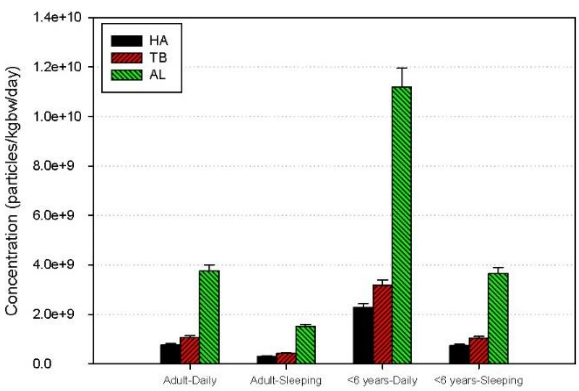

(c) Oxy product-65ppm (on)

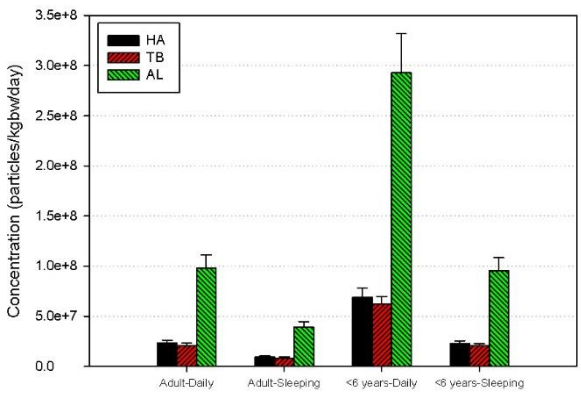

(d) Oxy product-6.5ppm (off)

Figure IV- 1 . The estimated number concentration by deposited regions.

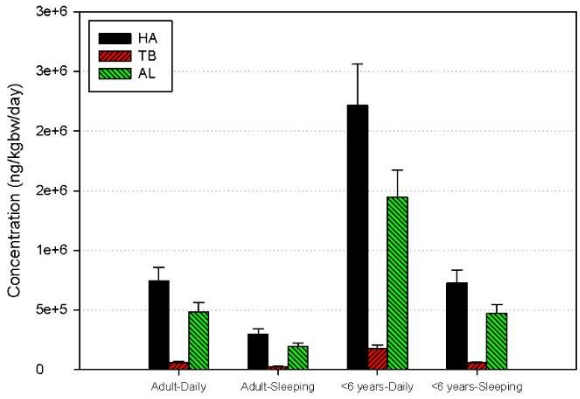

(a) Oxy product-6.5ppm (on)

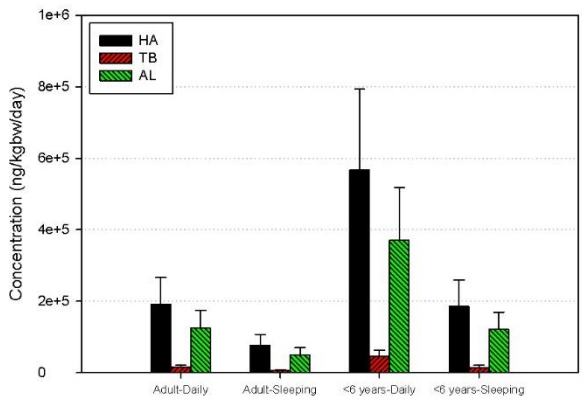

(b) Oxy product-6.5ppm (off)

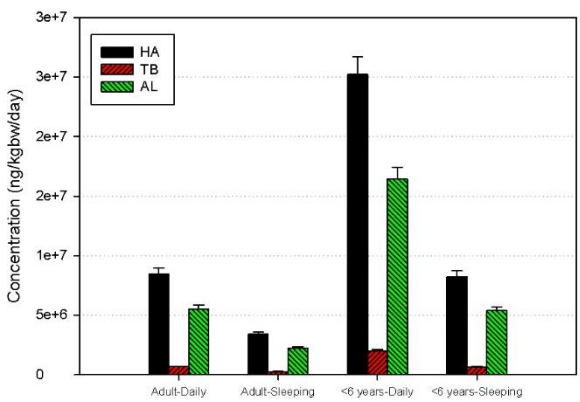

(c) Oxy product-65ppm (on)

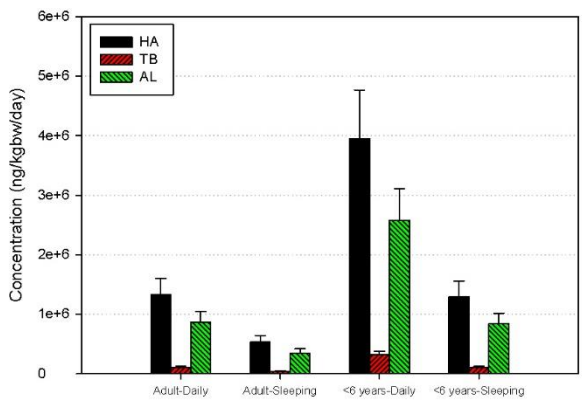

(d) Oxy product-6.5ppm (off)

Figure IV- 2 . The estimated mass concentration by deposited regions.

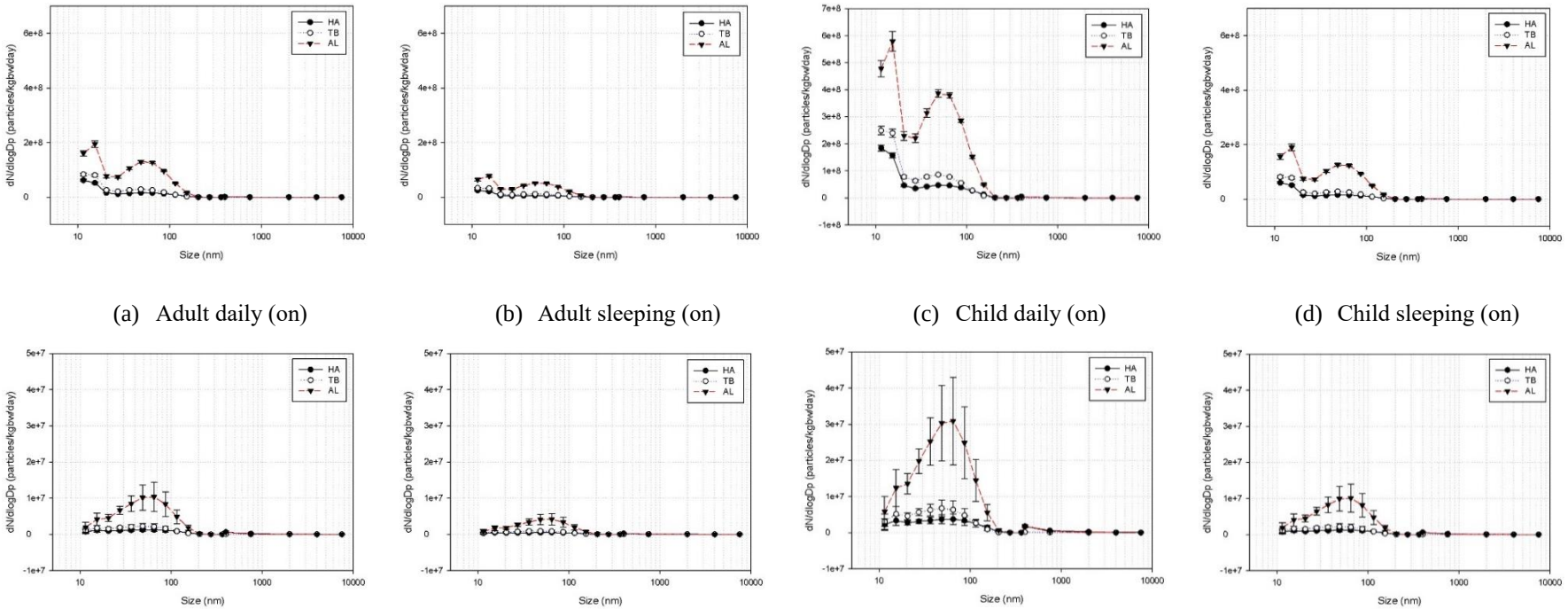

(a) Adult daily (on) (b) Adult sleeping (on) (c) Child daily (on) (d) Child sleeping (on)

(e) Adult daily (off) (f) Adult sleeping (on) (g) Child daily (on) (h) Child sleeping (on)

Figure IV- 3 . Particle size distribution (PSD) by scenarios at 6.5 ppm for Oxy product.

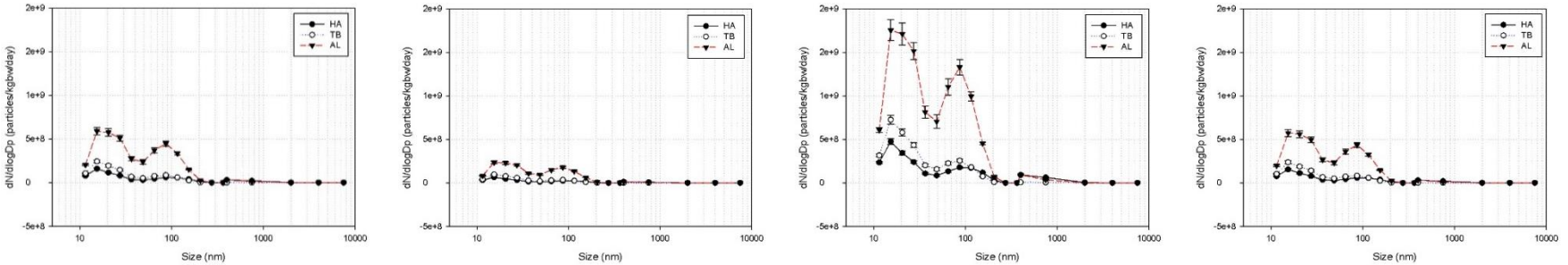

(a) Adult daily (on) (b) Adult sleeping (on) (c) Child daily (on) (d) Child sleeping (on)

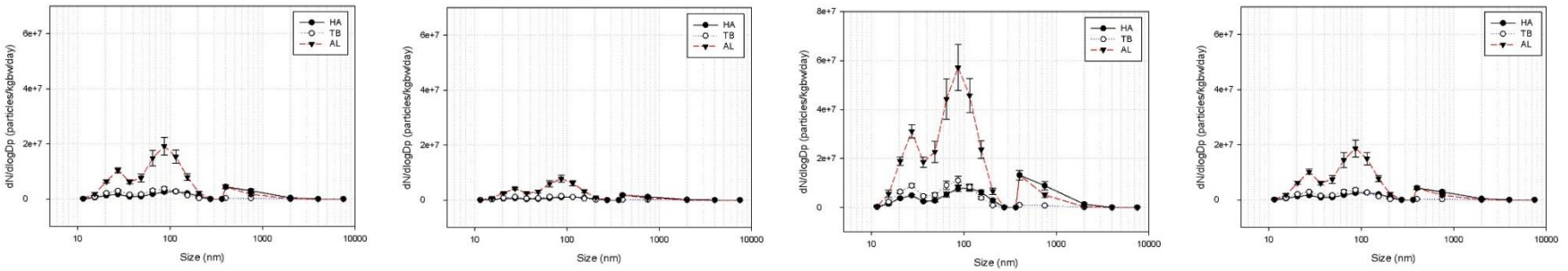

(e) Adult daily (off) (f) Adult sleeping (off) (g) Child daily (off) (h) Child sleeping (off)

Figure IV- 4 . Particle size distribution (PSD) by scenarios at 65 ppm for Oxy product.

IV-3-2. MPPD model

In this study, the deposition fractions of the two models are shown for the Oxy product results. Four variables in the setting of each model were used for concentration (6.5 ppm and 65 ppm) and activities such as daily and during sleep (body orientation). However, there was a slight difference between the activity in the same concentration and deposition fraction in each concentration.

The deposition fraction in figure Ⅳ-5 showed different concentrations in each five-lobe model and region. The Yeh-Schum five-lobe model had a lower overall deposition fraction than the age-specific five-lobe model. The deposition fraction in the Yeh-Schum model tended to be underestimated when compared with the condition of “21 years” as adult in the age-specific model.

In all scenarios as shown in figure Ⅳ-5, the deposition fraction is higher in the lower sections of both the lungs. In the graph of upper and lower depositions (Appendix Figure 10), the total deposition fraction in the lower part was the highest at 81% for the “3 months” scenario. With respect to regions, the head and pulmonary airways had the highest deposition fraction.

The deposition fraction tended to increase approximately two times in all scenarios when the diluted concentration increased 10 times. Figure Ⅳ-5 shows that the fraction

increased more than two times in all scenarios. Figure Ⅳ-6 shows the deposition fractions by lung generation. In all scenarios, the deposition fraction tended to gradually increase in the respiratory zone and then decrease. The deposition fractions increased by 1.5–3 times in the respiratory zone. In contrast, the mass/surface area tended to increase and decrease in the conducting zone. The deposited mass/area also increased by a maximum of 60 times at high concentrations (10 times difference in concentration) compared with that at low concentrations.

Figure Ⅳ-7 shows lung visualization by daily concentrations. These figures were obtained from the MPPD model, although the scale was not adjusted. Additionally, at the manufacturer's recommended dilution concentration of 6.5 ppm (× 200 dilution), the bronchial deposited mass was relatively large. However, as the dilution concentration increases 10 times, the lung has a relatively greater effect than the bronchus. Considering the red color indicating the highest deposition fractions, it seems that the younger the individual, the more likely it is that they have a high fraction (red dot) throughout the lung. Appendices figure 11 shows posterior lung visualization, with similar distributions in sleeping.

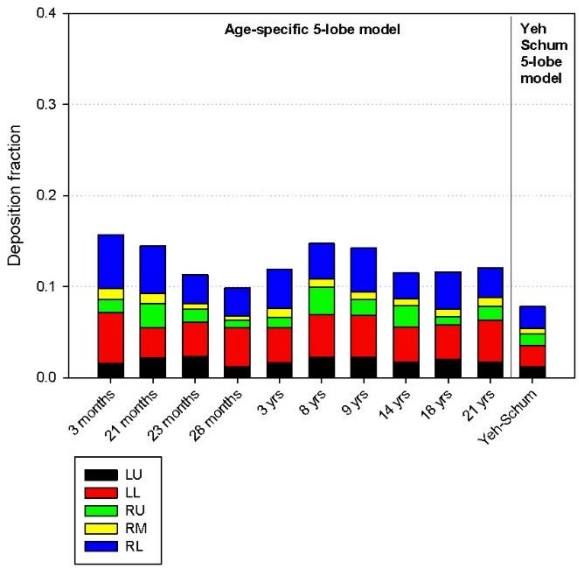

(a) Deposition fraction by the 5-lobes (6.5 ppm)

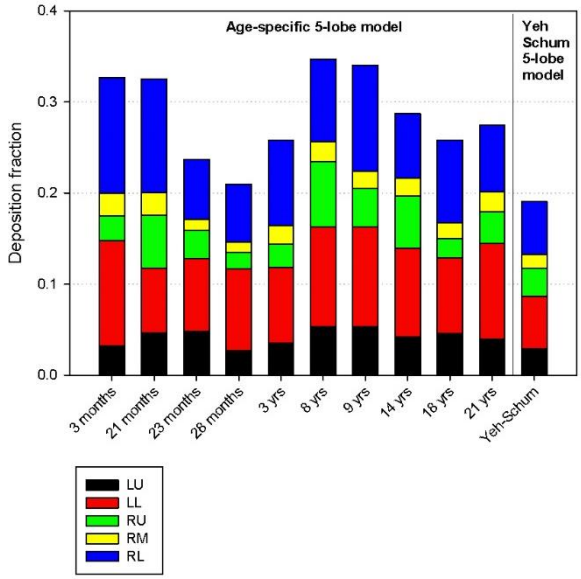

(b) Deposition fraction by the 5-lobes (65 ppm)

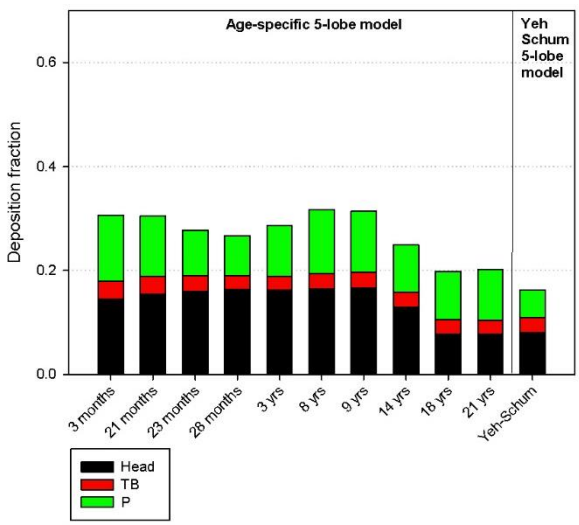

(c) Deposition fraction by regions (6.5 ppm)

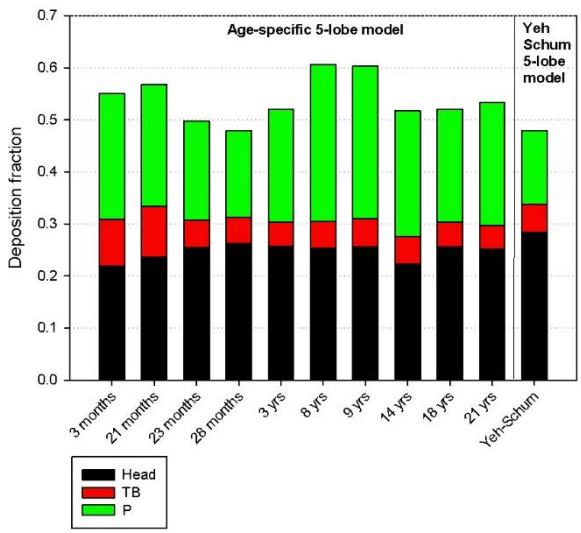

(d) Deposition fraction by regions (65 ppm)

Figure IV- 5 . Deposition fraction by the 5-lobes and the regions (LU (left upper), LL (left lower), RU (right upper), RL (right lower), RM (right middle), Head (Head airway), TB (tracheobronchial region), P (pulmonary region))

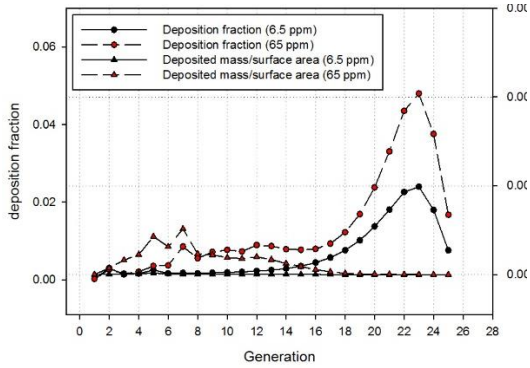

(a) 3 months

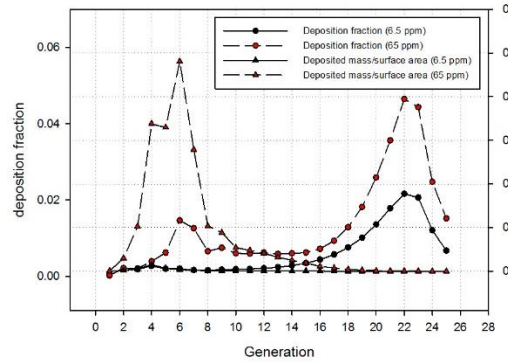

(b) 21 months

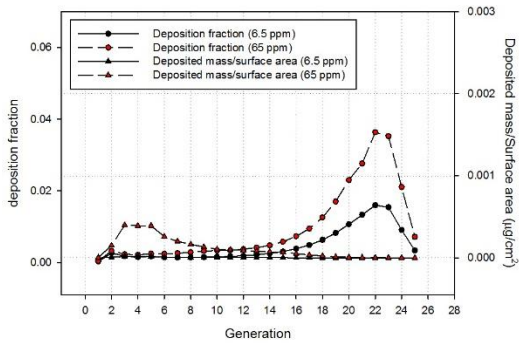

(c) 23 months

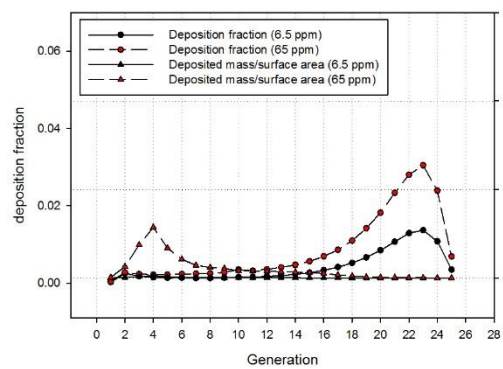

(d) 28 months

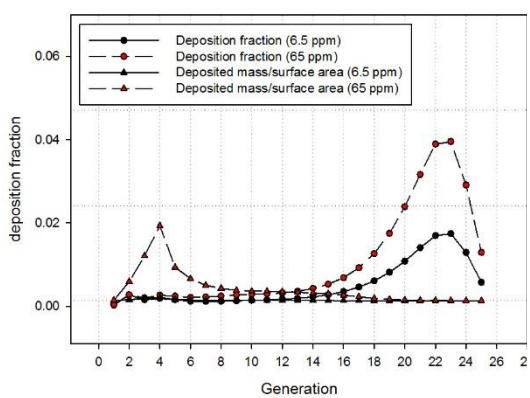

(e) 3 yrs

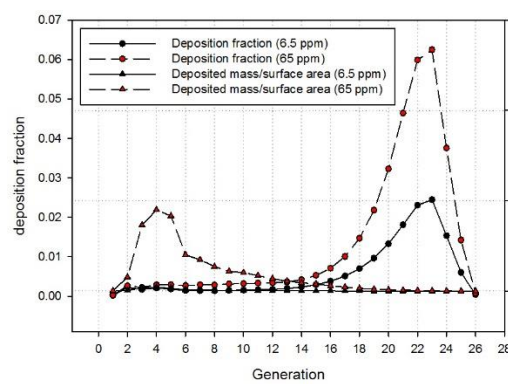

(f) 8 yrs

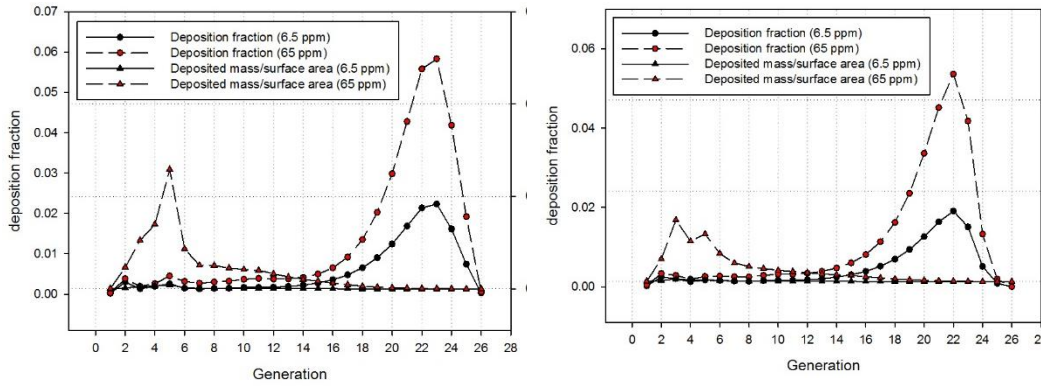

(g) 9 yrs (h) 14 yrs

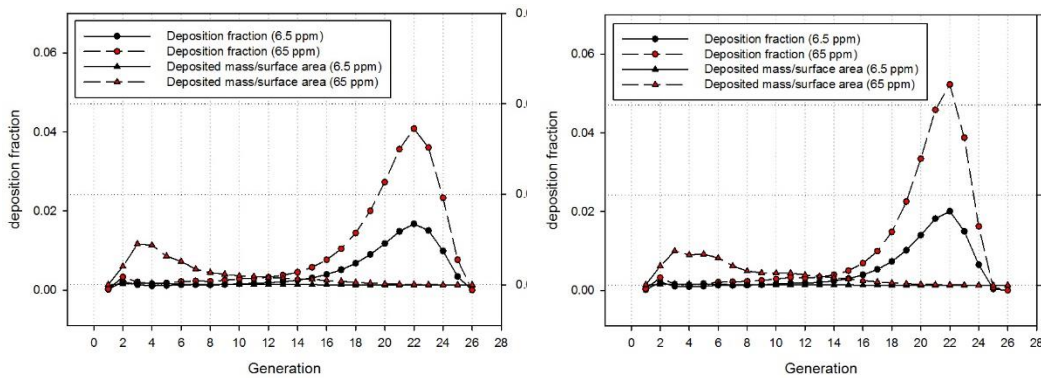

(i) 18 yrs (j) 21 yrs

Figure IV- 6 . Deposition fraction and deposited mass/surface area by generation of the lung by age (x axis (generation number) : conducting zone (1-16), transitional and respiratory zones (16-26)).

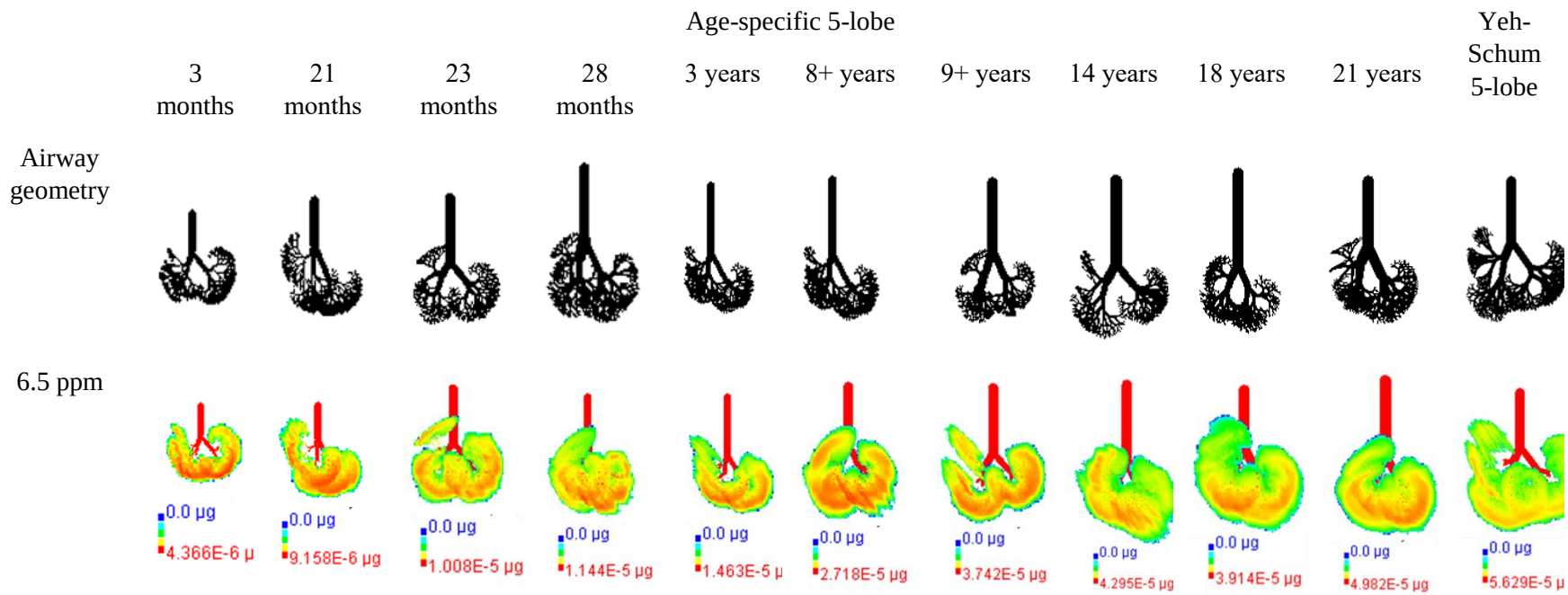
Age-specific 5-lobe
3 months
21 months
23 months
28 months
3 years
8+ years
9+ years
14 years
18 years
21 years
Yeh-Schum 5-lobe
Airway geometry
6.5 ppm
0.0 µg
4.366E-6 µ
0.0 µg
9.158E-6 µg
0.0 µg
1.008E-5 µg
0.0 µg
1.144E-5 µg
0.0 µg
1.463E-5 µ
0.0 µg
2.718E-5 µg
0.0 µg
3.742E-5 µg
0.0 µg
4.295E-5 µg
0.0 µg
3.914E-5 µg
0.0 µg
4.982E-5 µg
0.0 µg
5.629E-5 µ

65 ppm

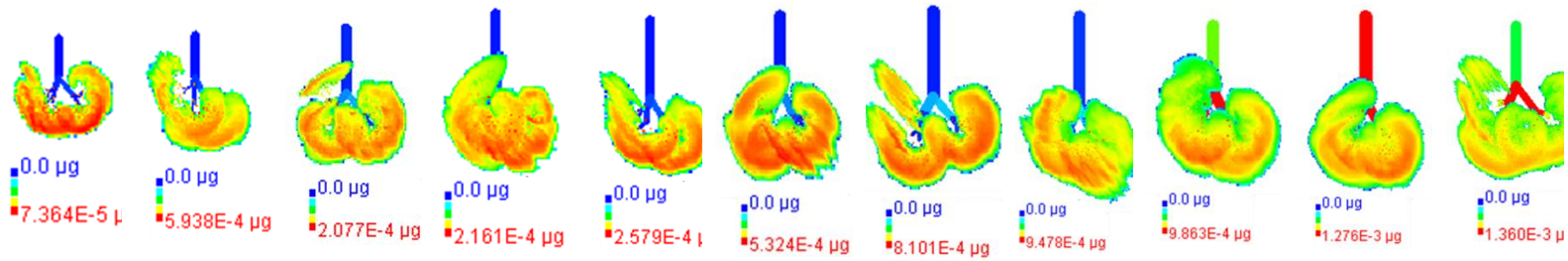

Figure IV- 7 . The lung visualization of deposited mass by concentration in daily (these figures had a different scale in all simulations).

IV-4. Discussion

This study aimed to estimate the inhaled and lung deposited doses in humans using the ICRP and MPPD models for the particles generated when a humidifier disinfectant containing PHMG is sprayed. It is challenging to determine the inhaled and deposited doses in the human lung because the complexity of the lung structure makes it difficult to obtain an accurate lung geometry model. Hence, the actual particle deposition is typically estimated using indirect methods, such as the ICRP model, as deposition models (Asgharian et al., 2006). In our study, the ICRP model was used, and the MPPD model, which applies different variables in various species, was used for comparison.

Although the ICRP model focuses on the dose and can convert the inhaled and deposited dose through a simple equation, the MPPD model shows the result of the deposition fraction. In this study, variables of age and life patterns were described, and the advantage of the MPPD model is that these variables are available in the age-specific model. These variables served as default in the MPPD model. However, the advantage of the ICRP model is that it can simply calculate the dose regardless of the particle size.

The daily inhaled and deposited doses in the ICRP model were high in children aged <6 years in all cases and was approximately three times higher in adults. In the MPPD model, infants aged <3 years also tended to have a higher deposition fraction than adults. Generally, children have a higher inhalation rate per BW or pulmonary surface area than do adults

(Ginsberg et al., 2005). The results may also support the evidence from previous epidemiologic studies indicating that a large number children aged <6 years had lung disease (Park et al., 2018a).

The results for PM_1 in the ICRP model were similar to those in the MPPD model. The head airway and pulmonary regions have the highest deposition fraction. It is because the MPPD model is based on the ICRP model. The similarity between the two models was also shown in the previous study (Park et al., 2018a)..

In the MPPD model, the deposition fractions in children aged 3–28 months are generally low. This is quite similar to the trend observed in the number of affected individuals aged from <1 to 6 years in the previous study that analyzed the number of the affected individuals by age. Although direct comparisons of two models were difficult due to the difference in input parameter and results, the results in children aged 3–28 months indicate that both the ICRP and MPPD models obtained higher deposited dose and deposition fractions at younger ages.

Particularly, the MPPD model, unlike the ICRP model, has the advantage of identifying the deposition fraction of the lung's more detailed structure and visualizing the lung. A ten-fold increase in the dilution concentration could increase the deposition fraction by approximately 20 and not 10 times. Moreover, the deposited mass was greater in the bronchus than in the lungs at the recommended dilution concentration. Recently, there is much interest in the effects on asthma due to exposure to humidifier disinfectants. In a

recent study, children who developed acute bronchiolitis at <3 years of age and who had humidifier disinfectant exposure showed a significantly increased risk for asthma in the preceding 12 months (Yoon et al., 2018). Therefore, considering the result of the MPPD model, it appears that exposure to the humidifier disinfectant also increased the risk of asthma and lung disease.

Previous studies have rarely estimated inhaled and deposited doses or fractions from measured data in a similar environment. However, this study is expected to obtain values close to the actual inhaled and deposited dose or fraction because it is based on results obtained for PHMG concentration in the air after moisture control.

IV-5. Conclusions

In this study, the inhaled and deposited doses or fraction was identified by the scenario according to the life patterns and age, reflecting the characteristics of the actual humidifier disinfectant incident using the ICRP and MPPD models.

Infants and young children showed high deposition dose or fraction in the ICRP and MPPD models. Particularly, the lower the number of months in the MPPD model, the higher the deposition fraction. We also found that it affects the bronchi and lungs, and the higher concentrations increase the deposition fraction.

The highest deposited dose based on the number concentration in the ICRP model was noted at 15.4 nm. Both models tended to have similar trends in deposition fraction or dose by region, and the pulmonary and head airways showed the highest dose.

CHAPTER V.

Summary and conclusions

The humidifier disinfectant incident was one of worse incidents caused by consumer products containing PHMG, which was the most widely sold product, accounting for the overwhelming majority of fatalities. This study was conducted using the real product in the incident and a similar environment because there have been few exposure assessment studies in realistic environmental conditions. Therefore, this study aimed to identify the characteristics of PHMG in aqueous solution and investigate the behavior of airborne particles generated by use of PHMG as a humidifier disinfectant; determine the difference in oligomer types and content between PHMG products and aerosols and estimate the airborne concentration of oligomers during humidifier use; and calculate the inhaled and deposited doses or fraction in the human lung using the ICRP and MPPD models for particles generated when a humidifier disinfectant containing PHMG was sprayed.

First, PHMG particles in the aqueous solution had a bimodal distribution near 100 nm. The PSD of PHMG in the air was slightly right-shifted in the region near 100 nm. This was estimated based on the particles analyzed by FE-SEM, which were mostly aggregated, and the single particle size was also approximately 20 nm. Most particles contributing to the mass concentration of PHMG were smaller than 1 μm, and the PM_1 concentration was almost 99% of the PM_{10} concentration regardless of the initial PHMG concentration. Additionally, without ventilation, the PHMG particles could remain in the air even after operating the humidifier at the concentration recommended by the manufacturer for the Oxy product, with a required period of approximately 2 h to reach

the background concentration. Although the three PHMG products were manufactured in different countries, we found that the behavior of airborne particles was mostly affected by the input PHMG concentration rather than differences due to the manufacturer of the product.

Second, although the same PHMG product was manufactured in different countries, PHMG raw materials consisted of different oligomers. Most of the three products consisted of type A–C, which has a linear structure and dimers; moreover, most of the branched or cyclic structure was composed of E2. The lower the concentration, the more the oligomer had a small number of monomers. PHMG in the air when the humidifier was sprayed had a similar component as the raw materials in the samples collected at 0.5 m, and the proportion of monomer of type C was high at 1 m. However, most samples were composed of E2 at 1 m because there is no E1 in the branched or cyclic structure. In the Oxy product that caused the most damage in the humidifier disinfectant incident, most monomers were C1 when the humidifier was sprayed based on the manufacturer-recommended dilution concentration (6.5 ppm; 200:1); moreover, the concentration in the air was 30.15 $\mu g/m^3$.

Finally, the inhaled and deposited doses or fractions were identified based on scenario according to the life patterns and age, reflecting the characteristics of the actual humidifier disinfectant incident using the ICRP and MPPD models. Infants and young children showed high deposition doses or fractions in the ICRP and MPPD models. Particularly, the lower was the number of months in the MPPD model, the higher was the

deposition fraction. The highest deposited dose based on number concentration in the ICRP model was found at 15.4 nm. Both models tended to have similar trends in deposition fraction or dose by region, and the highest dose was noted in the pulmonary and head airways.

Therefore, this study evaluated the characteristics of raw materials of humidifier disinfectant containing PHMG sprayed in the air and then estimated the inhaled and deposited doses in humans using the ICRP and MPPD models. Particles in raw materials of PHMG had a bimodal distribution in the region near 100 nm, and raw materials of PHMG consisted of linear type (type A–C) oligomers. Characteristics of PHMG in the air were identified, and most particles were PM_1 and existed as aggregated single particles of approximately 20 nm in size. Aerosol had a high proportion of monomers, and the proportions of type C monomers was high at 1 m. Infants and young children showed high deposition doses or fractions in the ICRP and MPPD models.

REFERENCES

ACCEH . The list of humidifier disinfectant tragedy incident. Asian Citizen's Cent er for Environment and Health, accessed 13 May 2019.

Albert M., Feiertag P., Hayn G., Saf R., Hönig H., 2003. Structure− Activity Rel ationships of Oligoguanidines Influence of Counterion, Diamine, and Avera ge Molecular Weight on Biocidal Activities. Biomacromolecules. 4 (6), 18 11-1817.

Aleshina E. Y., Yudanova T. N., Skokova I. F., 2001. Production and properties of polyvinyl alcohol spinning solutions containing protease C and polyhexa methylene guanidine. Fibre Chem. 33 (6), 421-423.

Alvarez-Fernández J., Quirce S., Calleja J., Cuevas M., Losada E., 1998. Hyperse nsitivity pneumonitis due to an ultrasonic humidifier. Allergy. 53 (2), 210-212.

An W. J., Pathak R. K., Lee B. H., Pandis S. N., 2007. Aerosol volatility measu rement using an improved thermodenuder: application to secondary organic aerosol. J. Aerosol Sci. 38 (3), 305-314.

Anderson W., Kozak D., Coleman V. A., Jämting Å. K., Trau M., 2013. A comp arative study of submicron particle sizing platforms: accuracy, precision an d resolution analysis of polydisperse particle size distributions. J. Colloid I

nterface Sci. 405, 322-330.

Bae J., Park M., Lee J., Song I., Ju Y., Lee C., Kwon J., Moon B., Oh H., 201 9. Quantitative MALDI-TOF mass spectrometric analysis of biocidal polyh examethylene guanidine (PHMG) oligomers in consumer products. Internati onal Journal of Mass Spectrometry. 435, 298-304.

Buchberger T., Himmelsbach M., Buchberger W. Analysis of Biocidal Oligoguanid ines and Oligobiguanides by High Performance Liquid Chromatography an d Mass Spectrometry.

Buseck P. R., Adachi K., 2008. Nanoparticles in the atmosphere. Elements. 4 (6), 389-394.

Chen A., Peng H., Blakey I., Whittaker A. K., 2017. Biocidal polymers: A mech anistic overview. Polymer Reviews. 57 (2), 276-310.

Cheon C. K., Jin H. S., Kang E. K., Kim H. B., Kim B.-J., Yu J., Park S. J., Hong S.-J., Park J. D., 2008. Epidemic acute interstitial pneumonia in chil dren occurred during the early 2006s. Korean journal of pediatrics. 51 (4), 383-390.

Choi S. H., Bae J.E., Oh H. B., Kwon J. H., 2016. Optimization of the Spectrop hotometric Method using Eosin Y for the Quantification of Guanidine Olig omers in Consumer Products. J. of the Korean Society for Environmental Analysis. 19 (1), 36-43.

Elizalde O., Leal G. P., Leiza J. R., 2000. Particle size distribution measurements of polymericdispersions: a comparative study. Part. Part. Syst. Charact. 17

(5-6), 236-243.

Fierz M., Vernooij M. G. C., Burtscher H., 2007. An improved low-flow thermod enuder. J. Aerosol Sci. 38 (11), 1163-1168. https://doi.org/10.1016/j.jaerosci. 2007.08.006.

Fissan H., Ristig S., Kaminski H., Asbach C., Epple M., 2014. Comparison of dif ferent characterization methods for nanoparticle dispersions before and after aerosolization. Anal. Methods. 6 (18), 7324-7334. https://doi.org/10.1039/c 4ay01203h.

Gilbert P., Moore L., 2005. Cationic antiseptics: diversity of action under a comm on epithet. Journal of applied microbiology. 99 (4), 703-715.

Ginsberg G. L., Perkovich Foos B., Firestone M. P., 2005. Review and analysis o f inhalation dosimetry methods for application to children's risk assessmen t. Journal of Toxicology and Environmental Health, Part A. 68 (8), 573-61 5.

Ham S., Kim S., Lee N., Kim P., Eom I., Tsai P. J., Lee K., Yoon C., 2015. C omparison of nanoparticle exposure levels based on facility type—small-sca le laboratories, large-scale manufacturing workplaces, and unintended nanop article-emitting workplaces. Aerosol Air Qual. Res. 15, 1967-1978. https://d oi.org/10.4209/aaqr.2015.03.0141.

Highsmith V. R., Rodes C. E., Hardy R. J., 1988. Indoor particle concentrations associated with use of tap water in portable humidifiers. Environ. Sci. Tec hnol. 22 (9), 1109-1112. https://doi.org/10.1021/es00174a019.

Hinds W. C. Aerosol technology: properties, behavior, and measurement of airbor ne particles: John Wiley & Sons, 1999.

Hofmann W., 2011. Modelling inhaled particle deposition in the human lung—a r eview. Journal of Aerosol Science. 42 (10), 693-724.

Hong S. B., Kim H. J., Huh J. W., Do K. H., Jang S. J., Song J. S., Choi S. J., Heo Y., Kim Y. B., Lim C. M., 2014. A cluster of lung injury associate d with home humidifier use: clinical, radiological and pathological descript ion of a new syndrome. Thorax. 69 (8), 694-702.

Hotze E. M., Phenrat T., Lowry G. V., 2010. Nanoparticle aggregation: challenges to understanding transport and reactivity in the environment. J. Environ. Qual. 39 (6), 1909-1924. https://doi.org/10.2134/jeq2009.0462.

Hung D. V., Tong S., Nakano Y., Tanaka F., Hamanaka D., Uchino T., 2010. M easurements of particle size distributions produced by humidifiers operating in high humidity storage environments. Biosyst. Eng. 107 (1), 54-60.

Hwang H. J., Nam J., Yang S. I., Kwon J.-H., Oh H. B., 2013. MALDI-TOF an alysis of polyhexamethylene guanidine (PHMG) oligomers used as a comm ercial antibacterial humidifier disinfectant. Bulletin of the Korean Chemical Society. 34 (6), 1708-1714.

KCDC. Interim report of epidemiological investigation on lung injury with unkno wn cause in Korea. Public Health Weekly Report. 4, 2011, pp. 817-839.

Kim H. J., Lee M. S., Hong S. B., Huh J. W., Do K. H., Jang S. J., Lim C. M., Chae E. J., Lee H., Jung M., 2014. A cluster of lung injury cases as

sociated with home humidifier use: an epidemiological investigation. Thora x. 69 (8), 703-708.

Kim H. R., Lee K., Park C. W., Song J. A., Park Y. J., Chung K. H., 2016. Po lyhexamethylene guanidine phosphate aerosol particles induce pulmonary in flammatory and fibrotic responses. Arch. Toxicol. 90 (3), 617-632.

Kim Y. Behavioral characteristics of mist containing PHMG emitted from ultrason ic humidifier. Graduate School of Public Health, Seoul National University, 2018.

Kudo T., Sekiguchi K., Sankoda K., Namiki N., Nii S., 2017. Effect of ultrasonic frequency on size distributions of nanosized mist generated by ultrasonic atomization. Ultrason. Sonochem. 37, 16-22.

Lee J. H., Kim Y. H., Kwon J. H., 2012. Fatal misuse of humidifier disinfectants in Korea: importance of screening risk assessment and implications for m anagement of chemicals in consumer products. Environ. Sci. Technol.

Lee J. H., Yu I. J., 2017. Human exposure to polyhexamethylene guanidine phosp hate from humidifiers in residential settings: cause of serious lung disease. Toxicol. Ind. Health. 33 (11), 835-842.

Mahl D., Diendorf J., Meyer Zaika W., Epple M., 2011. Possibilities and limitatio ns of different analytical methods for the size determination of a bimodal dispersion of metallic nanoparticles. Colloids Surf., A. 377 (1-3), 386-392.

Mashat B., 2016. Polyhexamethylene biguanide hydrochloride: features and applicat ions. British Journal of Environmental Sciences. 4 (1), 49-55.

O'Malley L. P., Hassan K. Z., Brittan H., Johnson N., Collins A. N., 2006. Chara cterization of the biocide polyhexamethylene biguanide by matrix-assisted l aser desorption ionization time-of-flight mass spectrometry. Journal of appli ed polymer science. 102 (5), 4928-4936.

Ostapenko Y. N., Brusin K. M., Zobnin Y. V., Shchupak A. Y., Vishnevetskiy M. K., Sentsov V. G., Novikova O. V., Alekseenko S. A., Lebed'Ko O. A., Puchkov Y. B., 2011. Acute cholestatic liver injury caused by polyhexame thyleneguanidine hydrochloride admixed to ethyl alcohol. Clin. Toxicol. 49 (6), 471-477.

Paek D., Koh Y., Park D. U., Cheong H. K., Do K. H., Lim C. M., Hong S. J., Kim Y. H., Leem J. H., Chung K. H., 2015. Nationwide study of humid ifier disinfectant lung injury in South Korea, 1994–2011. Incidence and do se–response relationships. Ann. Am. Thorac. Soc. 12 (12), 1813-1821.

Park D. U., Ryu S.-H., Lim H.-K., Kim S.-K., Ahn J., Roh H.-S., Choi Y.-Y., C ha W.-S., Lee E., Hong S.-B., 2016a. Characteristics of exposure to humid ifier disinfectant by lung injury patients. Korean Journal of Environmental Health Sciences. 42 (3), 147-159.

Park D. U., Ryu S.-H., Roh H.-S., 2016b. Distribution of health problems associat ed with humidifier disinfectant by year. Korean Journal of Environmental Health Sciences. 42 (6), 365-374.

Park D. U., Friesen M. C., Roh H. S., Choi Y. Y., Ahn J. J., Lim H. K., Kim S. K., Koh D. H., Jung H. J., Lee J. H., Cheong H. K., Lim S. Y., Lee

m J. H., Kim Y. H., Paek D. M., 2015. Estimating retrospective exposure of household humidifier disinfectants. Indoor Air. 25 (6), 631-40.

Park D. U., Ryu S. H., Roh H. S., Lee E., Cho H. J., Yoon J., Lee S. Y., Cho Y. A., Do K. H., Hong S. J., 2018a. Association of high-level humidifier disinfectant exposure with lung injury in preschool children. Sci. Total En viron. 616, 855-862.

Park J., Ham S., Jang M., Lee J., Kim S., Kim S., Lee K., Park D., Kwon J., K im H., 2017. Spatial–temporal dispersion of aerosolized nanoparticles durin g the use of consumer spray products and estimates of inhalation exposure. Environ. Sci. Technol. 51 (13), 7624-7638.

Park J., Yoon C., Lee K., 2018b. Comparison of modeled estimates of inhalation exposure to aerosols during use of consumer spray products. International j ournal of hygiene and environmental health. 221 (6), 941-950.

Qian L., Guan Y., He B., Xiao H., 2008. Modified guanidine polymers: synthesis and antimicrobial mechanism revealed by AFM. Polymer. 49 (10), 2471-24 75.

Sain A. E., Zook J., Davy B. M., Marr L. C., Dietrich A. M., 2018. Size and m ineral composition of airborne particles generated by an ultrasonic humidifi er. Indoor Air. 28 (1), 80-88.

Shiue S., Scherzer H., DeGraff Jr A., Cole S., 1990. Hypersensitivity pneumonitis associated with the use of ultrasonic humidifiers. New York state journal of medicine. 90 (5), 263-265.

Solodun Y., Monakhova Y., Kuballa T., Samokhvalov A., Rehm J., Lachenmeier D., 2011. Unrecorded alcohol consumption in Russia: toxic denaturants and disinfectants pose additional risks. Interdiscip. Toxicol. 4 (4), 198-205.

Song J. A., Park H. J., Yang M. J., Jung K. J., Yang H. S., Song C. W., Lee K., 2014. Polyhexamethyleneguanidine phosphate induces severe lung infla mmation, fibrosis, and thymic atrophy. Food Chem. Toxicol. 69, 267-275.

Souza T. G. F., Ciminelli V. S. T., Mohallem N. D. S. A comparison of TEM a nd DLS methods to characterize size distribution of ceramic nanoparticles. J. Phys. Conf. Ser. 733. IOP Publishing, 2016, pp. 012039.

Streicher R. P., Reh C. M., Key-Schwartz R., Schlecht P. C., Cassinelli M. E., 1 998. Determination of airborne isocyanate exposure. NIOSH manual of ana lytical methods, 115-140.

Umezawa M., Sekita K., Suzuki K.-i., Kubo-Irie M., Niki R., Ihara T., Sugamata M., Takeda K., 2013. Effect of aerosol particles generated by ultrasonic h umidifiers on the lung in mouse. Part. Fibre Toxicol. 10 (1), 64.

Wang W. N., Purwanto A., Lenggoro I. W., Okuyama K., Chang H., Jang H. D., 2008. Investigation on the correlations between droplet and particle size d istribution in ultrasonic spray pyrolysis. Ind. Eng. Chem. Res. 47 (5), 165 0-1659.

Wei D., Ma Q., Guan Y., Hu F., Zheng A., Zhang X., Teng Z., Jiang H., 2009. Structural characterization and antibacterial activity of oligoguanidine (poly hexamethylene guanidine hydrochloride). Materials Science and Engineering:

C. 29 (6), 1776-1780.

Xu R., 2015. Light scattering: a review of particle characterization applications. P articuology. 18, 11-21.

Yang X., Wu T., Liu B., Du Y., Li H., Zhao S., Lu Y., 2013. Matrix selection f or polymer guanidine analysis by MALDI–TOF MS. International Journal of Mass Spectrometry. 356, 1-6.

Yoon J., Lee S., Lee S, Kim E, Jung S., Cho H., Lee E., Yang S., Hong S., 20 18. Exposure to Humidifier Disinfectants Increases the Risk for Asthma in Children. American journal of respiratory and critical care medicine, 198(1 2), 1583-1586.

APPENDICES

Appendiċes table 1. Summary of geometric mean (GM) and geometric standard deviation (GSD) of PHMG concentration measured by real-time monitoring instruments

Working status	Concentration (ppm)	Product	SMPS (10-420 nm) [particles/cm^3] 0.5m			SMPS (10-420 nm) [particles/cm^3] 1m			OPS (0.3-10 μm) [particles/cm^3] 0.5 m		PAS ($PM_{1.0}$-PM_{10}) [μg/m^3] 0.5 m		
			<100	>100	Total Conc.	<100	>100	Total Conc.	0.3-1.0	1.0-10	$PM_{1.0}$	$PM_{2.5}$	PM_{10}
During operation	6.50	Oxy product	10,331	2,311	12,673	14,571	3,382	17,968	78	0.22	17	18	18
			(1.21)	(1.28)	(1.21)	(1.42)	(1.43)	(1.41)	(1.38)	(2.32)	(1.30)	(1.30)	(1.31)
	6.25	BOC product	11,585	2,707	14,343	8,882	2,494	11,394	57	0.06	16	16	16
			(1.23)	(1.30)	(1.22)	(1.81)	(1.82)	(1.80)	(1.23)	(1.75)	(1.46)	(1.43)	(1.43)
	6.25	Scunder product	12,980	2,869	15,897	8,092	2,405	10,576	78	0.08	14	14	14
			(1.28)	(1.28)	(1.26)	(1.25)	(1.30)	(1.21)	(1.19)	(1.62)	(1.35)	(1.35)	(1.35)
	65.00	Oxy product	34,604	18,305	53,004	41,529	26,644	68,214	2,026	10	202	205	210
			(1.20)	(1.23)	(1.20)	(1.17)	(1.19)	(1.17)	(1.16)	(1.50)	(1.11)	(1.11)	(1.10)

After operation	62.50	BOC product	26,995	14,778	41,842	21,939	13,262	35,242	1,814	5	181	183	183
			(1.28)	(1.28)	(1.27)	(1.25)	(1.25)	(1.24)	(1.10)	(1.72)	(1.12)	(1.13)	(1.13)
	62.50	Scunder product	27,302	13,885	41,337	18,012	11,571	29,655	1,937	7	170	171	171
			(1.50)	(1.52)	(1.49)	(1.15)	(1.20)	(1.15)	(1.10)	(1.53)	(1.10)	(1.10)	(1.10)
	0	D.W.	3,930	54	4,010	4,039	49	4,107	1	0.04	0.19	0.22	0.23
			(1.19)	(3.27)	(1.19)	(1.35)	(2.77)	(1.34)	(1.24)	(1.87)	(1.34)	(1.45)	(1.50)
	6.50	Oxy product	469	179	655	492	192	691	24	0.04	3	3	3
			(2.18)	(2.30)	(2.17)	(2.64)	(2.34)	(2.53)	(2.47)	(3.97)	(2.79)	(2.81)	(2.84)
	6.25	BOC product	295	134	432	420	189	614	10	0.01	2	2	2
			(2.32)	(2.11)	(2.24)	(2.70)	(2.59)	(2.64)	(2.65)	(2.76)	(2.61)	(2.60)	(2.61)
	6.25	Scunder product	351	104	459	209	119	342	7	0.02	1	1	1
			(2.50)	(2.75)	(2.52)	(3.51)	(3.10)	(3.21)	(3.25)	(3.14)	(3.43)	(3.43)	(3.43)
	65.00	Oxy product	573	698	1,280	689	935	1,639	198	2	22	23	23
			(2.65)	(2.26)	(2.42)	(3.02)	(2.39)	(2.64)	(2.49)	(2.76)	(2.42)	(2.43)	(2.44)

62.50	BOC product	350	317	673	490	534	1,036	152	1	13	13	13
		(2.92)	(2.80)	(2.83)	(3.53)	(2.92)	(3.21)	(2.87)	(2.99)	(2.98)	(3.00)	(3.02)
62.50	Scunder product	279	333	646	268	587	894	94	1	11	11	11
		(3.69)	(2.92)	(3.05)	(4.83)	(2.64)	(3.21)	(3.78)	(3.98)	(3.66)	(3.67)	(3.67)
0	D.W.	245	14	263	292	17	315	1	0.004	0.14	0.15	0.15
		(1.86)	(1.83)	(1.80)	(1.97)	(1.86)	(1.90)	(1.28)	(1.99)	(1.43)	(1.46)	(1.47)

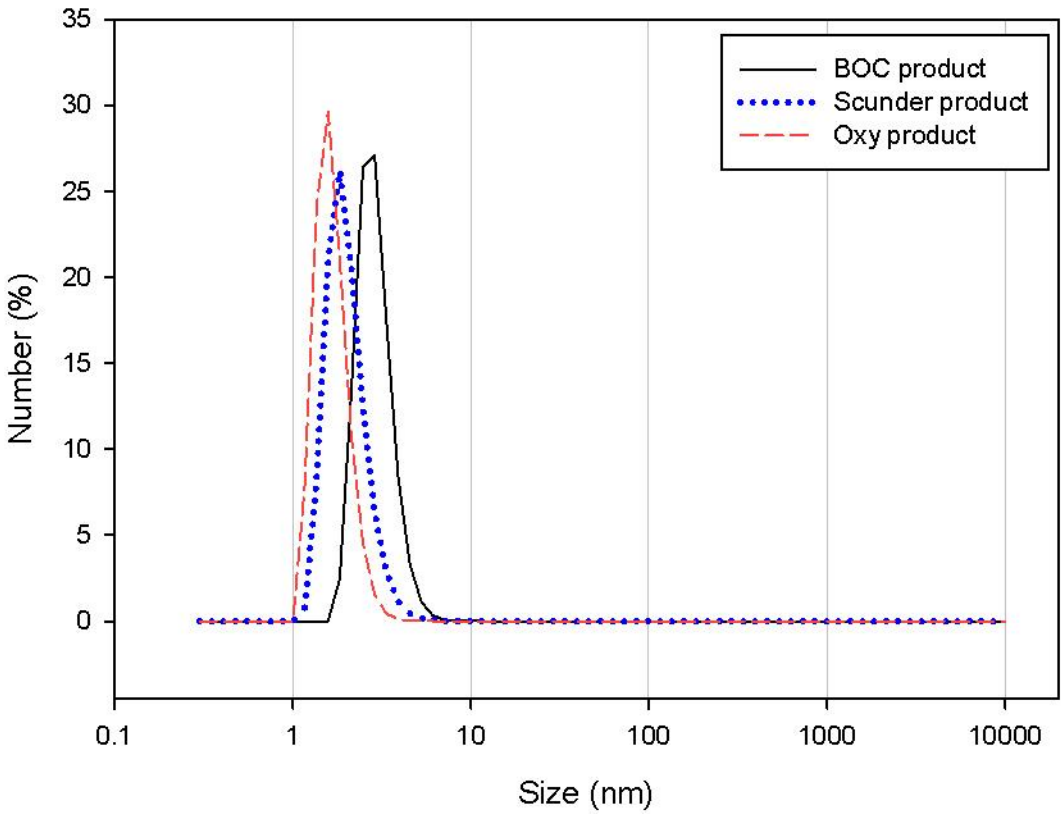

Appendices figure 1 . The relative number fraction distribution of PHMG products in aqueous solution analyzed by dynamic light scattering (DLS)

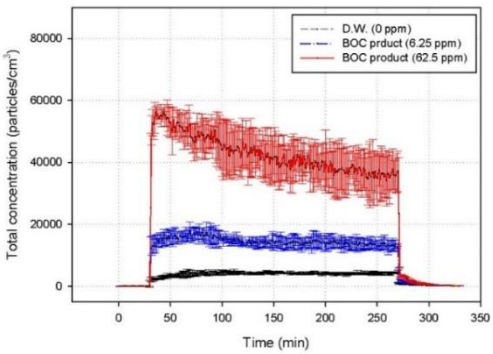

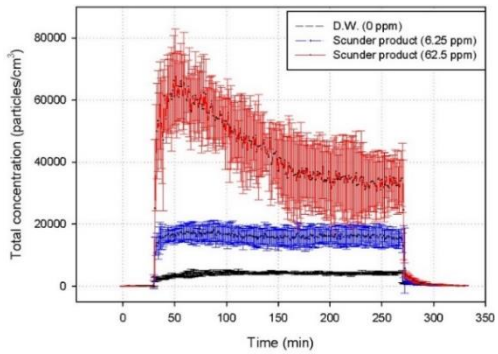

(d) The number concentration measured by SMPS
(10-420 nm; left : BOC product, right : Scunder product)

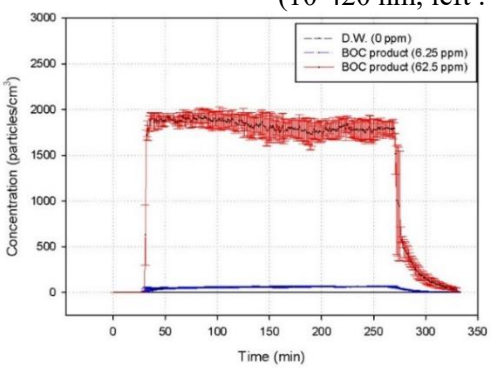

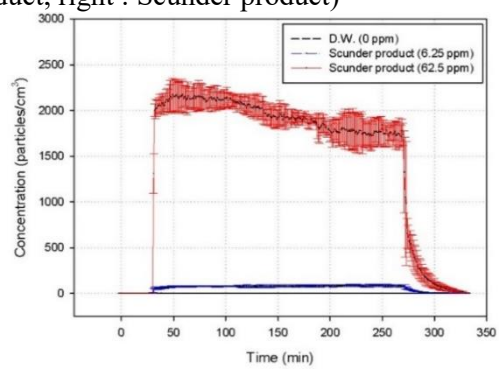

(e) The number concentration measured by OPS
(0.3-1.0 μm; left : BOC product, right : Scunder product)

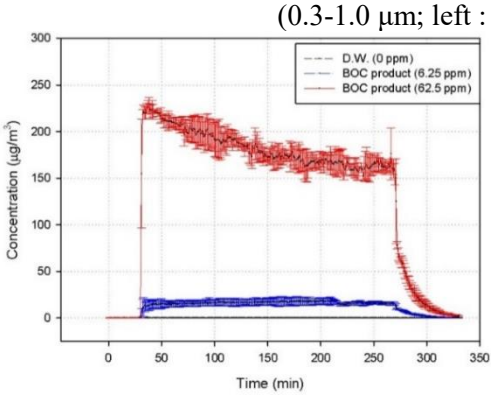

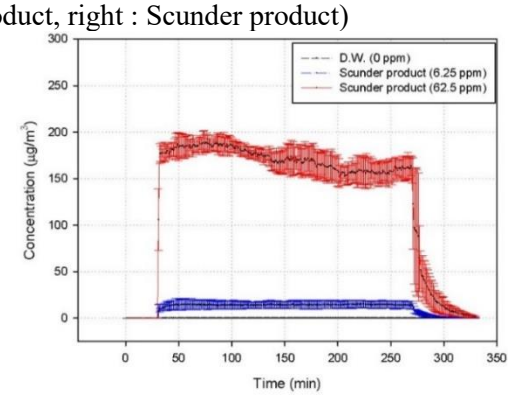

(f) The mass concentration measured by PAS
(PM1.0; left : BOC product, right : Scunder product)

Appendices figure 2. Time-varying concentration in airborne at different PHMG concentration for BOC and Scunder product.

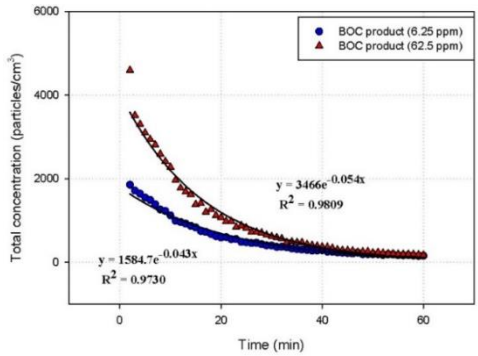

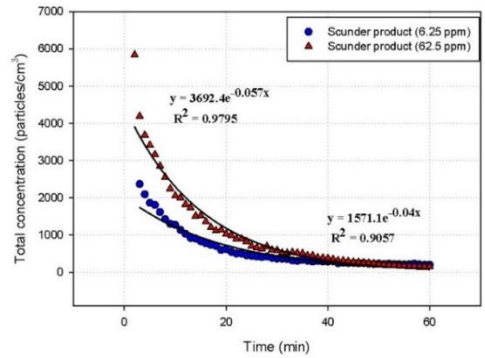

(a) The number concentration measured by SMPS
(10-420 nm; left : BOC product, right : Scunder product)

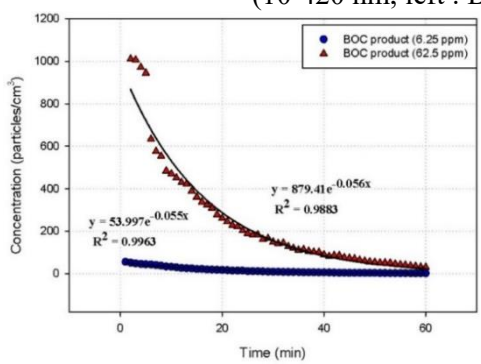

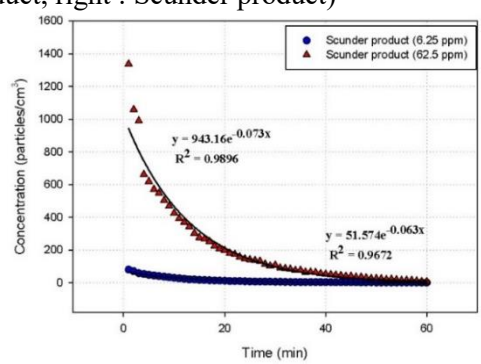

(b) The number concentration measured by OPS
(0.3-1.0 μm; left : BOC product, right : Scunder product)

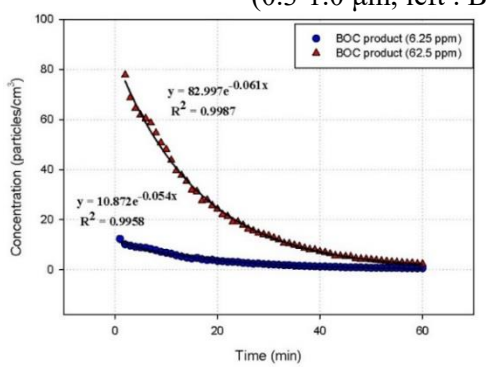

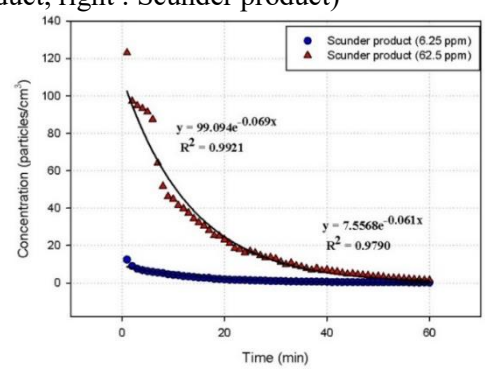

(c) The mass concentration measured by PAS
(PM1.0; left : BOC product, right : Scunder product)

Appendices figure 3 . Time-varying concentration including exponential regression curve after humidifier operation for BOC and Scunder products.

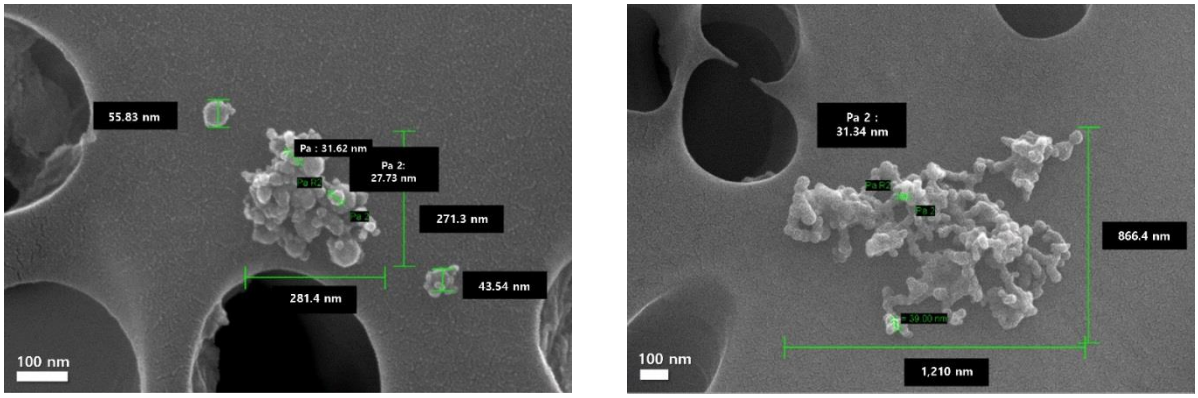

(c) Oxy product (left : 6.5 ppm, right : 65 ppm)

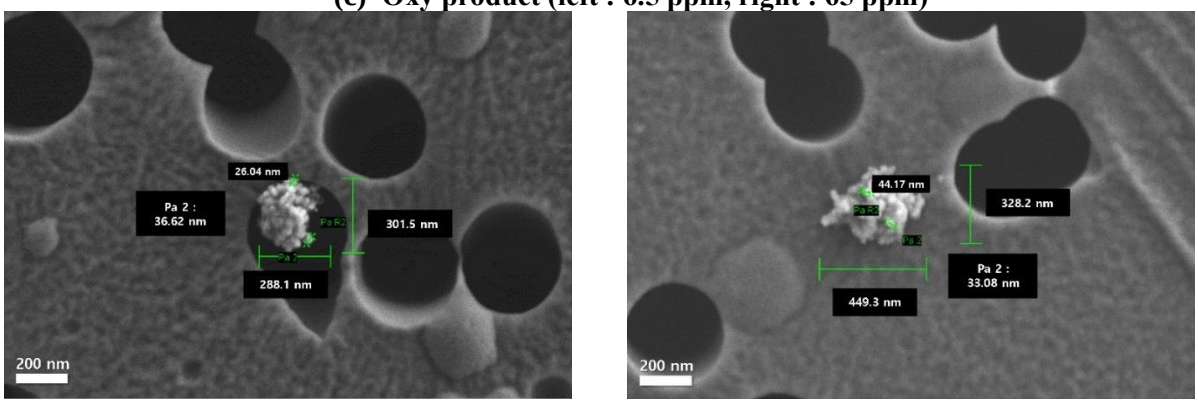

(d) BOC product (left : 6.25 ppm, right : 62.5 ppm)

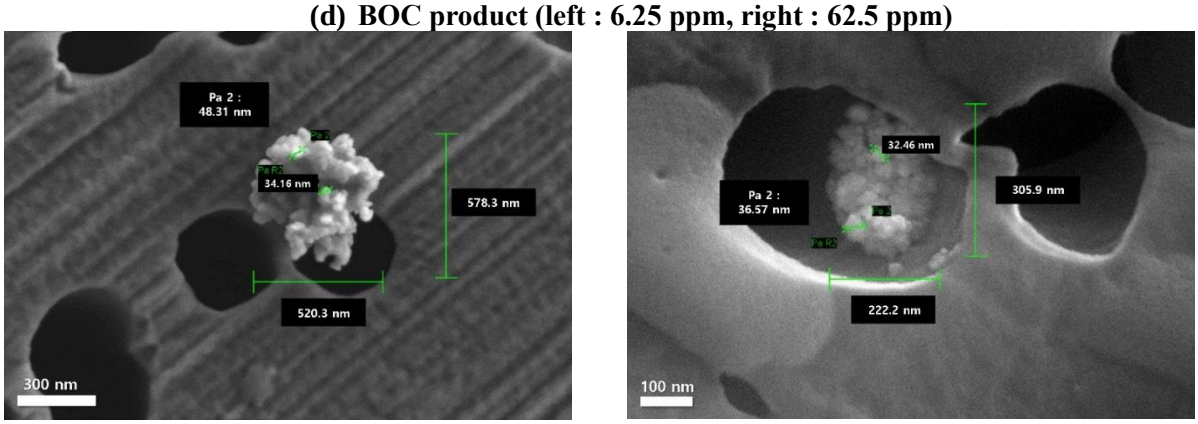

(c) Scunder product (left : 6.25 ppm, right : 62.5 ppm)

Appendices figure 4 . FE-SEM image of samples during humidifier operation at 1 m.

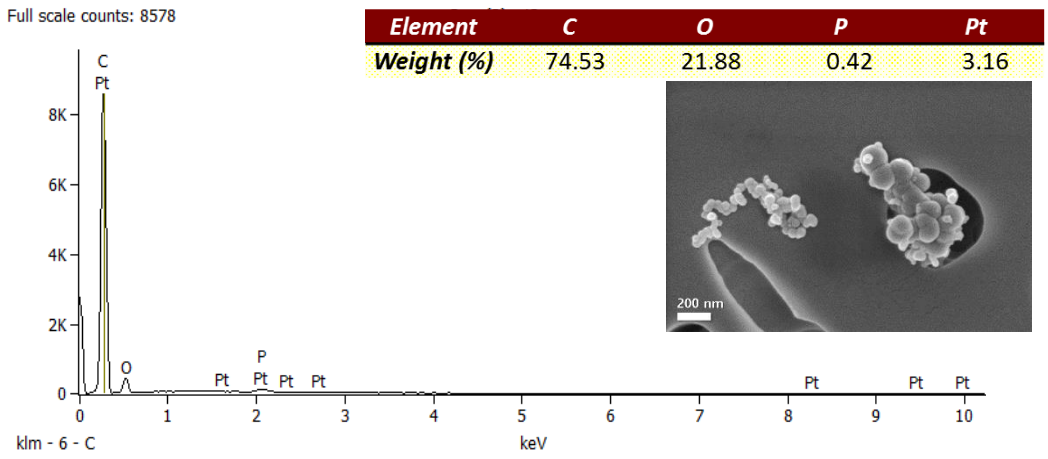

(a) Oxy product (65 ppm)

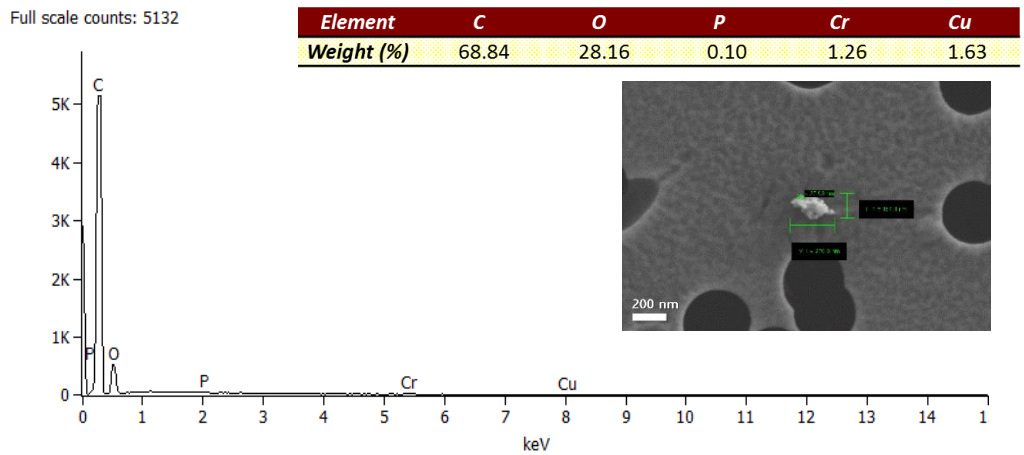

(b) BOC product (6.25 ppm)

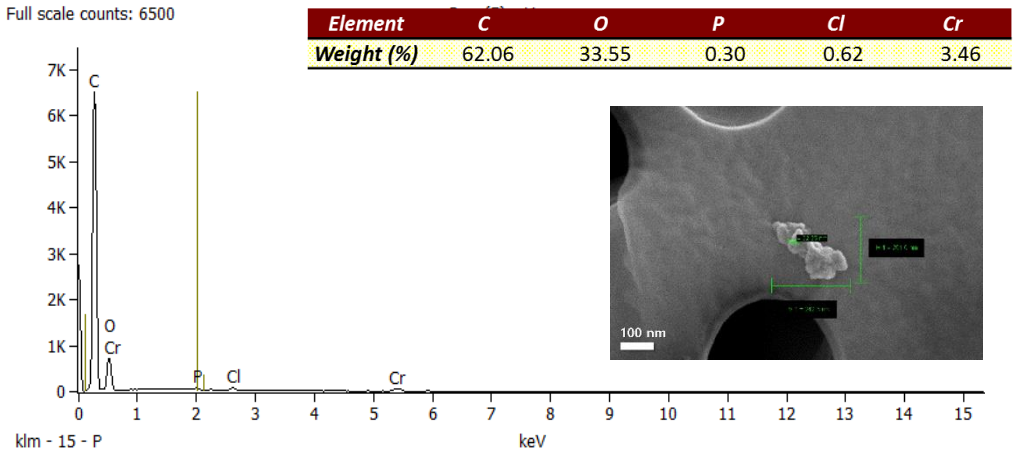

(c) Scunder product (62.5 ppm)

Appendices figure 5 . The analysis result of field emission-scanning electron microscope-energy dispersive spectrometry (FE-SEM-EDS) at 0.5 m.

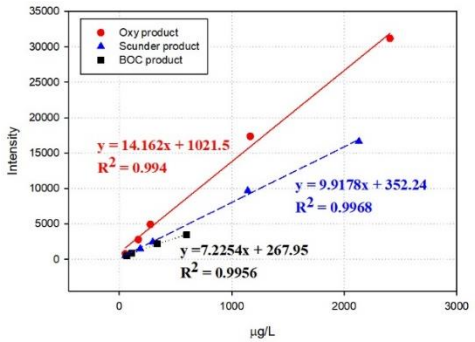

(a) Type A1

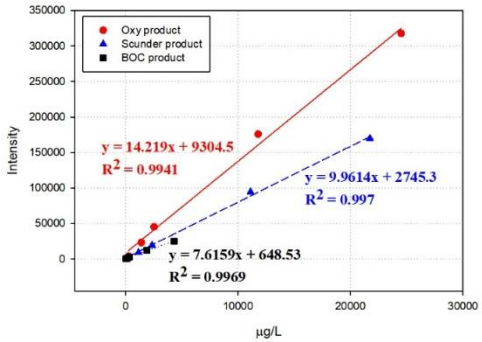

(b) Type A2

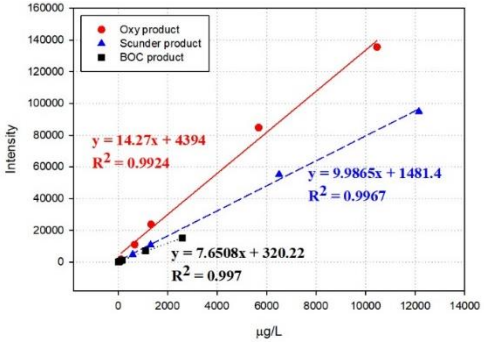

(c) Type A3

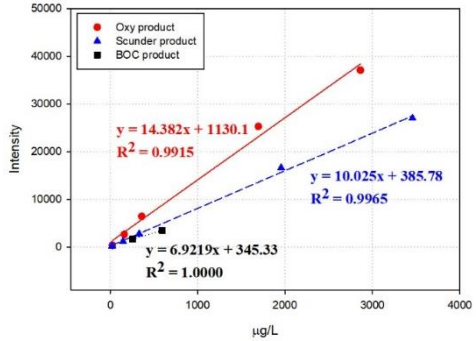

(d) Type A4

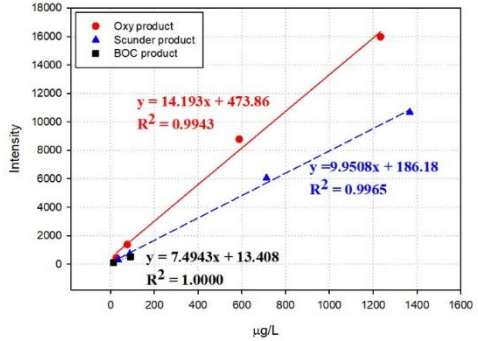

(e) Type A5

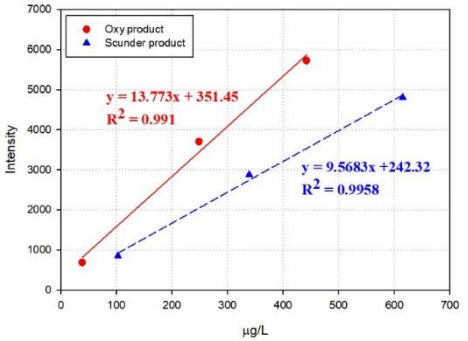

(f) Type A6

Appendices figure 6 . The linear graph of PHMG type A standard.

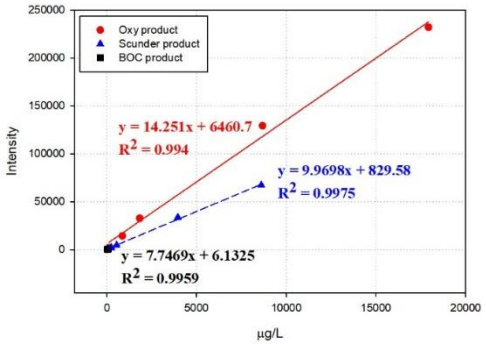

(a) Type B1

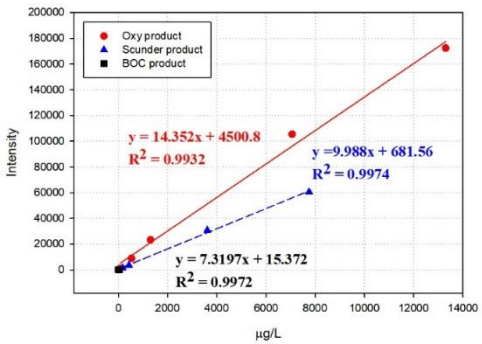

(b) Type B2

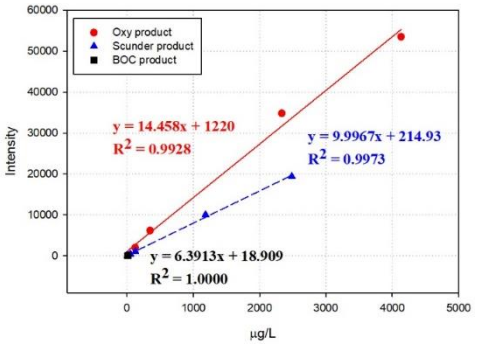

(c) Type B3

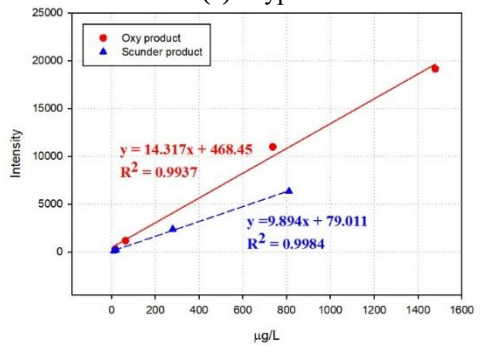

(d) Type B4

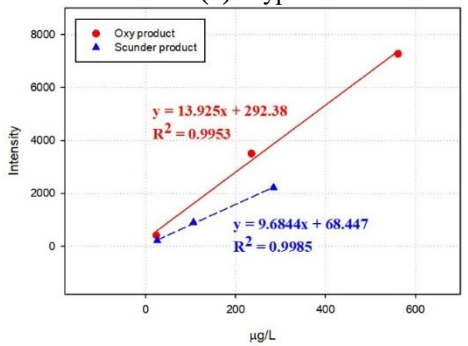

(e) Type B5

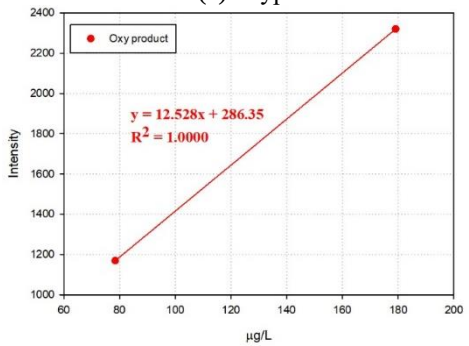

(f) Type B6

Appendices figure 7 . The linear graph of PHMG type B standard.

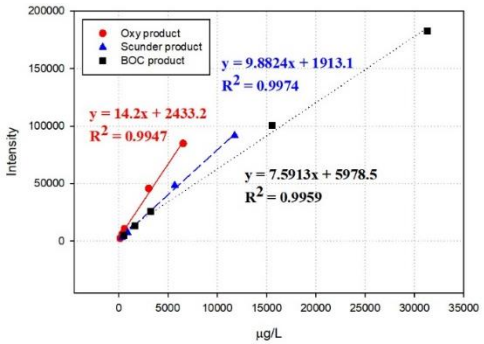

(a) Type C1

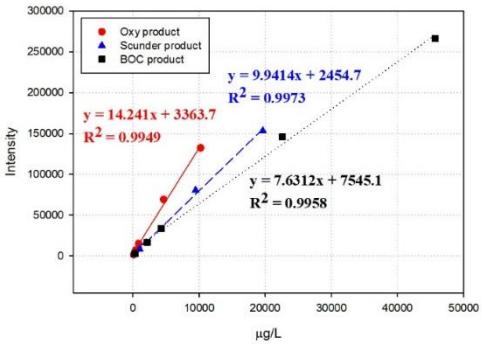

(b) Type C2

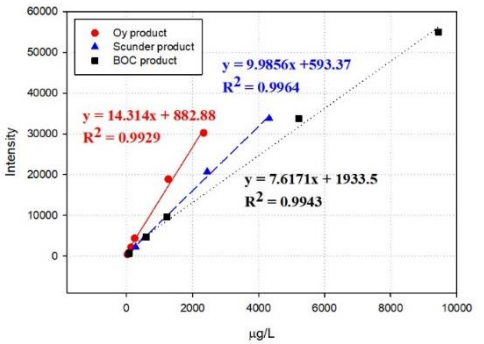

(c) Type C3

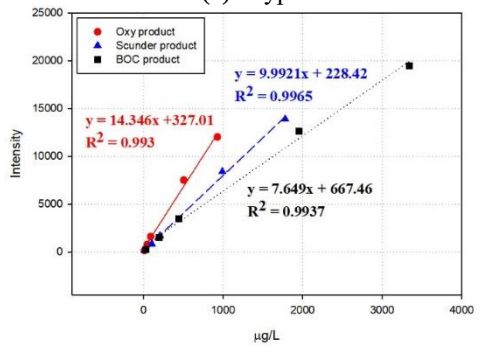

(d) Type C4

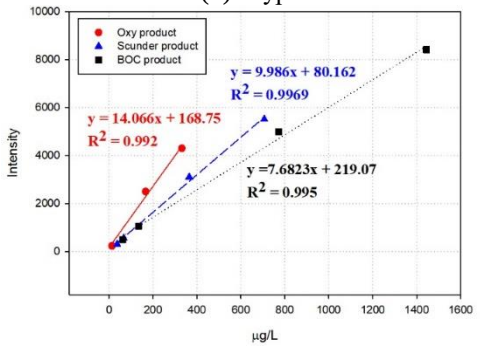

(e) Type C5

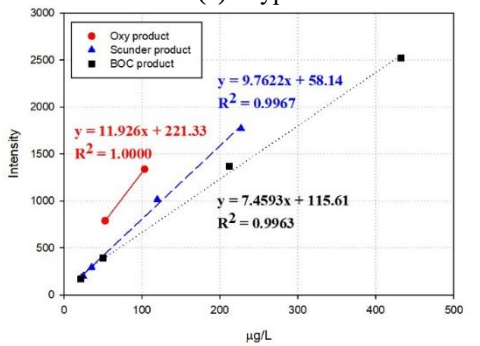

(f) Type C6

Appendices figure 8 . The linear graph of PHMG type C standard.

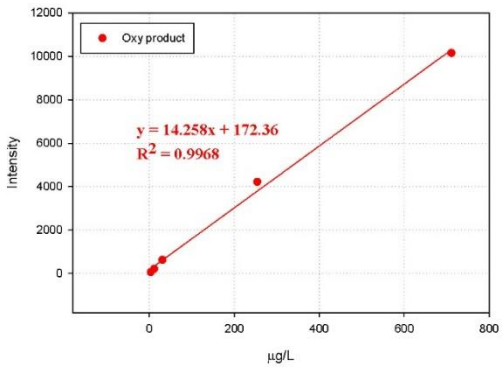

(a) Type D1

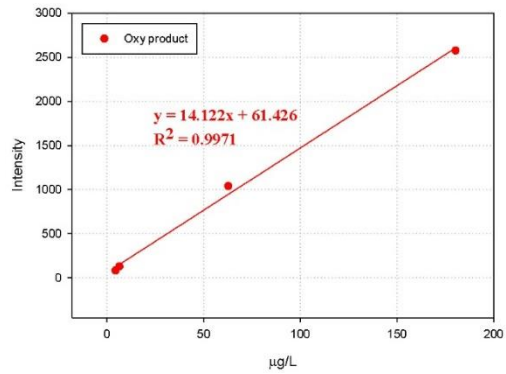

(b) Type D2

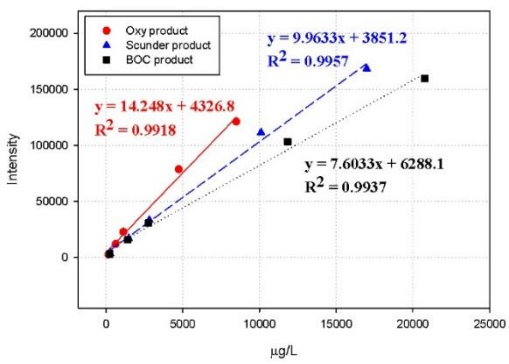

(c) Type E2

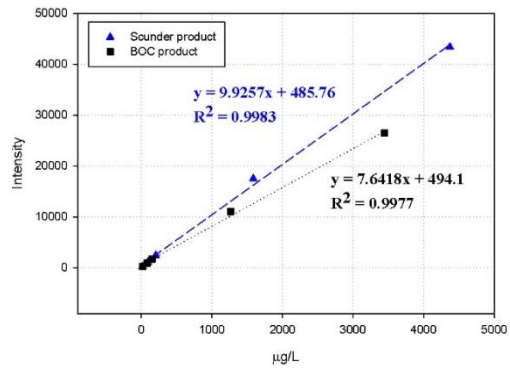

(e) Type E3

Appendices figure 9 . The linear graph of PHMG type D and E standard.

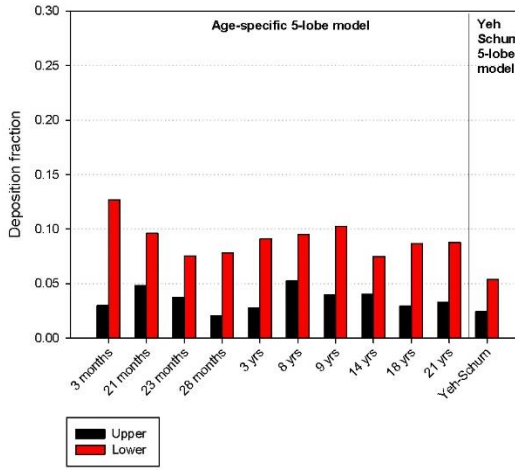

(a) Deposition fraction by upper and lower lung (x 200)

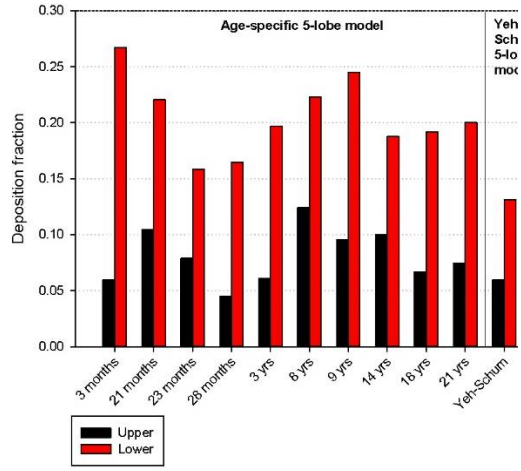

(b) Deposition fraction by upper and lower lung (x 20)

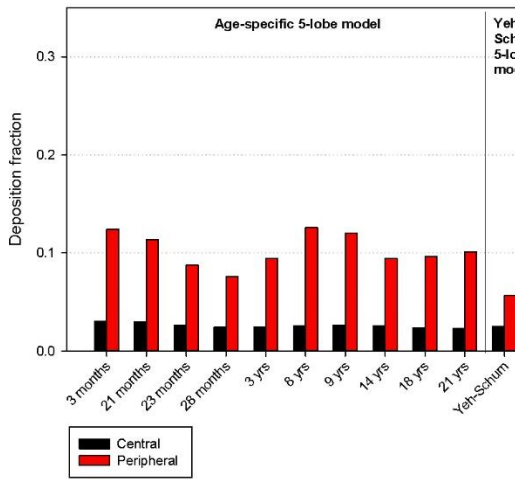

(c) Deposition fraction by central and peripheral lung (x 200)

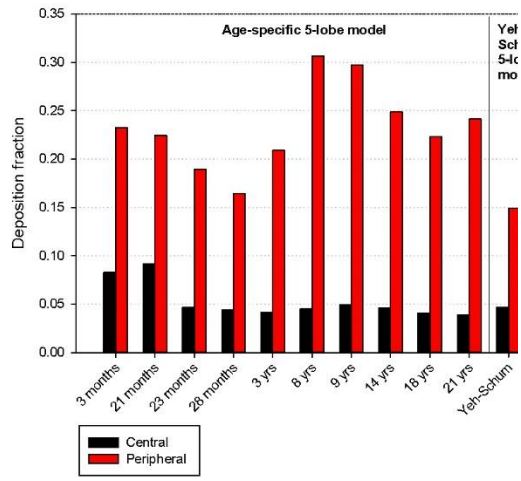

(d) Deposition fraction by central and peripheral lung (x 20)

Appendices figure １０. Deposition fraction by upper/lower and central/peripheral lung by concentrations.

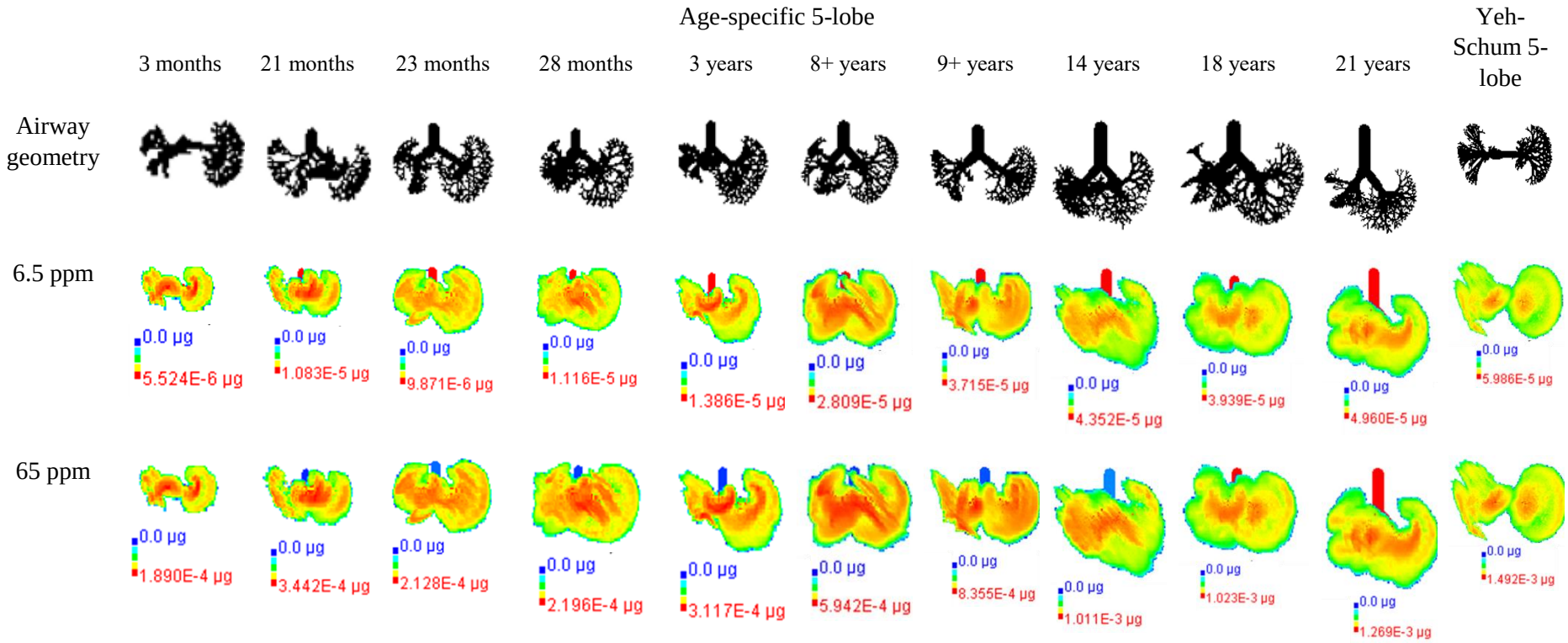

Appendices figure １１. The lung visualization of deposited mass by concentration in sleeping (these figures had a different scale in all simulation).

국문 초록

겨울과 봄이 춥고 건조한 한국은 주로 초음파식 가습기를 많이 사용한다. 그러나 가습기 저장탱크 내 미생물 번식으로 인한 가습기 폐질환은 과거에 문제가 되어 왔기때문에 국내에서는 1994년부터 2011년까지 초음파 가습기의 미생물 오염을 막기 위하여 가습기 살균제를 사용해왔다. 하지만 2011년 가습기 살균제 사용자들에서 심각한 폐질환이 발생하여 현재는 정부에 의해 판매가 금지되었다. 가습기 살균제에 사용되는 주요 원료로는 polyhexamethyleneguanidine (PHMG), oligo(2-(2-ethoxy)ethoxyethyl guanidine chloride (PGH), methylchloroisothiazolinone /methylisothiazolinone (CMIT/MIT)가 있었고, 그 중 PHMG가 함유된 제품이 가장 많은 피해자가 발생하였다. 따라서 본 연구의 목적은 첫번째로 수용액에서의 PHMG 입자특성을 확인하고, 가습기 살균제로 사용된 PHMG의 공기 중 거동을 조사하는 것, 두번째로 고분자인 PHMG 제품과 공기 중 에어로졸에서 PHMG 단량체(oligomer) 유형과 함유량을 파악하고, 공기 중 노출 농도를 추정하는 것, 세번째로 공기 중 가습기

살균제 입자를 ICRP 모델을 이용하여 인체에 흡입노출 되었을 때 흡입량과 침착량을 추정하는 것이다.

먼저, 다양한 PHMG를 이용하여 실험하기 위해 제조사가 다른 PHMG (한국, 미국 및 중국에서 제조) 제품을 선택했다. 수용액에서의 거동 특성을 확인하기 위해 동적 광산란 장치(DLS)를 이용하였으며, 공기 중 특성은 PHMG를 희석하여 높은 농도 (62.5–65ppm)와 낮은 농도 (6.25–6.5ppm)로 희석한 후, 실시간 모니터링 장비(SMPS, OPS, PAS)로 측정하였다. 이때 클린룸 내 수분을 제어하기 위해 수분제어장치를(diffusion dryer, thermodenuder) 실시간 모니터링 장비에 장착하였다. 또한 공기 중 형태학적 입자특성을 확인하기 위하여 전자현미경(FE-SEM-EDS)으로 분석하였다. DLS 결과는 공기 중 입자 분포에 비해 약간 오른쪽으로 치우친 (~ 100 nm) 이봉 분포(bimodal distribution)의 형태를 나타냈다. 전자현미경에 의해 확인 된 입자는 대략 20 nm 이상의 단일입자가 응집된 형태로 존재하였고, 공기 중에 분무되면서 PHMG 입자의 응집으로 크기가 증가된 것으로 추정된다. PHMG 원액 농도가 10 배 증가함에 따라, 실시간

모니터링 장비로 측정 한 공기 중 농도는 나노 입자의 경우 2–3 배, 1-10μm 입자의 경우 45–85 배 증가했다. 그러나 생성 된 입자의 99 %는 PM1이었다. 제조사에서 권장희석농도로(6.5 ppm) 가습기를 작동하고, 중단 한 이후에 환기를 하지 않는다면 배경 농도에 도달 할 때까지 PHMG 입자가 공기 중에 약 2 시간 존재할 수 있다. 따라서 PHMG 공기 중 거동특성은 제조업체가 다른 제품이라고 해서 크게 영향을 받지 않는 것으로 보인다.

두번째로, PHMG 구성 성분을 확인하기 위하여 LC-qToF를 이용하여 분석하였고, Unifi 프로그램을 이용하여 물질의 분자량과 구조를 고려하여 데이터 처리를 하였다. 가습기 분무 시 공기 중 샘플은 앞의 연구와 같은 조건으로 실험하였고, 샘플링은 임핀저를 이용하여 0.5 m와 1 m에서 8시간동안 채취하였다. PHMG 는 선형 타입(타입 A-C)과 가지 및 원형 타입 (타입 D-G)이 존재한다고 알려져 오고 있다. 원액분석결과 선행연구에서 알려진 것과 같이 다양한 타입이 존재하였고, 그 중 옥시 제품은 타입 A-E가 존재하였고, BOC와 Scunder 제품은 타입 A-E 중 타입 D를 제외하고 존재하였다. 또한 세 제품

구성성분 모두 단량체가 1-3개인 올리고머 수준으로 존재하였다. 공기 중에 분사된 PHMG 구성성분은 0.5 m 에서 채취된 샘플의 경우 원액구성성분과 유사한 패턴을 보였으나 농도가 낮거나 거리가 멀어지면(1 m) 주로 저분자인 단량체 (monomer, dimer)위주로 검출되었고, 주로 C 타입의 단량체인 monomer의 검출 비율이 높았다. 또한 공기 중 올리고머는 추정식을 이용하여 농도를 추정하였으며, 옥시제품의 권장희석배수인 200:1로 희석한 6.5 ppm에서 농도는 35.89 $\mu g/m^3$ 이었고, 65 ppm에서는 390.96 $\mu g/m^3$ 이었다.

마지막으로, 첫번째 연구인 실시간 기기로 측정한 공기 중 입자 농도 자료에 근거하여 인체 내 흡입 및 침착량을 ICRP 및 MPPD 흡입노출 모델을 사용하여 추정하였다. ICRP 모델은 일반 모집단의 폐에 침착되는 입자를 평가하는데 널리 사용되며 실험 데이터를 기반한 실험식을 사용하며, 이것을 발전시켜 개발한 것인 MPPD 모델이다. 이 연구에서 4 가지 유형의 시나리오는 노출 집단은 성인과 어린이, 그리고 환경은 일상생활과 수면시의 조합으로 사용되었다.

입력변수의 차이로 인해 두 모델이 차이는 있으나, 성인이 어린이에 비해 침착량 및 및착분률이 유사하거나 높은 경향을 보인다. 침착량 산정시 기관지내 침착부위는 3군데로 나뉘어 지는데, 머리기도, 기관지, 폐포 영역 각각의 노출량을 추정할 수 있다. 가습기가 분무 될 때, 15.4 nm에서 가장 높은 수농도의 침착량을 보였고, 질량농도에 의한 침착량은 두 모델 모두 폐포, 기관지, 머리기도 영역 순으로 높았다.

결론적으로, 본 연구는 가습기 살균제인 PHMG의 원액과 공기 중으로 분무시 입자 특성을 확인 한 후 ICRP 모델을 이용하여 인체 호흡기 내 흡입 및 침착량을 추정하였다. PHMG 원액 입자는 100 nm 근처의 영역에서 이봉 분포를 보였고, 주 성분은 주로 선형 유형의 올리고머로 구성되었다(타입 A-C). 공기 중 PHMG의 특성은 대부분의 입자가 PM_1이고 약 20-100 nm의 단일 입자가 응집 되어 존재하는 것으로 확인되었다. 공기 중 PHMG 에어로졸의 성분은 주로 올리고머 비율이 높았고, 0.5 m에서 측정된 샘플은 원액의 구성성분과 유사했으나 1 m에서 측정된 샘플은 단량체 중 타입 C가 높은 비율을 차지

하였다. 따라서 공기 중 입자의 대부분은 저분자인 단량체(주로 monomer, dimer 등)가 나노입자로 응집되어 있는 형태로 존재한다. ICRP 및 MPPD 모델을 사용하여 추정 된 흡입 및 침착량은 영아 및 어린이의 개월 수가 낮을수록 높은 수치를 보였다. 본 연구에서 제조사가 다양한 PHMG 제품을 이용하여 실험한 결과 전체적으로 세 제품이 유사하였기 때문에, 옥시 제품 외 PHMG를 함유한 다른 가습기 살균제 제품도 본 연구와 유사한 결과를 보일 것으로 생각된다.

주요어: 가습기 살균제, PHMG, 구아니딘계 살균제, 고분자, 올리고머, 단량체, 노출 모델, 침착 모델

학 번: 2015-30659